PB 151371

NBS

Technical Note No. 12

TRANSMISSION LOSS IN RADIO PROPAGATION - II

BY KENNETH A. NORTON

U. S. DEPARTMENT OF COMMERCE
NATIONAL BUREAU OF STANDARDS

NATIONAL BUREAU OF STANDARDS
Technical Note

12

June, 1959

Transmission Loss in Radio Propagation: II

by

Kenneth A. Norton

NBS Technical Notes are designed to supplement the Bureau's regular publications program. They provide a means for making available scientific data that are of transient or limited interest. Technical Notes may be listed or referred to in the open literature. They are for sale by the Office of Technical Services, U. S. Department of Commerce, Washington 25, D. C.

DISTRIBUTED BY

UNITED STATES DEPARTMENT OF COMMERCE

OFFICE OF TECHNICAL SERVICES

WASHINGTON 25, D. C.

Price $ 3.00

This Technical Note was originally given limited distribution as NBS Report No. 5092, dated July 25, 1957. Since that time parts of this report have been published in the following references:

(1) K. A. Norton, "Low and medium frequency radio propagation", Proc. of the International Congress on the Propagation of Radio Waves at Liege, Belgium, October, 1958, to be published by the Academic Press.

(2) K. A. Norton, "System loss in radio wave propagation", J. Research, NBS, 63D, pp. 53-73, July-August, 1959.

(3) K. A. Norton, "System loss in radio wave propagation", Letter to the Editor, Proc. I. R. E., to be published.

All of the material in reference (1) is included in this Technical Note. Some of the material in references (2) and (3) is new, particularly the definitions of the new terms "system loss" and "propagation loss". The transmission loss concept was adopted by the C.C.I.R. at its IXth Plenary Assembly in Los Angeles as is discussed more fully in reference (3) above.

TRANSMISSION LOSS IN RADIO PROPAGATION: II

by

Kenneth A. Norton

SUMMARY

In an earlier report with this title the concept of transmission loss was defined and its advantages explained. In this report a survey will be made of the transmission losses expected for a wide range of conditions, i. e., for distances from 10 to 10, 000 statute miles; for radio frequencies from 10 kc to 100, 000 Mc; for vertical or horizontal polarization; for ground waves, ionospheric waves, and tropospheric waves; over sea water or over land which may be either rough or smooth; and for various geographical and climatological regions.

Note: The attention of the reader is called to additional terms, discussed in appendix III, which must be added to the transmission losses shown in this report when the antennas are near the surface. These terms arise from changes in the antenna radiation resistances which occur when the antennas are near the surface, and represent important corrections to the transmission loss, particularly at the lower frequencies where the antennas, assumed to be 30 feet above the surface for many of the calculations, are only very small fractions of a wavelength above the surface.

TRANSMISSION LOSS IN RADIO PROPAGATION: II

by

Kenneth A. Norton

1. Transmission Loss in Radio Propagation

We will be concerned primarily with the transmission loss* encountered in the propagation of radio energy between a transmitting and a receiving antenna. Simple methods will be given for determining the magnitude of this transmission loss and its variation in space and time (fading) for any frequency in the presently-used portion of the radio spectrum and for any kind of transmission path likely to be encountered in practice. In addition, methods will be given for estimating radio noise and interference levels. When combined, these two methods make possible the estimation of the transmitter power and antenna gain required for satisfactory communication, navigation, or other specific uses of the transmissions.

The transmission loss in a radio system involving propagation between antennas is simply the ratio of the radio frequency power, p_r, radiated from the transmitting antenna divided by the resulting radio frequency power, p_a, available from an equivalent loss-free receiving antenna; thus the system transmission loss = (p_r/p_a). We see that the transmission loss of a system is a dimensionless number greater than unity, and that it will often be convenient to express this in decibels; the transmission loss, L, expressed in decibels, is thus always positive:

$$L = 10 \log_{10} (p_r/p_a) = P_r - P_a \qquad (1)^\dagger$$

---

* See references 1, 2 and 3.

† Throughout this report capital letters will be used to denote the ratios, expressed in decibels, of the corresponding quantities designated with lower-case type; e.g., $P_r = 10 \log_{10} p_r$.

This particular choice of definition excludes from the transmission loss the transmitting and receiving antenna circuit losses* and any loss which occurs in any transmission lines which may be used between the transmitter and the transmitting antenna or between the receiving antenna and the receiver. This exclusion has the advantage that it results in a measure of loss which is attributable solely to the transmission medium including the path antenna gain, G_p, which arises from the directivities of the transmitting and receiving antennas. In addition to the actual transmission loss, L, of the system, it is also convenient to define the basic transmission loss, L_b, to be the transmission loss expected if the actual antennas were replaced by isotropic antennas;† this also serves to define the path antenna gain:

$$G_p \equiv L_b - L \tag{2}$$

Consider first an idealized isotropic transmitting antenna in free space radiating a power, p_r, expressed in watts. Such an antenna produces a field intensity of $p_r/4\pi d^2$ watts per square mile at a distance d expressed in miles provided $d >> \lambda$. The absorbing area of a perfectly conducting, isotropic receiving antenna in free space is equal to $\lambda^2/4\pi$ where λ is the free-space wavelength expressed in miles; the resulting radio frequency power available from such a receiving antenna when placed at a distance $d >> \lambda$ from the isotropic transmitting antenna is thus $p_a = p_r(\lambda/4\pi d)^2$. Thus we find

---

* Antenna circuit loss includes the ground losses arising from the induction field of the antenna, but excludes losses occurring in the radiation field.

† In some of the past literature on radio wave propagation, the intensities of the expected fields have been given in terms of E, the field strength expressed in decibels above one microvolt per meter for one kilowatt effective power radiated from a half-wave dipole. It can be shown that L_b and E are simply and precisely related by $L_b = 139.367 + 20 \log_{10} f_{mc} - E$.

that the basic transmission loss, L_{bf}, for isotropic antennas in free space* is given by:

$$L_{bf} = 10\log_{10}(p_r/p_a) = 10\log_{10}(4\pi d/\lambda)^2 = 36.58 + 20\log_{10} d + 20\log_{10} f_{Mc} \tag{3}$$

In the above f_{Mc} denotes the radio frequency expressed in megacycles. Fig. 1 shows this basic transmission loss for isotropic antennas in free space. For $d = 2\lambda$, $L_{bf} = 28$ db and thus (3) is only approximate when the indicated values of L_{bf} are less than, say, 30 db.

In fact, whenever the calculated transmission loss is less than, say 30 db, we must consider that the problem involves a transfer of an appreciable portion of the power between the transmitting and receiving antennas by other than radiation. For example, there is a direct coupling between the antennas via their induction and electrostatic fields, and this is a negligible factor in the calculation of the transmission loss only when $L > 30$ db. When high gain antennas are used, their separation must be much greater than 2λ in order to maintain the condition $L > 30$ db.

For an actual radio transmission system there will always be some path antenna gain so that the transmission loss $L = L_b - G_p$ will be less than the basic transmission loss. In some systems the free space gains G_t and G_r of both the transmitting and receiving antennas, respectively, will be fully realized so that $G_p = G_t + G_r$. For example, with half-wave dipoles having a common equatorial plane and separated by a distance $d >> \lambda$ in free space $G_t = G_r = 2.15$ db so that $G_p = 4.30$ db; the transmission loss for such a system is thus just 4.3 db less than that given by (3) and shown on Fig. 1. Similarly, electrically short dipoles have gains

---

* In some of the past literature on radio wave propagation, the intensities of the expected fields have been given in terms of $A \equiv L_b - L_{bf}$, the attenuation relative to that expected for propagation in free space; in the case of surface wave propagation with vertical polarization, the attenuation has usually been expressed relative to an inverse distance field which is twice the free space field and thus $A' = L_b - L_{bf} + 6.021$ in this case.

BASIC TRANSMISSION LOSS IN FREE SPACE
ISOTROPIC ANTENNAS AT BOTH TERMINALS

$$L_{bf} = 36.58 + 20 \log_{10} D + 20 \log_{10} f_{Mc}$$

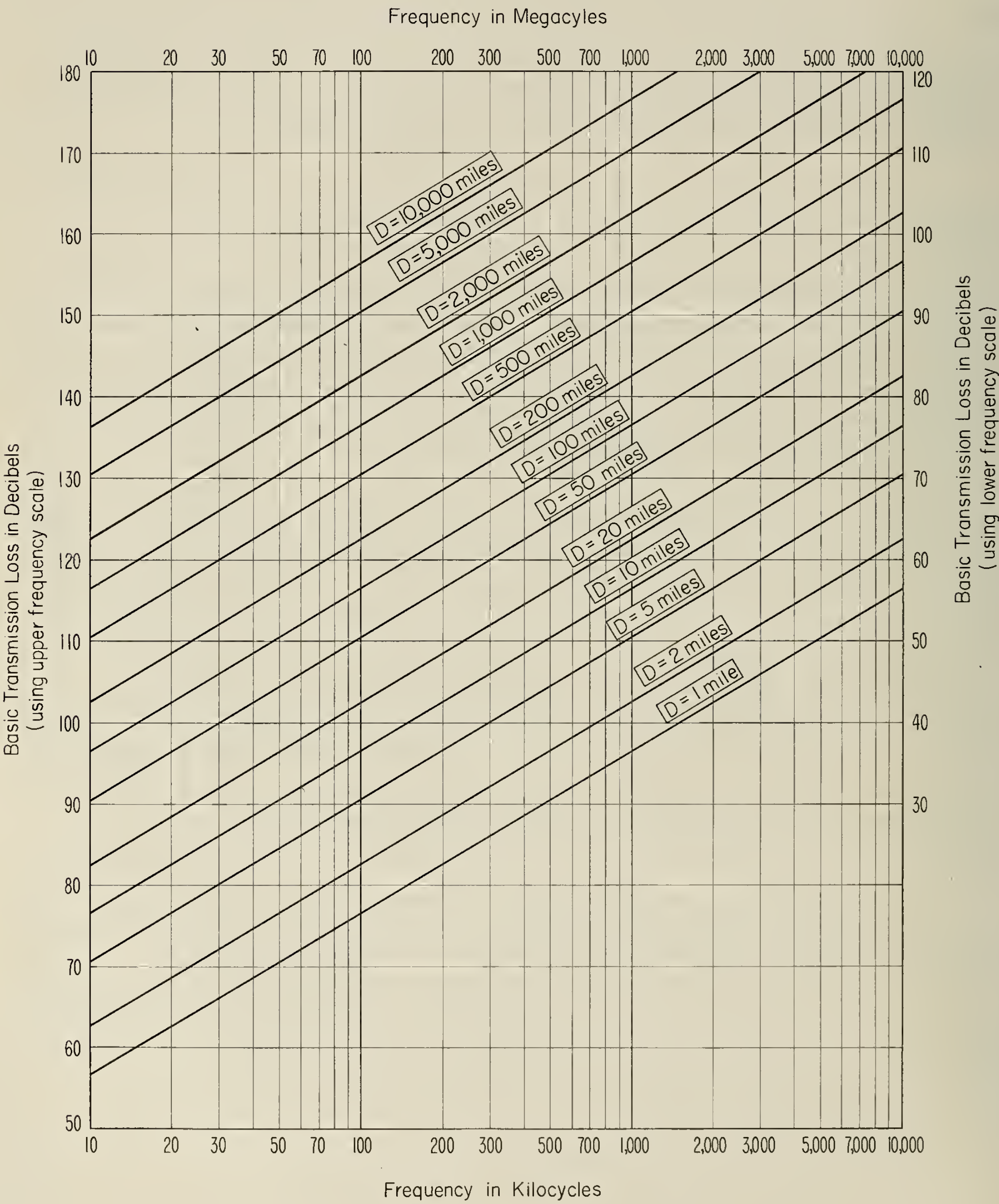

Figure 1

$G_t = G_r = 1.76$ db so that $G_p = 3.52$ db for propagation between appropriately oriented electrically short dipoles in free space.

The free space gain of a large receiving antenna with an effective absorbing area of a_e square meters will increase with increasing frequency at sufficiently high frequencies:

$$G_r = 10 \log_{10} a_e + 20 \log_{10} f_{Mc} - 38.54 \tag{4}$$

$$(\text{For } f_{Mc} > 100/\sqrt{a_e})$$

For example, a large parabolic antenna will have an effective absorbing area a_e between 50 and 70 per cent of its actual area.

2. Transmission Loss in Free Space

Before considering the additional influences of the earth's surface and of its atmosphere on the propagation and transmission loss of the radio waves, it is instructive to consider first the characteristics of the transmission loss in free space for three kinds of systems which are typical of most of the applications encountered in practice.

Consider first a broadcast type of system in which essentially non-directional antennas are used at both terminals of the transmission path. For example, if half wave dipoles were used we have already seen that the system transmission loss, L, will be just 4.3 db less than that given by (3) and shown on Fig. 1. For such systems we see that the loss increases rapidly with increasing frequency because of the decreasing absorbing area of the receiving antenna. For this reason such systems should, in general, use the lowest available frequencies.

Consider next a type of broadcast service in which a directional array may be used at one end of the path: television is an example since the televiewers in remote areas consistently use high gain receiving antennas. If we assume that a half-wave dipole is used at the other terminal, we may combine (3) and (4) and obtain for the system transmission loss:

$$L_f = 72.97 + 20 \log_{10} d - 10 \log_{10} a_e \tag{5}$$

Note that the free space transmission loss in this case is independent of frequency. In this case again, because of the additional loss arising from the effects of irregular terrain* which increase with increasing frequency, it is generally desirable to keep this kind of broadcasting service at the lowest available frequencies.

Finally consider a point-to-point type of service in which two identical high gain (and thus highly directional) antennas are used at each terminal of the transmission path. For such a system the free space transmission loss may be obtained from:

$$L_f = 113.67 + 20 \log_{10} d - 20 \log_{10} f_{Mc} - 20 \log_{10} a_e \qquad (6)$$

For services of this type it is clear that the highest frequencies free from the effects of atmospheric absorption are likely to be the most efficient. The above formula is applicable only to line-of-sight systems with first Fresnel-zone clearance over terrain which appears rough to the radio waves, and we will consider later within-line-of-sight smooth-terrain systems and beyond-the-horizon systems employing tropospheric scatter.

Rayleigh's criterion of the roughness may be used to determine whether a surface appears to the radio waves to be rough or smooth:

$$R = \frac{4\pi \sigma_h \sin \psi}{\lambda} \qquad (7)$$

In the above equation σ_h denotes the standard deviation of the terrain heights relative to a smoothed mean height (see Fig. 2), $\psi = \psi_T = \psi_R$ denotes the grazing angle with the smoothed mean surface and λ is the wavelength expressed in the same units as σ_h. When R is less than 0.1, there will be a well defined specular reflection from the ground, but when $R > 10$, the reflected wave will be substantially weaker and will usually have a very small magnitude.†

The concept of first Fresnel-zone clearance provides a means of determining when the effects of the ground may be neglected so that the simple formula (6) may be used for determining the expected

---

* See reference 2.

† See references 4, 5 and 6.

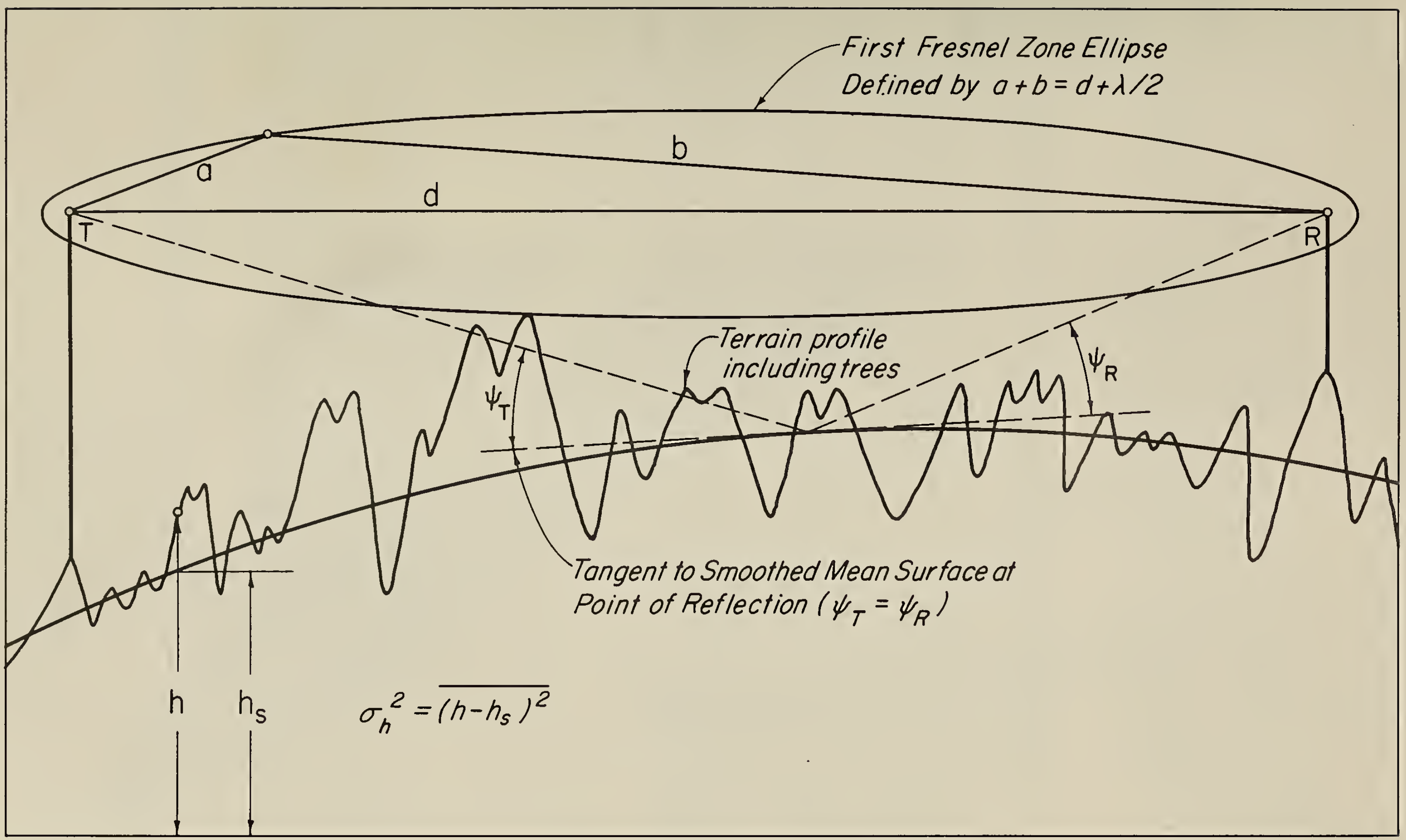

FIG. 2 PATH WITH FIRST FRESNEL ZONE CLEARANCE

transmission loss to a first approximation. Fig. 2 illustrates the first Fresnel zone concept. When the terrain along the path just touches the elliptical first Fresnel-zone defined by the locus of points such that $a + b = d + \lambda/2$, the path is considered to have first Fresnel-zone clearance for a system with wavelength λ. On Fig. 2, T and R represent the locations of the transmitting and receiving antennas. The presence of the ground will have only a small effect on the propagation, provided the antennas are sufficiently elevated so that none of the terrain lies within the first Fresnel zone and if, in addition, $R > 10$ so that the surface appears rough to the radio waves.*

3. Transmission Loss for Ground Wave Propagation

The ground wave is that component of the total received field which has not been reflected (or scattered) from either the ionosphere or the troposphere. It is convenient to divide the ground wave into two components:† a space wave and a surface wave.** The space wave is the sum of a direct wave and a ground-reflected wave. Figs. 3 and 4 give examples of space wave propagation.‡ Near the radio horizon the ground-reflected wave is out of phase with the direct wave, and the received fields are quite weak; as the receiving antenna is raised, the relative phase increases until finally the direct and ground-reflected waves are in phase--at the lobe maxima shown on Figs. 3 and 4. At still higher heights the relative

---

* See references 7 and 8.

† See references 3, 9, 10, 11, 12, and 13.

** The term Norton surface wave has been used in several recent papers in order to distinguish this component of the ground wave from the Zenneck surface wave with which it has sometimes been confused; the latter does not exist in practice as shown by Wise in reference 14. A recent discussion of surface waves by Wait in reference 15 further clarifies the physical nature of this and other surface wave components.

‡ See references 16 and 17 for a further discussion of air-to-ground propagation.

SPACE WAVE PROPAGATION BETWEEN VERTICAL HALF-WAVE DIPOLES
OVER A SMOOTH SPHERICAL SURFACE

GROUND TERMINAL ANTENNA HEIGHT 35 FEET; FREQUENCY 328 MC

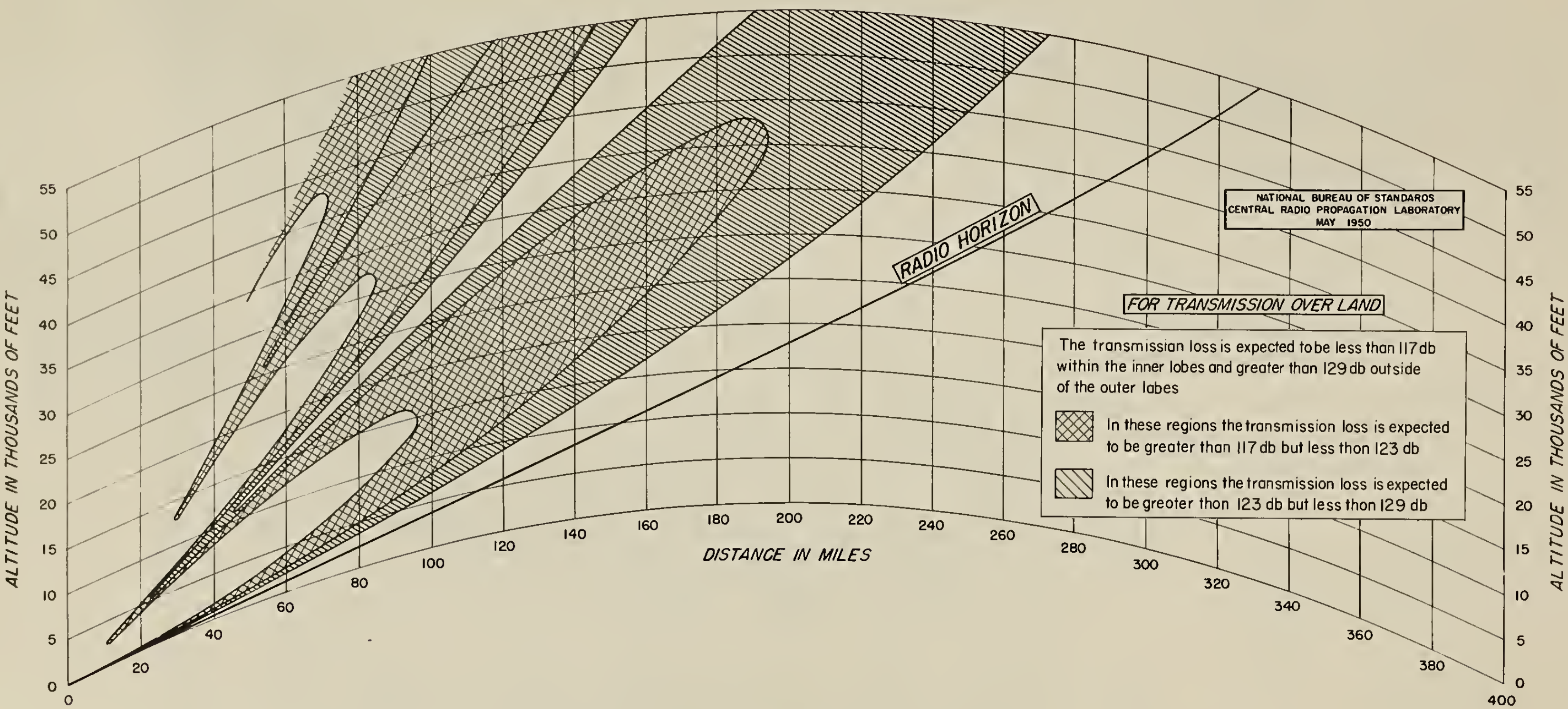

Figure 3

SPACE WAVE PROPAGATION BETWEEN VERTICAL HALF-WAVE DIPOLES OVER A SMOOTH SPHERICAL EARTH

GROUND TERMINAL ANTENNA HEIGHT 115 FEET; FREQUENCY 328 MC

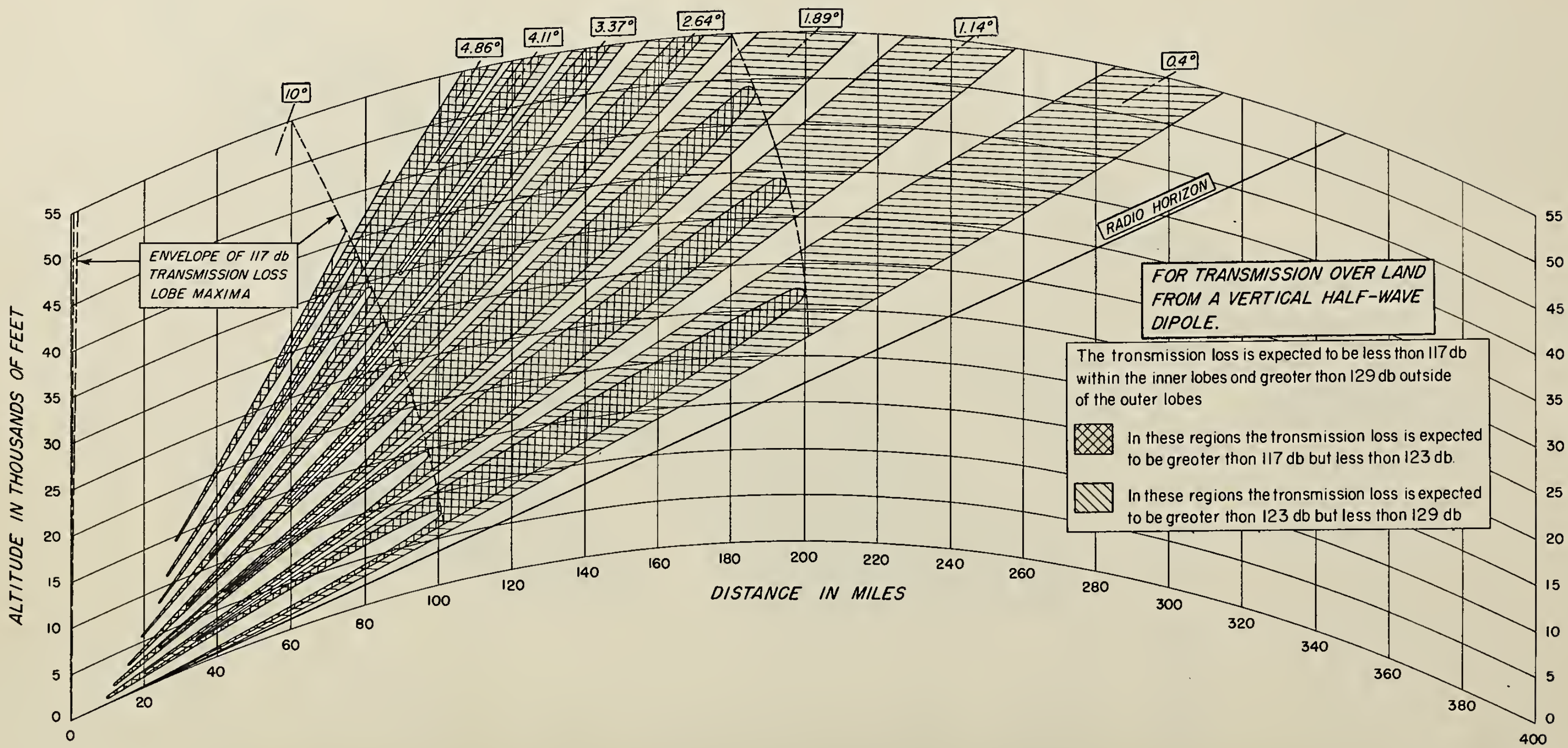

Figure 4

phase continues to increase, lobe minima and maxima occurring where the direct and ground reflected waves are out-of-phase and in-phase. Figs. 3 and 4 may be used to show approximately what happens at some other radio frequency, f_{Mc}, and ground antenna height, h, if we modify the transmission losses indicated on these figures by adding 20 log $(f_{Mc}/328)$ and, at the same time, determine h for Fig. 3 by $(h/35) = (328/f_{Mc})$ and for Fig. 4 by $(h/115) = (328/f_{Mc})$.

Figs. 3 and 4 correspond to smooth earth conditions, i. e., for $R << 0.1$. In this case the space wave field strength may be represented approximately by:

$$F = 2 F_o \sin(2\pi h \sin \psi/\lambda) \qquad (8)$$

For example, the above equation represents very accurately the expected field strength for propagation from a horizontal dipole over a smooth, flat, perfectly conducting surface, where F_o is the field strength in free space, F is the expected field strength at a receiving point corresponding to a grazing angle ψ, and h is the height of the ground terminal antenna above the smooth surface. The maximum of the first lobe ($F = 2F_o$) occurs when $(2\pi h \sin \psi/\lambda) = \pi/2$; according to Rayleigh's criterion $(4\pi \sigma_h \sin \psi/\lambda)$ must be less than 0.1 for the surface to appear smooth to the radio waves. Combining these two results we find that σ_h must be less than $h/10\pi$, independent of the frequency, if we are to expect (8) to apply at the angle ψ corresponding to the maximum of the first lobe. At still higher angles the requirements for smoothness of the terrain are correspondingly more stringent. At lower grazing angles, however, the terrain may be correspondingly rougher; for example, at the angle below the first lobe maximum where $F = 0.2 F_o$ corresponding to a transmission loss 20 db greater than at the maximum of the lobe, σ_h must be less than 0.5h for the earth to be considered sufficiently smooth for (8) to apply and where $F = 0.02 F_o$ corresponding to a transmission loss 40 db greater than at the lobe maxima, σ_h may be as large as 5h. Thus we see that the large reductions in the received field below the maximum of the first lobe as shown on Figs. 3 and 4 and indicated by (8) are expected to occur even over comparatively rough terrain.

For propagation conditions such that R is large, i. e., high frequencies, very rough terrain, or large grazing angles, the ground reflected wave may be described statistically. It has been found* that the Rayleigh distribution is appropriate for this purpose when R is very large, say $R > 100$, and that a combination of a constant specular component plus a random Rayleigh component is required for $0.01 < R < 100$. Fig. 5 shows theoretical probability distributions for this case with the parameter K increasing from $(-\infty)$ for $R < 0.01$ to values of K greater than 20 for $R > 100$. Here K is the level in decibels of the mean power in the random, Rayleigh distributed, component relative to that of the steady component. As an example of the use of probability distributions of this kind for describing space wave propagation conditions, suppose we have an air-to-air communication system operating at 328 Mc. As we fly over irregular terrain at a fixed high altitude away from another aircraft at the same altitude (See Fig. 6), the grazing angle ψ decreases from a comparatively large value to zero on the radio horizon, and this corresponds to a decrease of R from a very large value to zero on the radio horizon. Thus at short distances the ground-reflected wave will fluctuate in magnitude over a range indicated by the $K = 20$ curve on Fig. 5, while at larger ranges these fluctuations will occur over smaller and smaller ranges corresponding to the smaller values of K.

The above statistical description of space wave propagation over rough terrain is appropriate for propagation paths with Fresnel-zone clearance. For still smaller antenna heights involving propagation very near to or just below grazing incidence, the received space wave is log normally distributed.† For example, a study** of the fields received on over-land paths from television stations in the frequency range from 50 to 220 Mc and on receiving antennas with heights in the range from 12 to 30 feet indicates that the standard deviation of the received fields is of the order of 6 to 10 db about mean values of the order of magnitude expected for propagation over a smooth surface.

Finally, when the transmitting and receiving antennas are both actually on the surface, the received ground wave is a surface wave. Furthermore, when the transmitting and receiving antennas

---

* See references 4, 6 and 18.

† See references 2 and 19.

** See reference 19.

DISTRIBUTION OF THE RESULTANT AMPLITUDE
OF A CONSTANT VECTOR PLUS A RAYLEIGH DISTRIBUTED VECTOR

Power in Random Component is K Decibels
Relative to Power in Constant Component

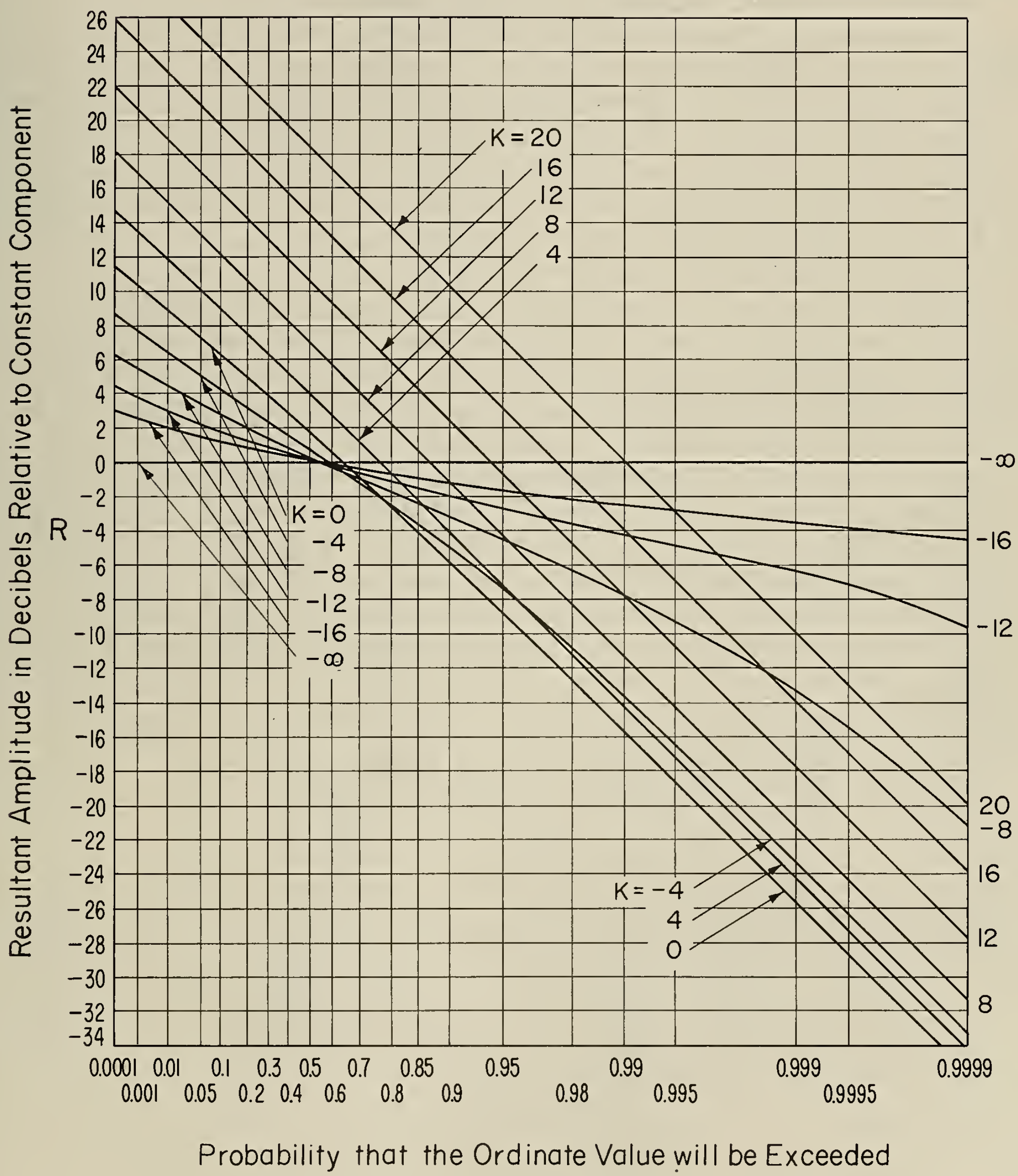

Figure 5

TRANSMISSION LOSS EXPECTED BETWEEN VERTICAL HALF WAVE DIPOLES IN AIR-TO-AIR PROPAGATION ON 328 MC BETWEEN TWO AIRCRAFT FLYING OVER IRREGULAR TERRAIN AT THE SAME ALTITUDE

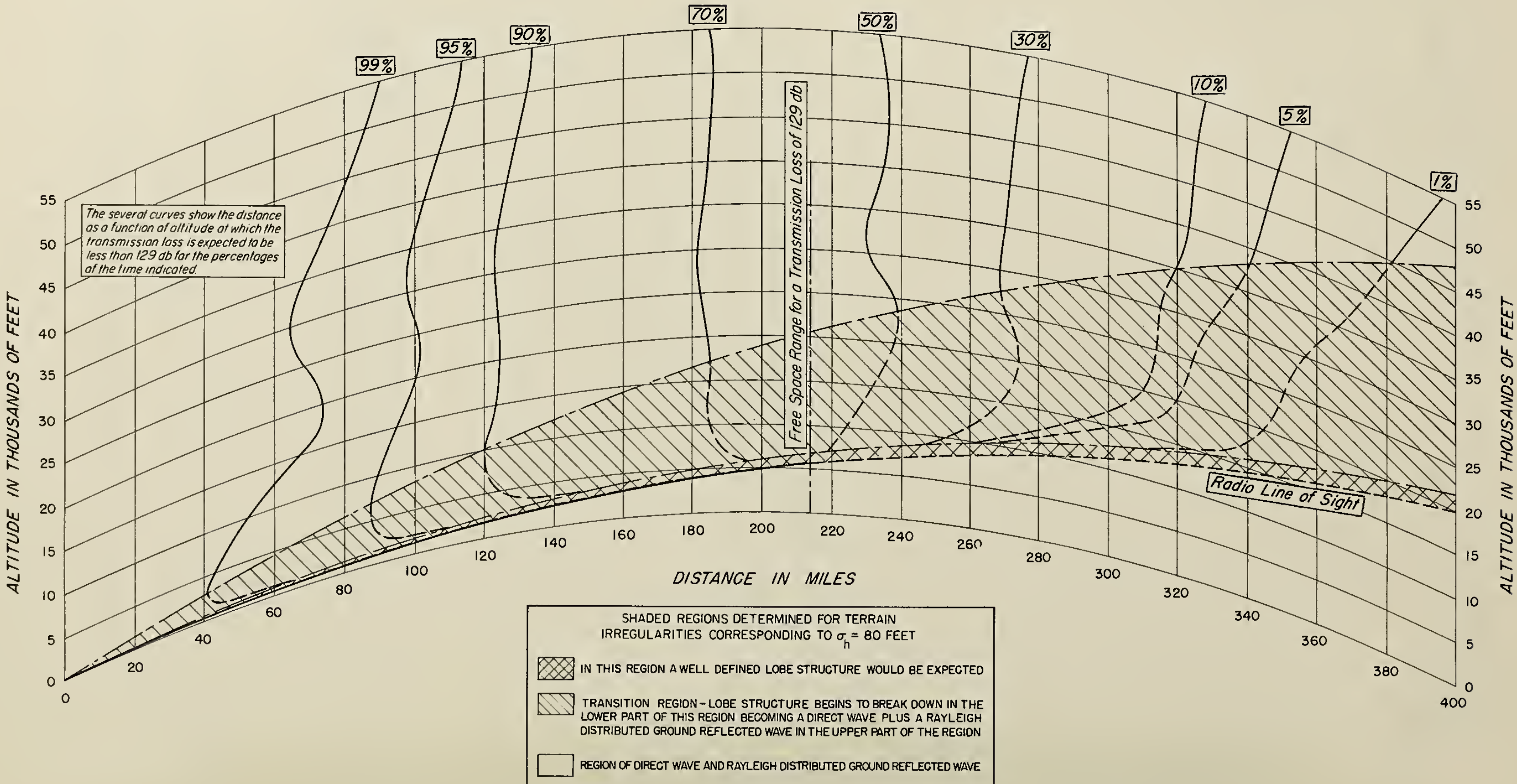

FIGURE 6

are both only a small fraction of a wavelength above the surface, the received ground wave is still primarily a surface wave together with a small space-wave component. The transmission loss in surface wave propagation* is very much influenced by the electrical constants of the ground, especially its conductivity. Although efforts have been made to correlate these ground constants with soil types so that predictions of the effective ground conductivity could be made, such studies have not been very successful so far. However, a publication of the National Bureau of Standards is available† which gives the measured values of effective ground conductivity for various propagation paths in the United States. For propagation over average land one may use an effective ground conductivity of 5 milli-mhos per meter and an effective dielectric constant of 15 although individual over land paths may have substantially different ground constants, while over the sea the effective ground conductivity is of the order of 5 mhos per meter with an effective dielectric constant of 80.

Figs. 7, 8, 9, and 10 show the basic transmission loss expected for ground wave propagation over a smooth spherical earth with the transmitting and receiving antennas both at a height of 30 feet, for either vertical or horizontal polarization and with ground constants typical of over land and over sea water paths. At frequencies less than 10 Mc, the antenna heights are less than a wavelength and the ground waves shown for vertical polarization are primarily surface waves, whereas for frequencies greater than 100 Mc the ground waves with these antenna heights are primarily space waves with only a small surface wave component. Note that the proximity of the earth at low frequencies doubles the received fields for vertically polarized waves, but suppresses the propagation of horizontally polarized waves: i. e., horizontally polarized surface waves are highly attenuated. However, at the higher frequencies involving primarily space wave propagation, the expected transmission loss becomes independent of the polarization used.

On frequencies above 10,000 Mc the radio waves are appreciably absorbed by the oxygen and water vapor in the atmosphere. Fig. 11 shows the total gaseous atmospheric absorption near the surface at Washington, D. C. The absorption shown on Fig. 11 is the median value; for small percentages of the time the absorption will be considerably greater as a result of absorption

---

* See references 9, 10, 11, and 12.

† See reference 20.

BASIC TRANSMISSION LOSS EXPECTED FOR GROUND WAVES PROPAGATED OVER A SMOOTH SPHERICAL EARTH

OVER LAND: $\sigma = 0.005$ MHOS/METER, $\epsilon = 15$

POLARIZATION: VERTICAL

TRANSMITTING AND RECEIVING ANTENNAS BOTH 30 FEET ABOVE THE SURFACE

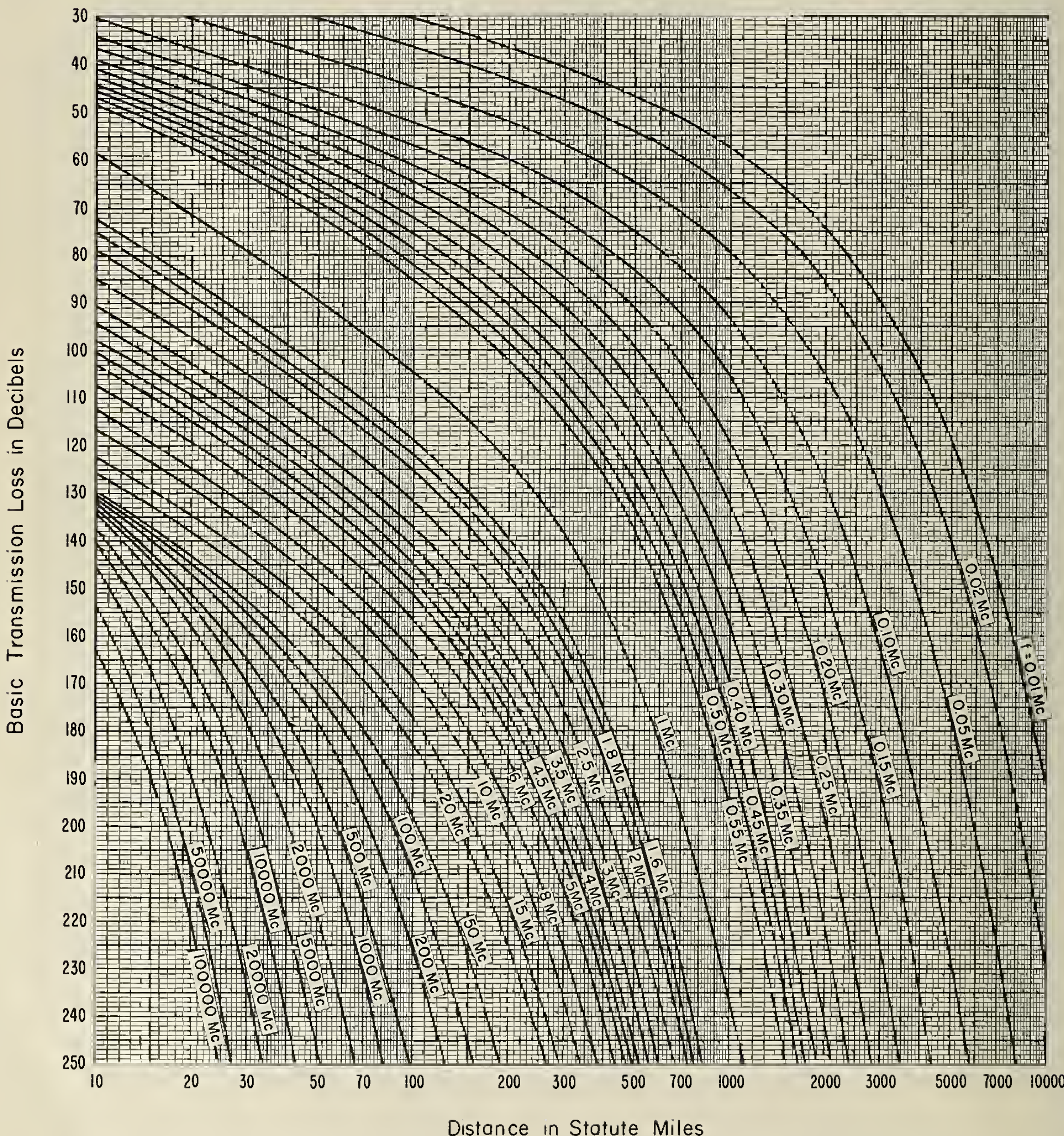

Figure 7

BASIC TRANSMISSION LOSS EXPECTED FOR GROUND WAVES
PROPAGATED OVER A SMOOTH SPHERICAL EARTH

OVER SEAWATER: σ = 5 MHOS/METER, ϵ = 80

POLARIZATION: VERTICAL

TRANSMITTING AND RECEIVING ANTENNAS BOTH 30 FEET ABOVE THE SURFACE

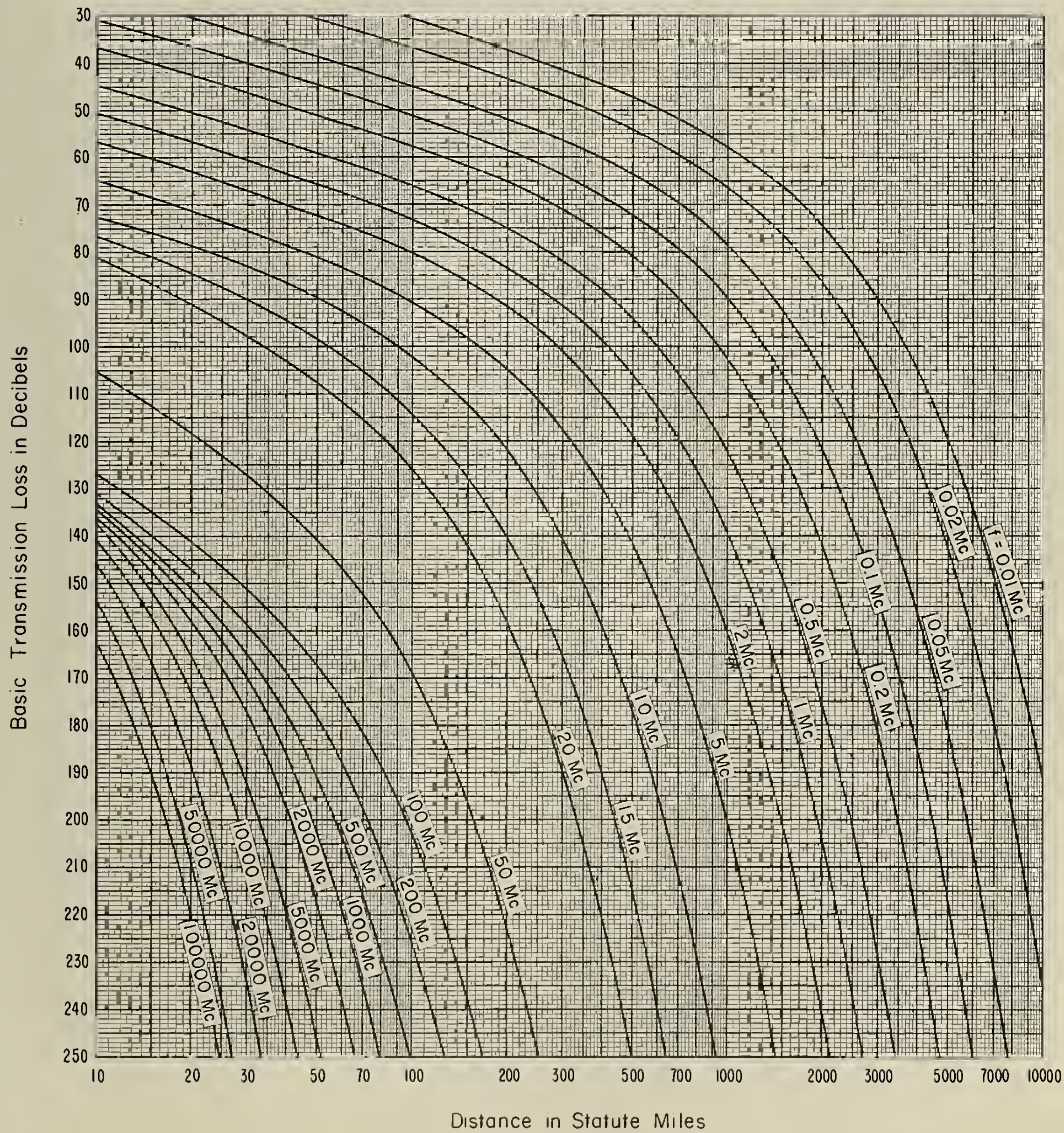

Figure 8

BASIC TRANSMISSION LOSS EXPECTED FOR GROUND WAVES PROPAGATED OVER A SMOOTH SPHERICAL EARTH

OVER LAND: $\sigma = 0.005$ MHOS/METER, $\epsilon = 15$

POLARIZATION: HORIZONTAL

TRANSMITTING AND RECEIVING ANTENNAS BOTH 30 FEET ABOVE THE SURFACE

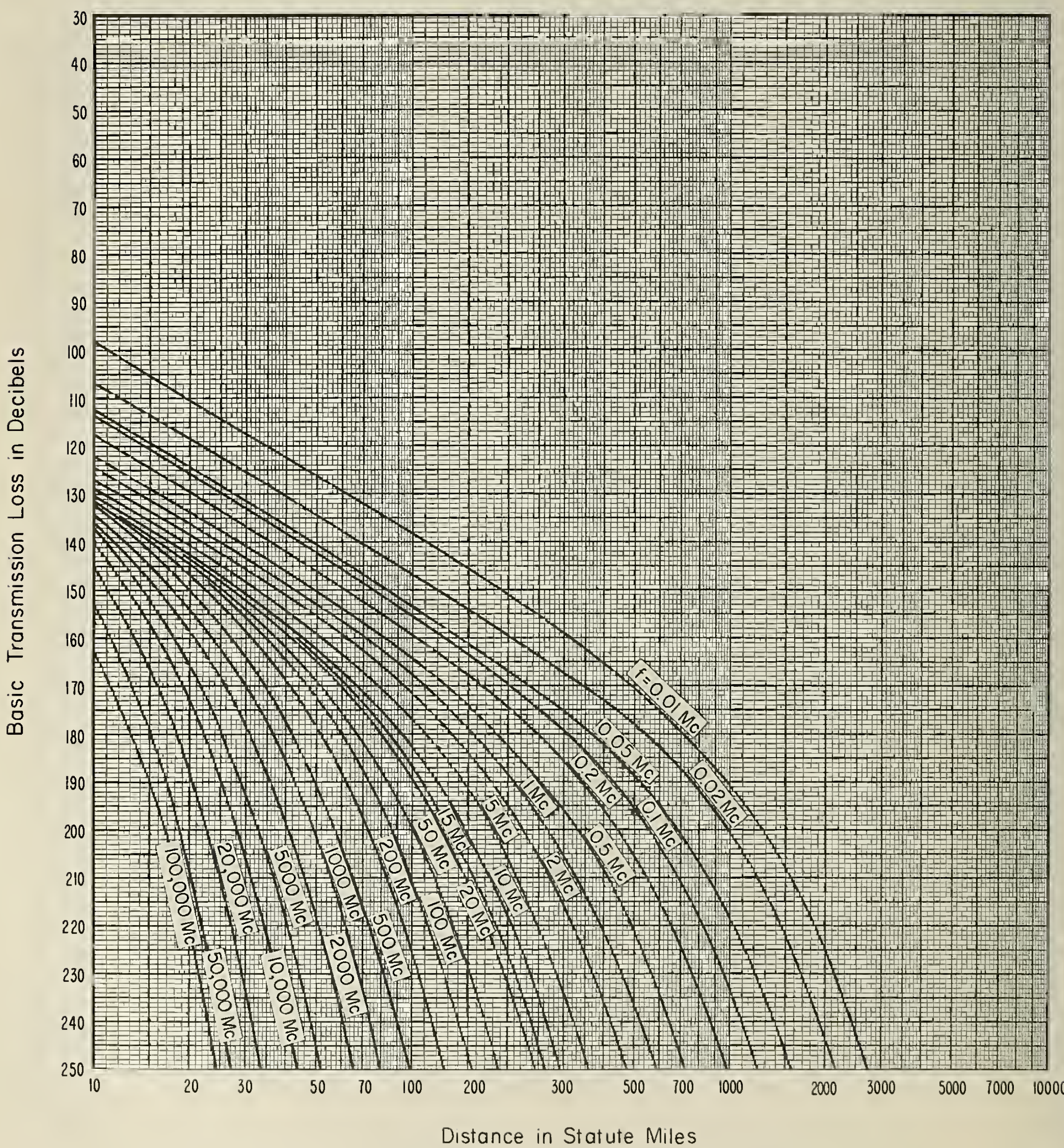

Figure 9

BASIC TRANSMISSION LOSS EXPECTED FOR GROUND WAVES PROPAGATED OVER A SMOOTH SPHERICAL EARTH

OVER SEAWATER: σ = 5 MHOS/METER, ϵ = 80

POLARIZATION: HORIZONTAL

TRANSMITTING AND RECEIVING ANTENNAS BOTH 30 FEET ABOVE THE SURFACE

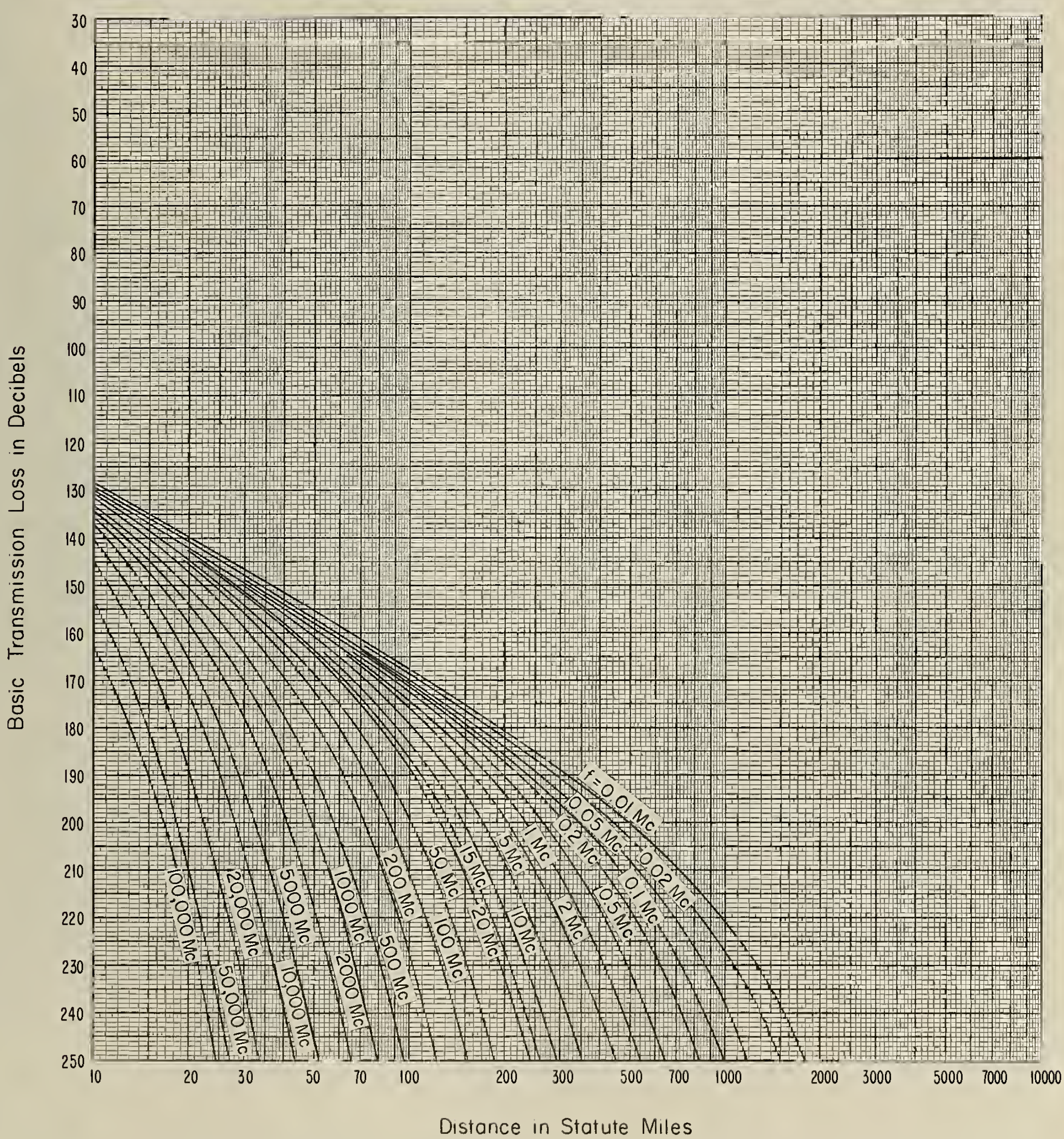

Figure 10

AVERAGE GASEOUS ATMOSPHERIC ABSORPTION
NEAR THE GROUND AT WASHINGTON, D.C.
Meteorological Data From the Ratner Report
July 11, 1957

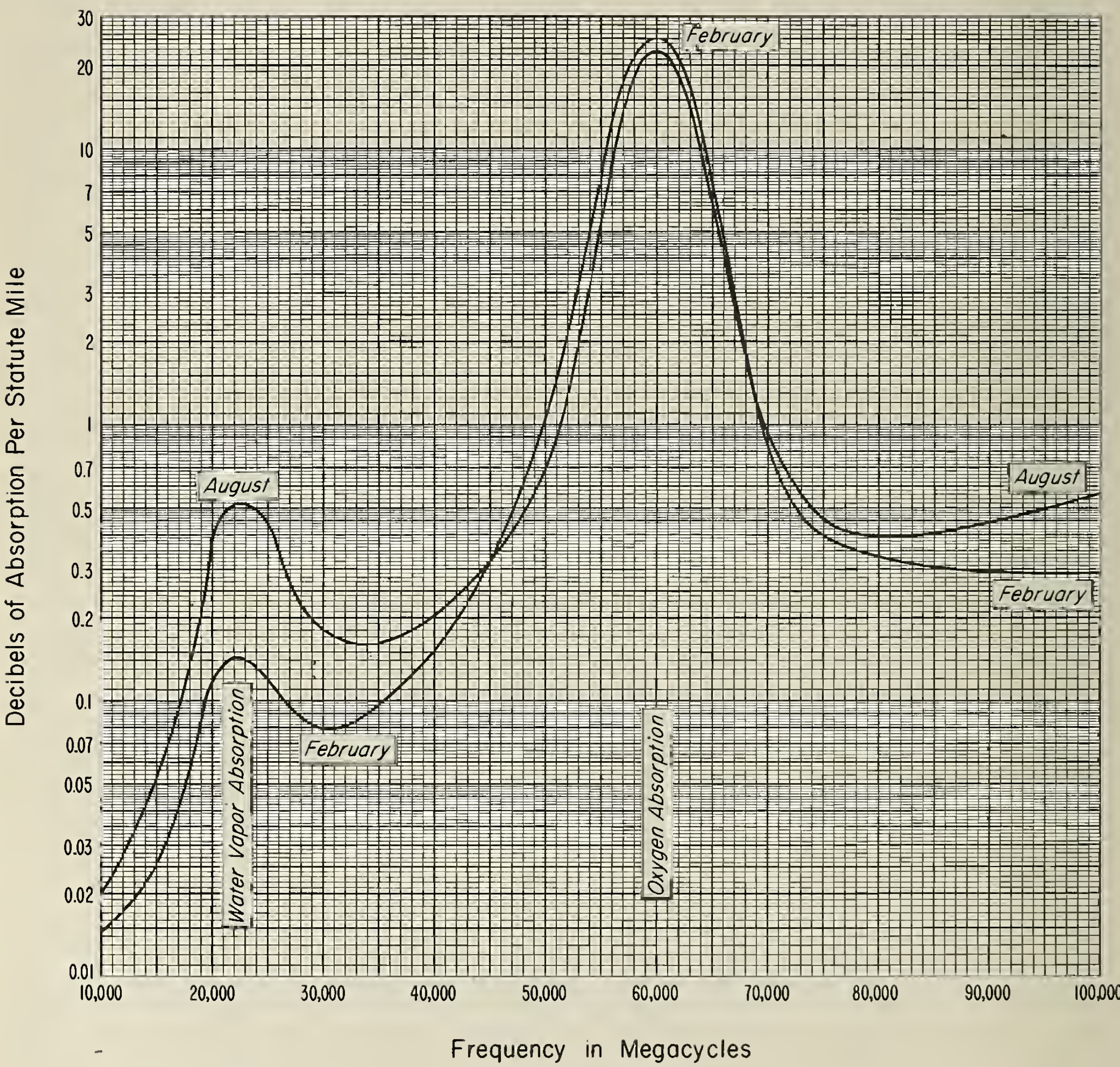

Figure II

by rain.* The transmission losses shown on Figs. 7, 8, 9, and 10 for frequencies above 10,000 Mc were estimated by using the August absorption shown on Fig. 11.

The heights of the antennas are very important in ground wave propagation at the higher frequencies. This is illustrated on Fig. 12 which shows for a frequency of 50 Mc the great reduction in transmission loss expected when the antenna height at one terminal is increased from zero up to 10,000 feet while the other antenna height is increased from zero up to 30 feet.

4. Transmission Loss for Ionospheric Propagation

Radio waves with frequencies less than the maximum usable frequency for a given transmission path are reflected by the ionized regions of the upper atmosphere with sufficient intensity so that they often provide a mode of transmission with less loss than that involved in ground wave propagation. The maximum frequency usable on a given ionospheric transmission path depends upon the length of the path, its geographical location, the time of day, the season of the year, and the phase of the sunspot cycle. Predictions of these maximum usable frequencies are published regularly three months in advance by the Central Radio Propagation Laboratory.† Fig. 13 is an example of these predictions showing how the maximum usable frequencies vary with local time and with geographical location for a path 4,000 kilometers long. This particular chart is for February, 1957, a period near sunspot maximum as may be seen on Fig. 14 which shows the smoothed Zurich sunspot numbers from 1750 to 1957. The sunspot numbers shown on Fig. 14 are averaged over a period of 13 months, but the author has shown in unpublished work that the sunspot numbers obtained by averaging over a period of three months are just as well correlated with ionospheric propagation conditions and thus provide a more useful index for prediction purposes. Fig. 15 shows a typical correlation between the observed maximum usable frequencies and these three-months-smoothed sunspot numbers.

---

* See references 21, 22 and 23.

† See references 24 and 25.

BASIC TRANSMISSION LOSS EXPECTED IN PROPAGATION OVER A SMOOTH SPHERICAL EARTH AT 50 MEGACYCLES

HORIZONTAL POLARIZATION; σ =0.005 MHOS/METER; ϵ = 15 FOR THE TERMINAL ANTENNA HEIGHTS INDICATED

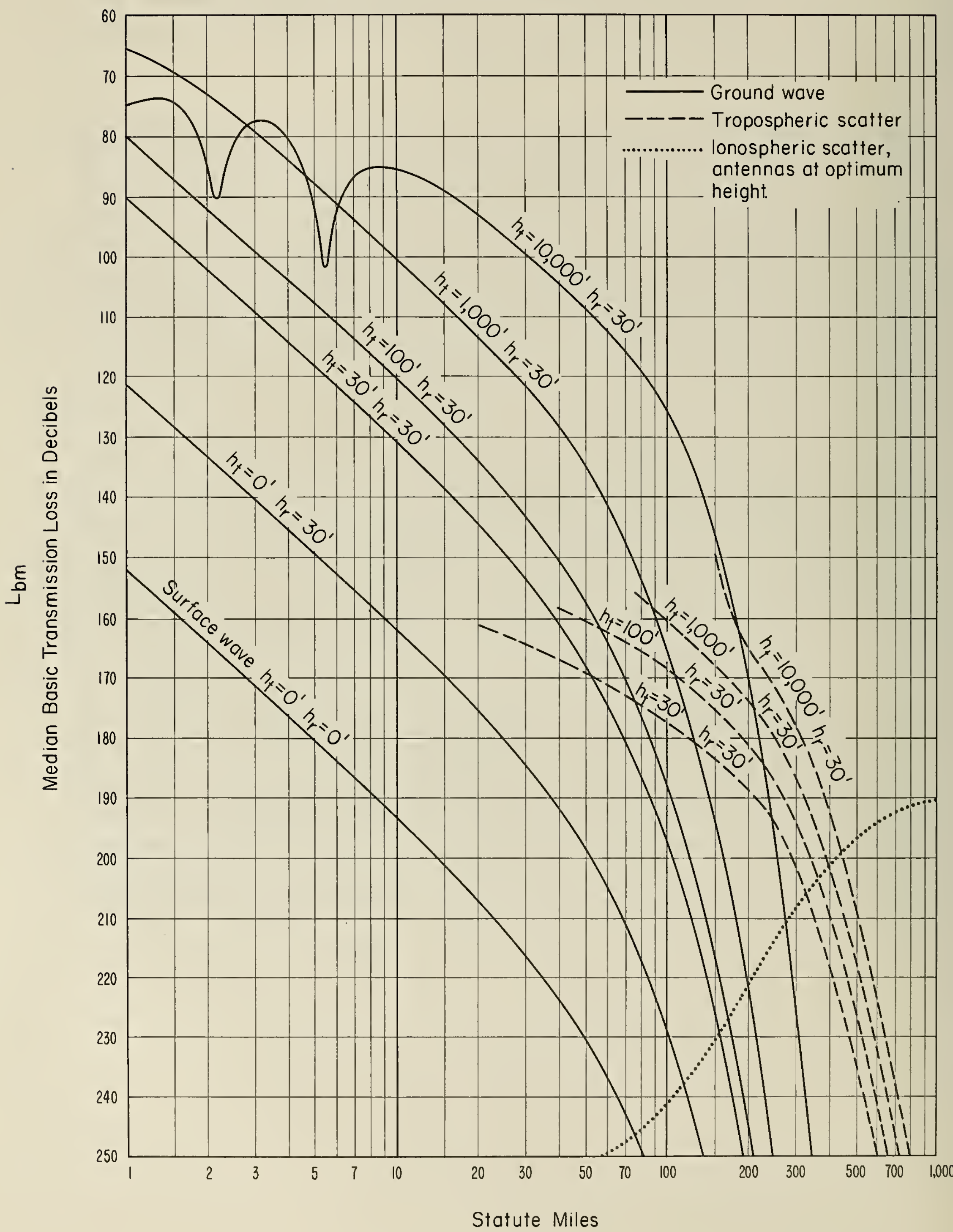

Figure 12

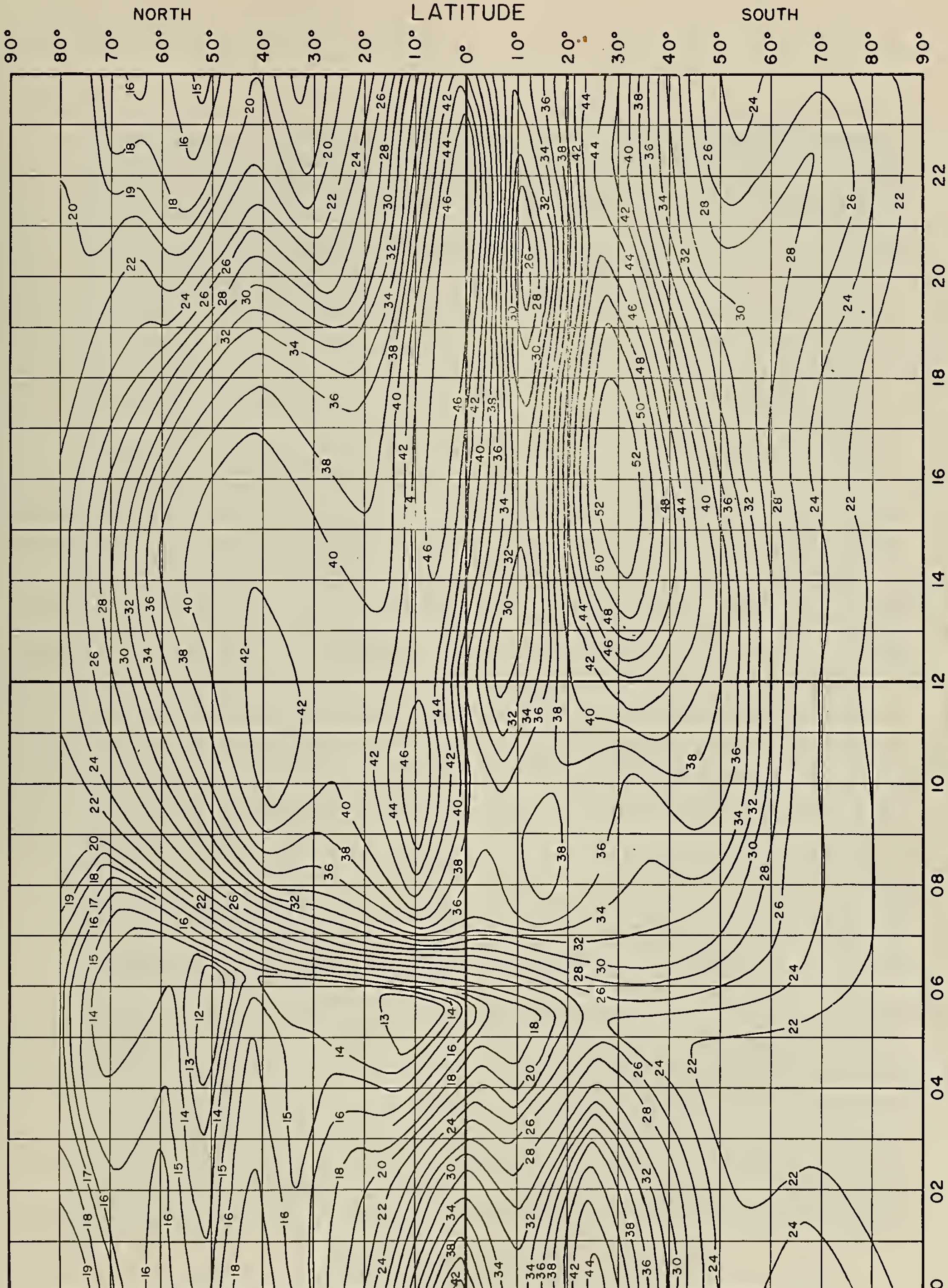

FIG.13 MEDIAN F2-4000-MUF, IN Mc, W ZONE, PREDICTED FOR FEBRUARY 1957

SECULAR VARIATIONS EXHIBITED BY PAST SUNSPOT CYCLES

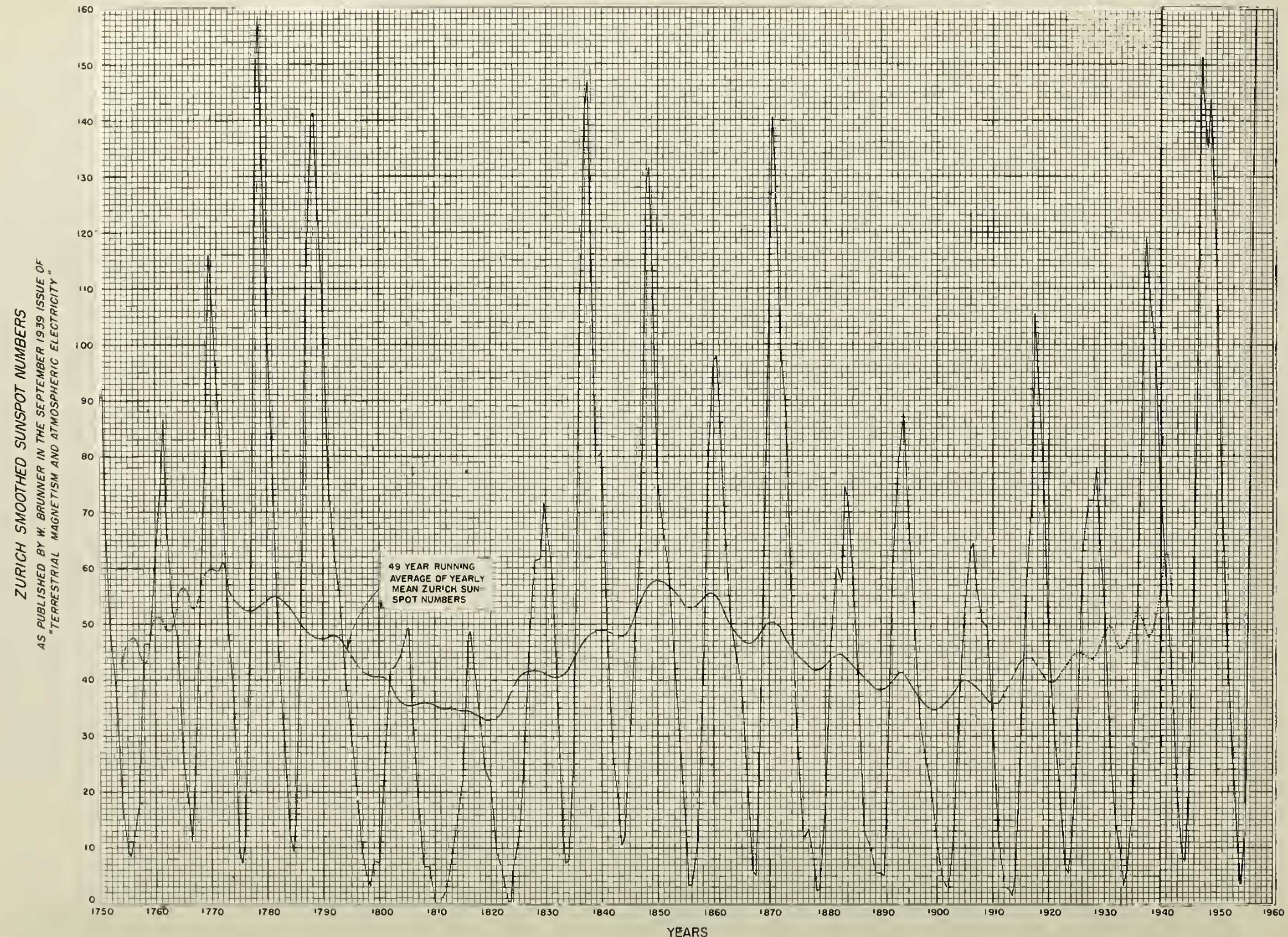

Figure 14

CORRELATION OF THE MONTHLY MEDIAN WASHINGTON 2 P.M. MAXIMUM USABLE FREQUENCIES FOR FEBRUARY WITH THE THREE-MONTHS-SMOOTHED ZURICH SUNSPOT NUMBERS

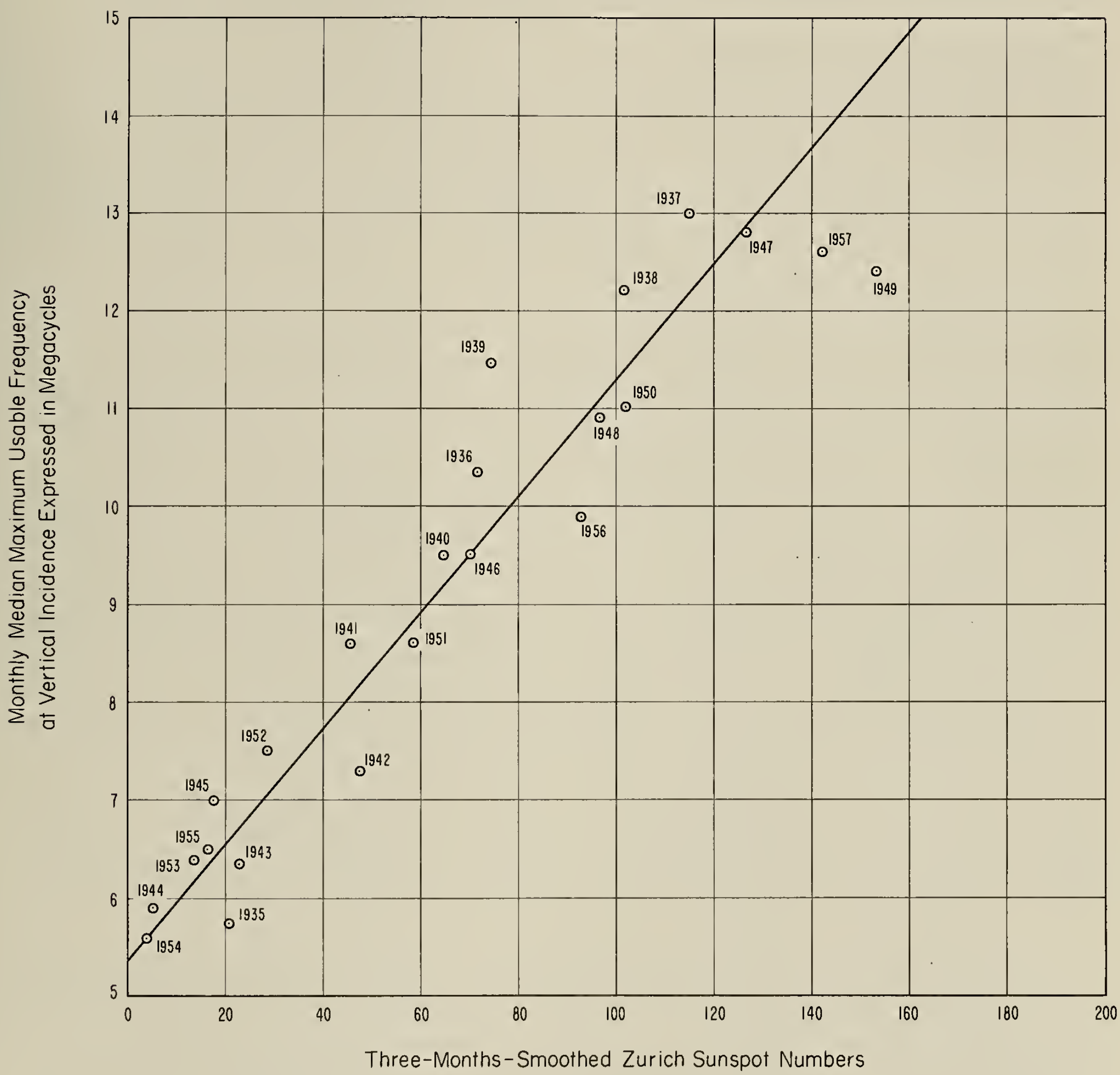

Figure 15

4.1 Very Low Frequency Ionospheric Propagation

At the very low frequencies below 30 kc, the ionosphere reflects the waves at relatively low heights, about 70 km in the daytime and 90 km at night. At these low heights the ionization gradients are sufficiently large so that the ionosphere behaves as a sharp boundary, and it is convenient to use wave guide theory for determining the phase and amplitude of the received waves; good discussions of this theory are presented in the June, 1957 issue of the Proceedings of the Institute of Radio Engineers. Figures 16, 17, 18, and 19 give examples for this frequency range of the transmission loss expected in propagation between vertical electric dipoles over land and over sea and for day and night conditions. The values shown on these four figures were computed by the methods described by Wait; [26] [27] the minima and maxima shown are caused by interference between the ground wave and ionospheric wave modes at distances less than about 1,000 miles, and are caused by interference between the several ionospheric modes at the larger distances. At these long wavelengths the fading of the received waves is caused by a gradual shift from midday to midnight conditions and consequently has a very long period; thus at certain distances the received field may remain weak throughout the day or the night. The comparison between the calculated and observed locations and magnitudes of such anomalies provides a useful means for determining the effective constants of the ionosphere. The dimensionless constant L/H provides a measure of the effective conductivity of the ionospheric boundary, and the values of this constant assumed in these examples were determined by a comparison with observations of transmission loss. It is expected that L/H will also vary somewhat with the geomagnetic latitude of the receiving point, but such variations are not expected to have a large influence on the transmission loss.

It should be noted on Figs. 16 - 19 that values are shown for the transmission loss expected at distances beyond the antipode of the transmitter (about 12,500 miles), and at these larger distances a stronger signal would be expected from the shorter great circle path corresponding to transmission in the opposite direction; when short pulses are transmitted, these signals traveling in opposite directions [28] will interfere with each other, and the results given on these figures should be useful in determining the magnitude of this multipath problem.

TRANSMISSION LOSS EXPECTED BETWEEN SHORT VERTICAL ELECTRIC DIPOLE ANTENNAS

Day Over Land $\sigma = 0.00477$ Mhos/Meter; Ionospheric Constant L/H=0.1; h=70 km

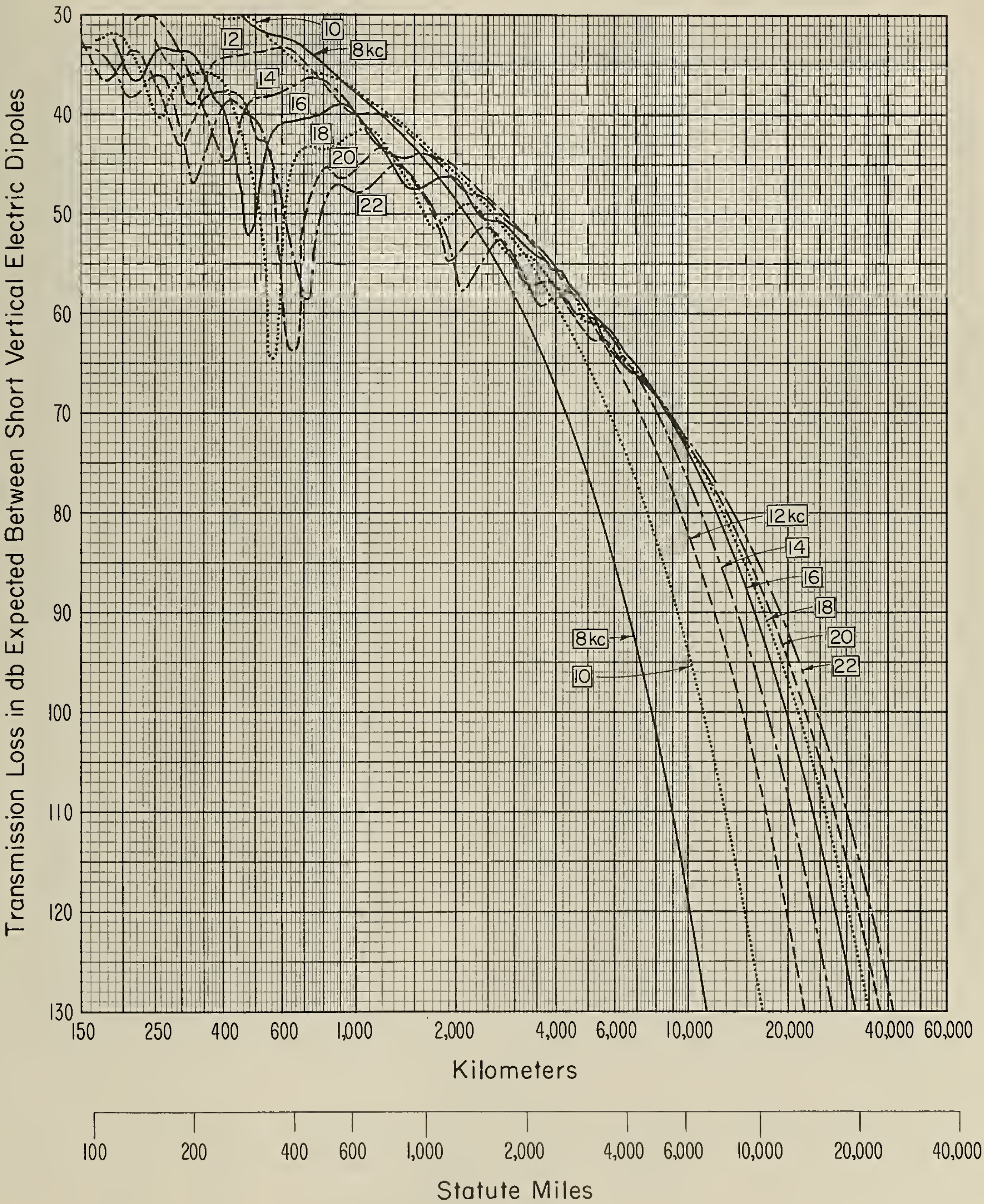

Figure 16

TRANSMISSION LOSS EXPECTED BETWEEN SHORT VERTICAL ELECTRIC DIPOLE ANTENNAS

Day Over Sea $\sigma = \infty$

Ionospheric Constant L/H = 0.1; h = 70 km

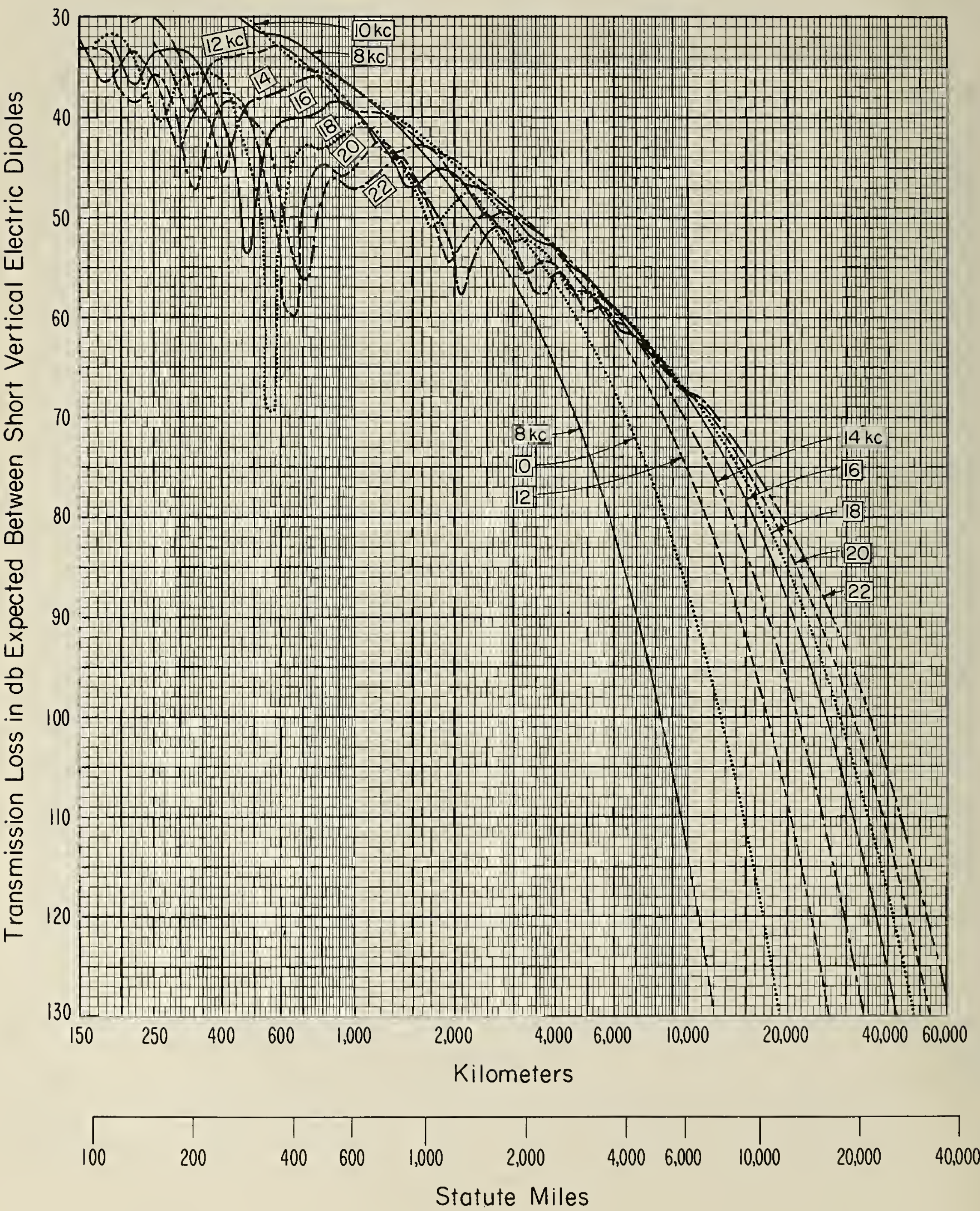

Figure 17

TRANSMISSION LOSS EXPECTED BETWEEN SHORT VERTICAL ELECTRIC DIPOLE ANTENNAS

Night Over Land $\sigma = 0.00371$ Mhos/Meter
Ionospheric Constant $L/H = 0.05$; $h = 90$ km

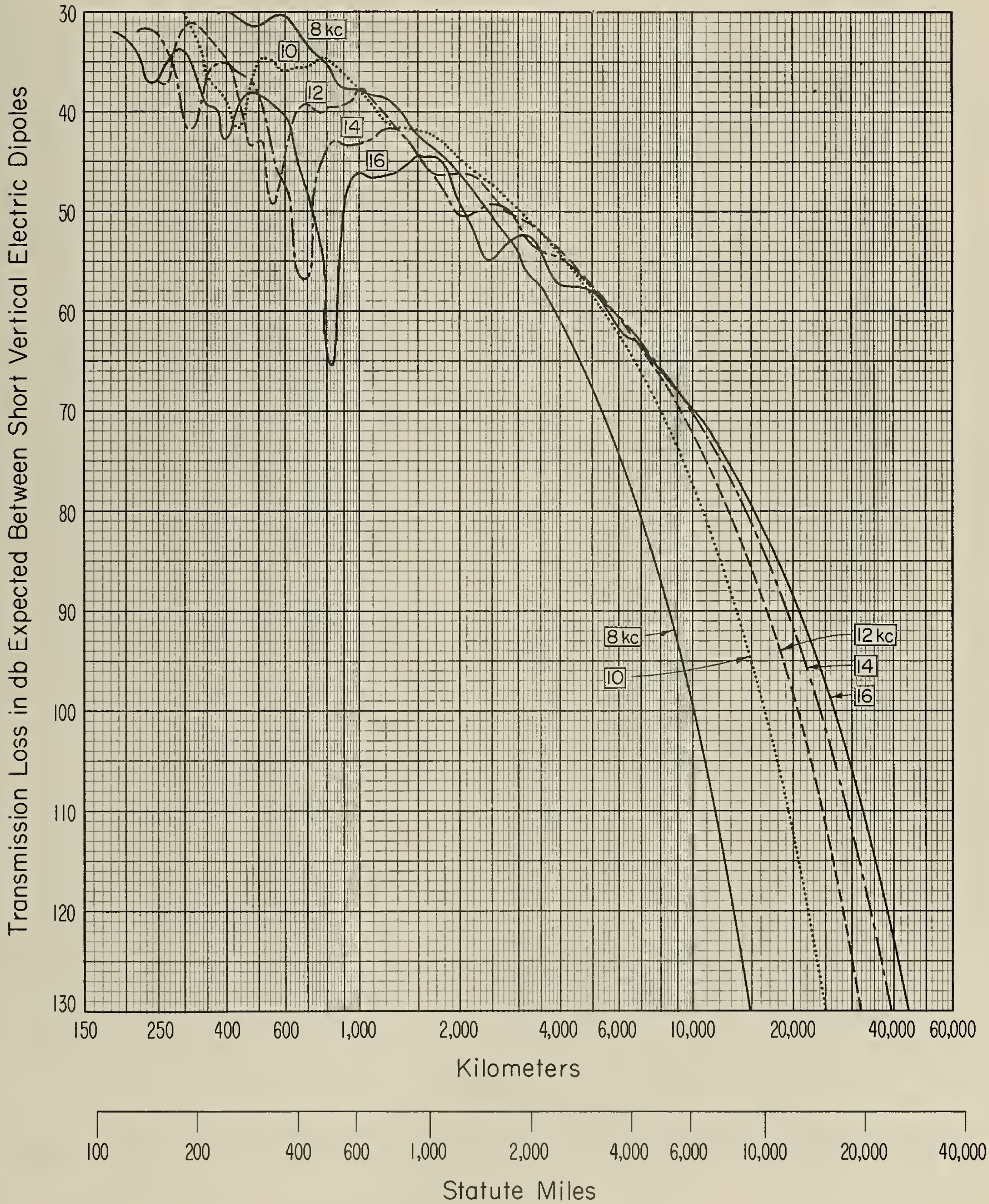

Figure 18

TRANSMISSION LOSS EXPECTED BETWEEN SHORT VERTICAL ELECTRIC DIPOLE ANTENNAS

Night Over Sea $\sigma = \infty$
Ionospheric Constant $L/H = 0.05$; $h = 90$ km

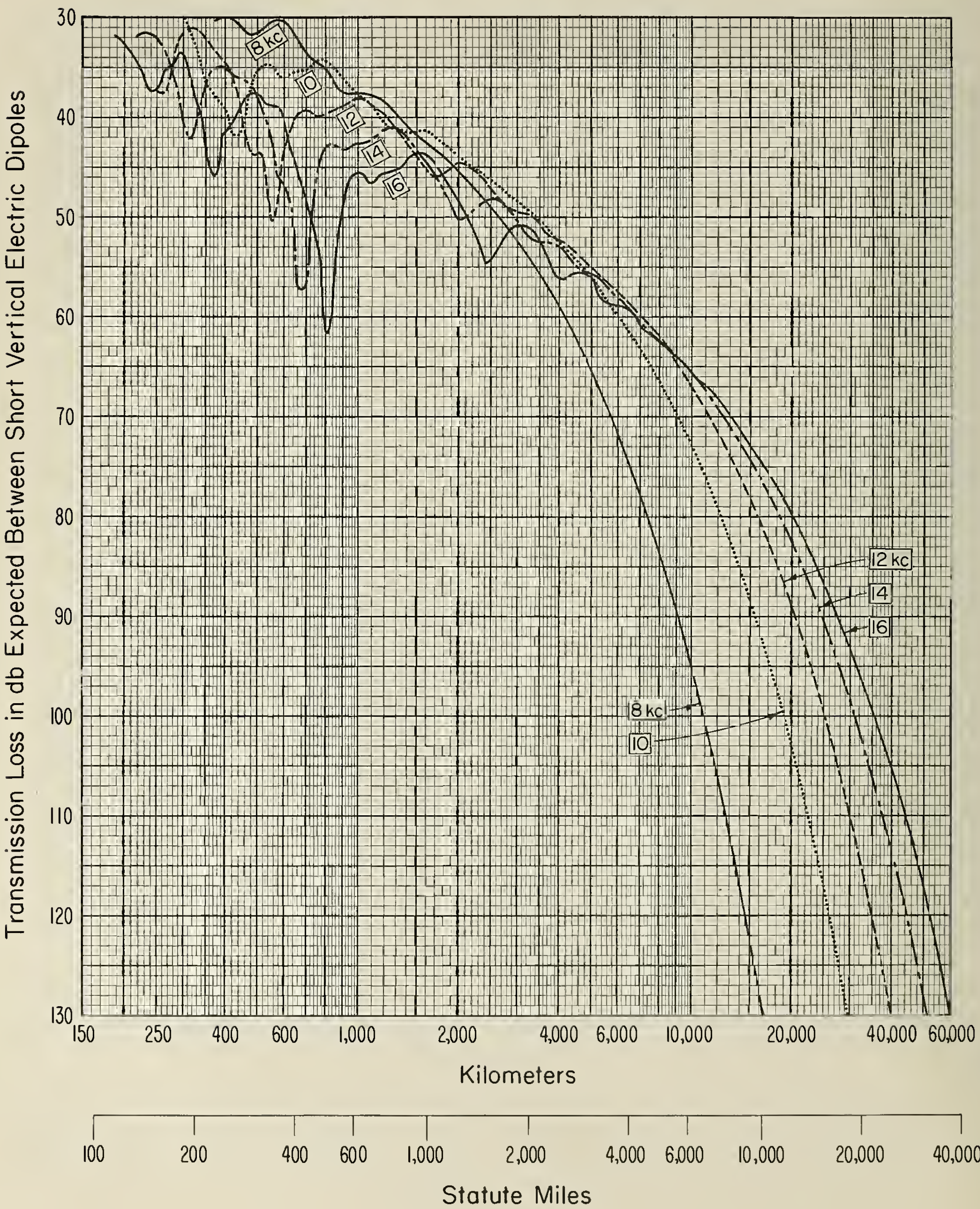

Figure 19

We will see in a later section how convergence at the curved surface of the ionosphere is expected to affect the transmission loss; in calculating the losses shown on Figs. 16-19, allowance was made only for the convergence expected in the vertical plane and on the assumption that the ionosphere is smooth. Allowance for convergence in the horizontal plane leads to large additional reductions in the transmission loss expected near the antipode—12,441 miles—and near 24,881 miles and 37,322 miles. For a smooth, spherical ionosphere, we should subtract the horizontal plane convergence $C_h = 10 \log_{10}[d(\text{miles})/3960 \sin\{d(\text{miles})/3960\}]$ from the transmission losses shown; at distances, ρ, from the antipodal points less than 100 miles but greater than 0.1λ, we may write $C_h = 40.948 - 10 \log_{10} \rho(\text{miles})$; the value right at the antipodal points is given by $C_h = 34.210 + 10 \log_{10} f_{kc}$, but this latter includes both long and short great circle path energy.

The available experimental data indicate that the parameters of the ionosphere chosen for these calculations lead to about the right conclusions over the range of frequencies from 10 to 20 kc, but at 8 kc the calculated losses are somewhat greater than those observed.

Finally, it should be noted that mixtures of day and night and land and sea conditions are to be expected over these long paths, and suitable methods of calculation have yet to be developed for such mixed paths. It will likely be possible, however, to develop empirical methods for combining the results given here to obtain good estimates of the transmission loss expected on such mixed paths in much the same manner as has been used for estimating the transmission loss expected in ground wave propagation over mixed paths. [29] [30]

4.2 Low and Medium Frequency Ionospheric Propagation

As we increase the radio frequency well above 30 kc, the ionosphere behaves much less as a sharp boundary and instead gradually refracts the waves back to the receiving point only after they have penetrated many kilometers into it, this penetration being greater the higher the radio frequency. The available evidence appears to indicate that the D and E regions of the ionosphere, which extend from 70 to 110 km, are turbulent, consisting of "blobs" of ionization which drift with the mean wind with velocities often in excess of 100 miles per hour. An interesting discussion of these irregular ionospheric motions is given in a recent article by Gautier. [31] The radio waves will travel along many different paths through this turbulent ionized medium, the received field being the resultant vector sum of the waves received after propagation along these different paths. At sufficiently high frequencies, the relative phases of these waves will be random, and the resultant received field will have a Rayleigh distributed amplitude as shown on Fig. 5; on this figure K represents the ratio in decibels between the field intensity of the random ionospheric waves and a steady ground wave or, in the case of a single ionospheric mode, K represents the ratio in decibels between the field intensity of the random ionospheric waves and the steady, specularly-reflected component. Thus it becomes convenient, particularly for frequencies above 30 kc, to determine the transmission loss separately for the ionospheric and ground wave modes of propagation. Figs. 20 and 21 show the transmission loss expected at 100 kc between short vertical electric dipole antennas for the ground wave and several ionospheric wave modes of propagation over land and over the sea, and for day and night conditions. The method of calculation used in determining the results shown on Figs. 20 and 21 involves a combination of ray and wave theory. Fig. 22 illustrates the geometry of our model and some of the assumptions made in the calculations. The waves are refracted in the troposphere down towards the earth and, as a consequence, the distance, d_1, traveled for a given ray angle of elevation, ψ, before the waves arrive back at the earth is substantially larger than if there were no atmosphere.

We have idealized our problem by assuming for all points along the path that the ionosphere has the same height, h, and the same reflection coefficient, while the ground is assumed to have the same electrical constants even for propagation all the way to the antipode at a distance of about 12,500 miles. The actual ionosphere and ground reflection conditions over particular propagation paths are obviously much different from these idealized paths, but our present model seems better for expository purposes. The principle of stationary phase (essentially the same as Fermat's principle) leads to the conclusion that the received waves may be considered to travel along several discrete ray paths between the transmitter and the receiver. All of these paths are great circle paths, the shortest corresponding to the ground wave mode of propagation. The other paths involve m reflections at the ionosphere, and the waves propagated along these other paths arrive at the receiving point at successively later times. By transmitting short pulses, it is possible to observe these several modes independently at a distant receiving point, and in this way their physical reality has been verified. The term "mode of propagation" here, and in the remainder of the ionospheric propagation discussions, refers to the waves propagated along one of these ray paths, and has a distinctly different meaning from the usage in the previous section where the modes of propagation were the wave guide modes which are simply the successive terms in a mathematical expression for the field. The use of short pulses to make possible the separate reception of each of these modes is a very useful device for radio navigation and, in this connection, the estimation of the time of arrival of the successive modes becomes of great practical importance. These time delays have been studied both theoretically [32/] [33/] [34/] and experimentally [35/] [36/] [37/] [38/] and the reader is referred to the references for information of this kind; here we will be primarily interested only in their transmission losses.

MEDIAN TRANSMISSION LOSS OVER LAND AT 100 kc

$\sigma = 0.005$ Mhos/meter; $\epsilon = 15$

Day h = 70 km; Night h = 90 km

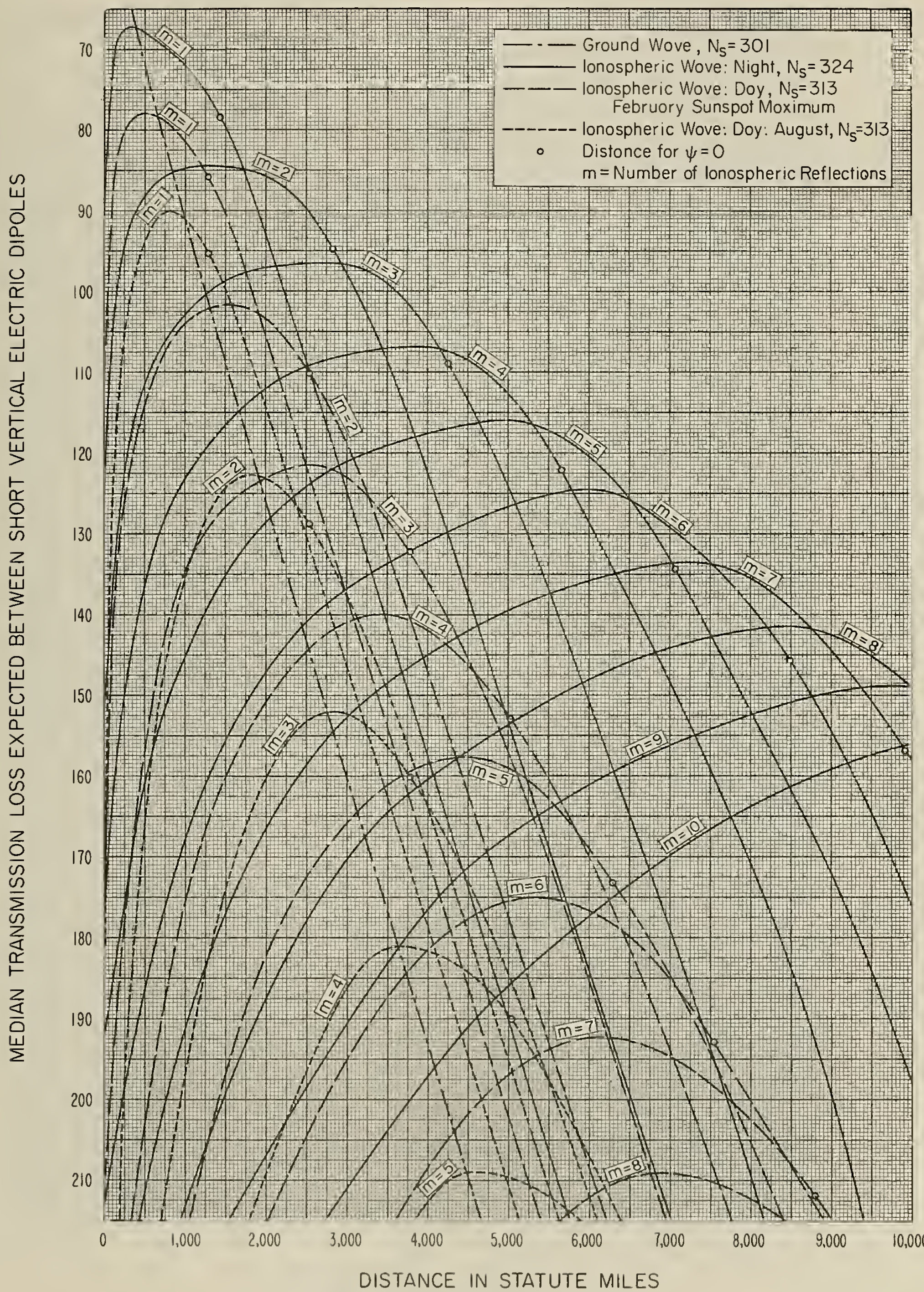

Figure 20

MEDIAN TRANSMISSION LOSS OVER SEA AT 100 kc

$\sigma = 5$ Mhos/meter; $\epsilon = 80$

Day h = 70 km; Night h = 90 km

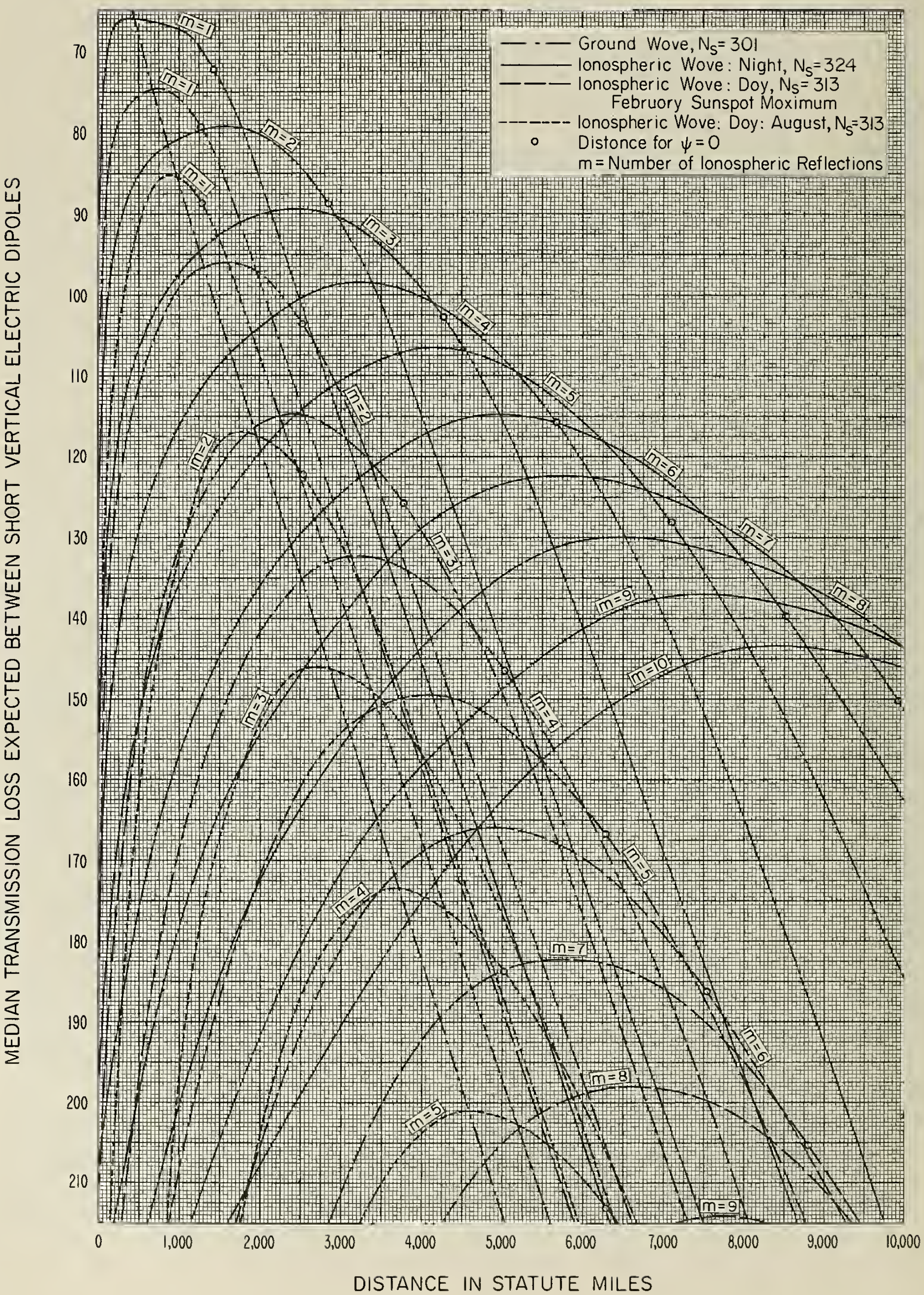

Figure 21

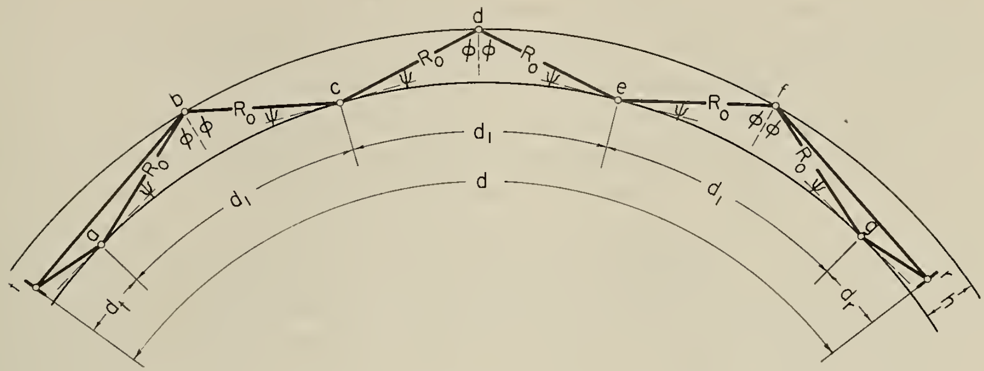

Case (a) ψ Positive and m = 3

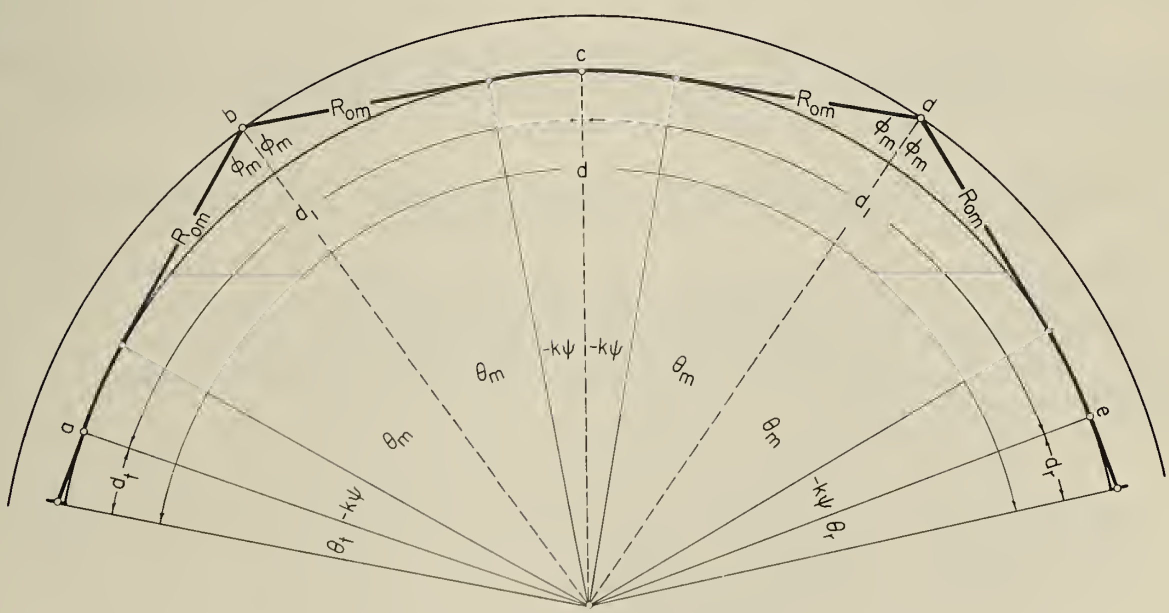

Case (b) ψ Negative and m = 2; $k = 1 - \dfrac{d\tau}{d\psi}$

Figure 22

Consider the phase of a radio wave for a given ray path, $\Omega(\psi) = 2\pi R/\lambda$, where λ is the wavelength and R is the total length of the ray path between the transmitter and the receiver. Now consider the variation of this phase for all possible adjacent paths between the transmitter and the receiver as we vary the angle of elevation, ψ, and azimuth, χ; it should be clear (a) that $\Omega(\psi)$ will be a minimum with respect to variations in χ for the set of rays lying in the great circle plane, i. e., for $\chi = 0$ and (b), of this set there will be m + 1 points of stationary phase, $\Omega'(\psi) = 0$, for the ray representing the ground wave and for the m rays reflected at the ionosphere in such a way that the angle of incidence, ϕ, at the ionosphere (for example, at b, d, and f on Fig. 22) is equal to the angle of reflection, and also (for $m > 1$) that the angle of incidence, $(90° - \psi)$, at the ground (for example, at a, c, e, and g on Fig. 22) is equal to the angle of reflection at the ground. When the angle of elevation, ψ, is positive, the waves may be considered to travel both along the direct ray path, tb, from the transmitter to the ionosphere and along the ground-reflected ray path, tab; the reflection points b and f at the ionosphere and c and e at the ground will be very slightly different for the direct and ground-reflected ray paths, but this small difference is ignored in our calculations. Note that the angle of elevation, ψ, can be negative as is illustrated on Fig. 22, case (b).

The following formula may be used to calculate the median transmission loss of an ionospheric mode of propagation involving m reflections at the ionosphere and a ray path of length, R:

$$L_m = L_{bf}(R) + A_t(\psi) + A_r(\psi) + (m - 1)\, A_g(\psi) - C_m(R, 0.5) + P + mA(\phi, 0.5) \tag{9}$$

Each of the terms in the above is expressed in decibels; $L_{bf}(R)$ denotes the basic free space transmission loss (Set d = R in (3) in Section 1) for the ray distance, R. We see by Fig. 22 that we may calculate R as follows:

$$R \cong d_t + d_r + 2m\, R_o \qquad (\psi > 0) \tag{10}$$

$$R \cong d_t + d_r + 2m\,(R_{om} - k\,a\,\psi) \qquad (\psi \le 0) \tag{11}$$

$$d_t = \sqrt{(k\,a \tan\psi)^2 + 2\,k\,a\,h_t} - k\,a \tan\psi \tag{12}$$

The distance, d_r, is determined by a formula similar to (12) with h_t replaced by h_r; in this equation ka is the effective earth's radius, and k has been chosen equal to 4/3 in our ionospheric examples. Methods for estimating k as a function of time and geographical location are given in a later section. It is convenient to choose several values of ψ at conveniently spaced intervals and then to calculate all of the remaining factors at these particular values of ψ.

The space wave radiation factors, $A_t(\psi)$, and $A_r(\psi)$ include the gains of the transmitting and receiving antennas, respectively, relative to that of an isotropic antenna in free space, and allow for the radiation patterns of the antennas and the loss arising from the proximity of the antennas to the curved earth. The magnitude of $A_t(\psi)$ can be determined from $A_t(\psi) = L_i(\psi) - L_{bf}(R_o + d_t)$, where $L_i(\psi)$ denotes the transmission loss expected for the ground wave mode propagated between the actual transmitting antenna and an isotropic receiving antenna placed at the first point of reflection in the ionosphere, while $L_{bf}(R_o + d_t)$ is the corresponding basic free space transmission loss at this distance. Figs. 23 and 24 give typical values of $A_t(\psi)$ expected for short vertical electric dipoles 30 feet above the ground; in this case we may express $A_t(\psi)$ as follows:

$$A_t(\psi) = 20 \log_{10} |F| - 1.761 - 20 \log_{10} \cos \psi - 20 \log_{10} f(q) \tag{13}$$

In the above $|F|$ is a "cut-back" factor. When ψ is large and positive, $|F|$ is just $|1 + R_v(\psi)|$ where R_v is the complex Fresnel reflection coefficient for plane vertically polarized waves incident on the ground at the grazing angle ψ; when ψ is small or negative, the curvature of the earth becomes important and the values of $|F|$ have then been determined by formulas recently developed by Wait. 39/ 40/ The term 1.761 is just the gain of the short dipole; the term $20 \log_{10} \cos \psi$ allows for the cosine pattern of the dipole; and finally f(q) is the height gain factor given by equation (19) in reference (11) which allows for the effect of the height, h_t, of the antenna above the surface. The "cut-back" factor $|F|$ was calculated for a spherical surface of radius, a_e = ka, with k = 4/3; this provides approximately for the effect of air refraction.

The factor $(m - 1)A_g(\psi)$ allows for loss on reflection at the ground, for example at c and e on Fig. 22 in Case (a) and at c in Case (b). The amount of this loss will depend on the polarization of

EFFECTIVE SPACE WAVE RADIATION AT A LARGE DISTANCE FROM A SHORT VERTICAL DIPOLE 30 FEET ABOVE A SPHERICAL EARTH

Earth's radius 4/3 actual value to allow for the bending near the surface in a standard atmosphere; ground constants $\sigma = 0.005$ mhos/meter, $\epsilon = 15$

$h > (5/f_{Mc}^{2/3})$ kilometers

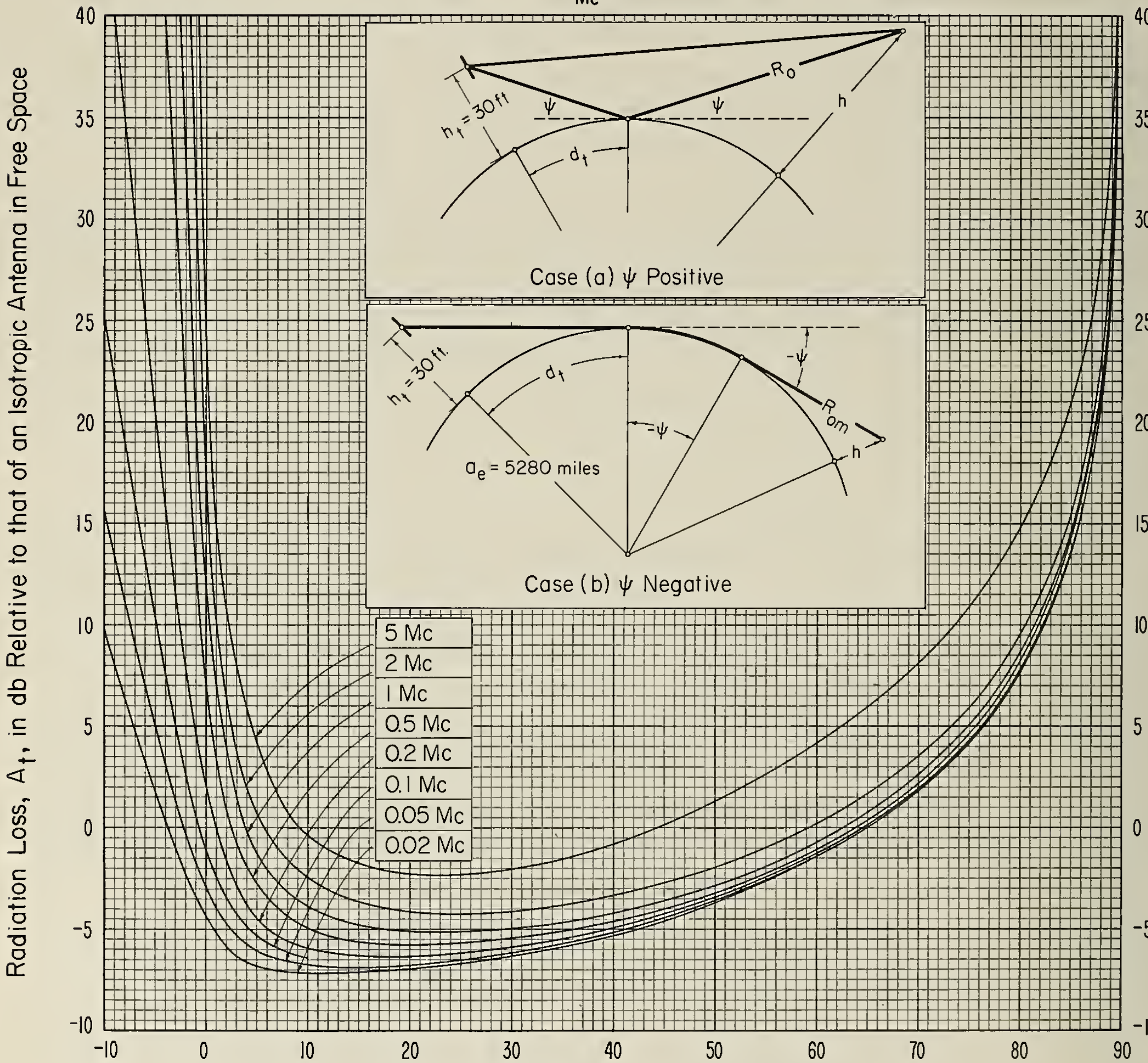

Figure 23

EFFECTIVE SPACE WAVE RADIATION AT A LARGE DISTANCE FROM A SHORT VERTICAL DIPOLE 30 FEET ABOVE A SPHERICAL EARTH

Earth's radius 4/3 actual value to allow for the bending near the surface in a standard atmosphere; ground constants $\sigma = 5$ mhos/meter, $\epsilon = 80$

$h > (5/f_{Mc}^{2/3})$ kilometers

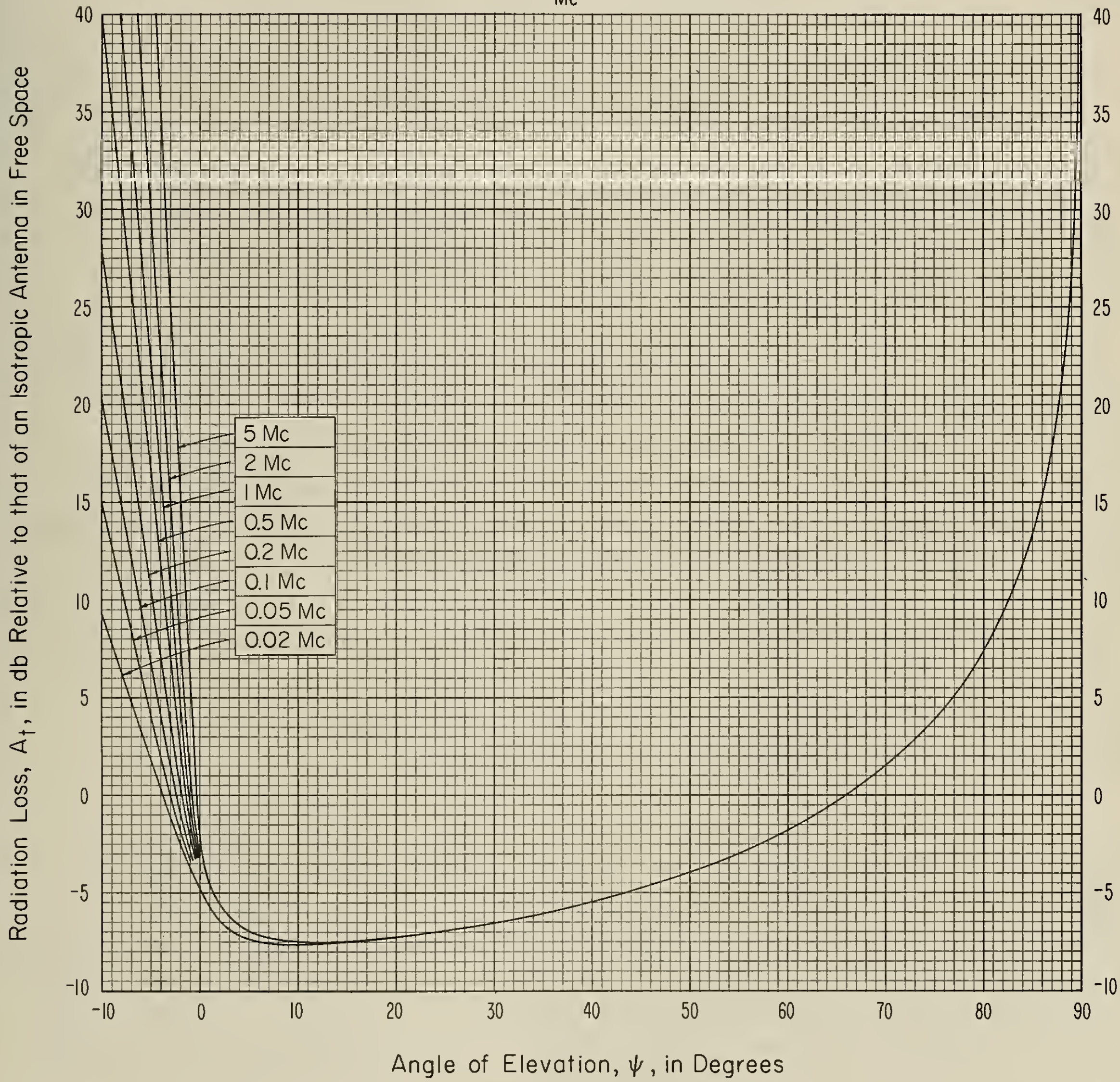

Figure 24

the downcoming waves. Since the waves reflected from the ionosphere will have both vertically and horizontally polarized components, even when the incident waves are linearly polarized, it becomes necessary to know the relative amounts of energy associated with each polarization in the downcoming waves. This problem is not easy to solve precisely, and we have obtained an estimate for $A_g(\psi)$ by assuming, quite arbitrarily, that the energy in the downcoming waves is equally divided between the two polarizations. Thus, for angles $\psi > 2°$, we have:

$$A_g(\psi) \cong -10 \log_{10} [(|R_v^2| + |R_h^2|)/2] \qquad \psi > 2° \qquad (14)$$

where R_v and R_h are the complex Fresnel reflection coefficients for vertical and horizontal polarization, respectively. Since the value determined by (14) represents only a few decibels, the use of the above approximate expression will not lead to serious errors.

It has been shown by Rice [41] and by Fock [42] that $A_g(0) = 6.021$ db when ψ equals zero (in the limit as R_{om}/λ is very large, i.e., for $h > (5/f_{Mc}^{2/3})$ kilometers) regardless of the polarization or ground constants; their results can also be used to compute $A_g(\psi)$ for other values of ψ, but we have instead assumed that $A_g(\psi)$ can be calculated for $\psi \leq 0$ by the following approximate formula:

$$A_g(\psi) \cong 6.021 - 2\,A_t(0) + 2\,A_t(\psi) \qquad (\psi \leq 0) \qquad (15)$$

For values of ψ between 0 and 2°, it is easy to sketch in a smooth curve between the results given by (14) and (15).

We turn next to a consideration of the convergence factor $C_m(R, p)$ which provides a measure of the focusing of the energy on reflection at the curved surface of the ionosphere exceeded with probability p. Fig. 25 is a geometrical construction which demonstrates the nature of this focusing of rays in the vertical plane for ψ near zero. At the antipode of the transmitter, half way around the earth, the rays are also focused in the horizontal plane. A detailed discussion of this phenomenon is given in Appendix I. For rays leaving the earth's surface at grazing incidence ($\psi \leq 0$) and at the antipode ($m\,\theta = 90°$), it is necessary to use a wave treatment of the problem, the amount of the focusing then being a function of the frequency. At points substantially removed from these caustics, geometrical optics leads to the following

GEOMETRICAL CONSTRUCTION DEMONSTRATING THE CONVERGENCE
OF RAYS NEAR GRAZING INCIDENCE

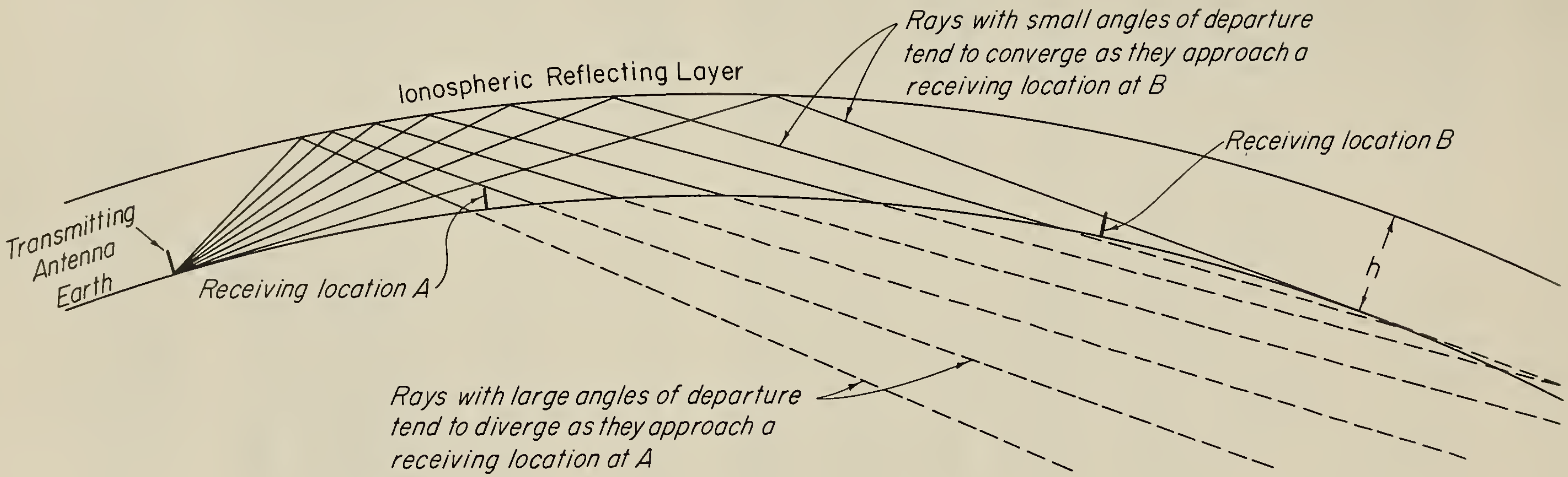

Figure 25

formula for $C_m(R)$ which provides for a smooth ionosphere a measure in decibels of the expected increase in the received field due to this focusing.

$$C_m(R) = 10 \log_{10} c_m = 10 \log_{10} \left\{ \frac{R_o}{- a \sin \psi \, (d\theta/d\psi)} \right\}_v \cdot \left\{ \frac{2m\, R_o \cos \psi}{a \sin 2m\,\theta} \right\}_h \tag{16}$$

$$\frac{d\theta}{d\psi} = - \frac{\sin(\theta - \tau)}{\cos \psi \cos \phi} + \frac{d\tau}{d\psi} \tag{17}$$

In the above τ denotes the total bending of a radio wave in passing through the troposphere, and methods of calculating τ are given in a later section. The two factors in (16) correspond to the focusing in the vertical and horizontal planes, respectively. Equation (16) may be used except near the caustics ($\psi \le 0$) and ($m\,\theta = 90°$). When $\psi \le 0$ and $m\,\theta \ne 90°$, we may use:

$$C_m(R) = 20 \log_{10} [R_{om} - 92.153\, \psi \,(\text{degrees})] + (10/3) \log_{10} f_{kc}$$

$$- 10 \log_{10} [\sin 2m\,(\theta_m - 4/3\, \psi)] + (40/3) \log_{10} m - 60.694 \tag{18}$$

When $\psi > 0$ and we are at a distance in wavelengths (ρ/λ) from the antipode, we may use:

$$C_m(\rho) = 20 \log_{10} (R_a/\pi a) + 10 \log_{10} \left\{ \frac{\cos^2 \psi}{- \sin \psi \, (d\theta/d\psi)} \right\} - 10 \log_{10} m$$

$$+ 10 \log_{10} f_{kc} + 10 \log_{10} [J_o(2\pi \cos \psi \, \rho/\lambda)]^2 + 36.172 \qquad (\psi > 0) \tag{19}$$

The above may be used for $m \ge 9$ at night since ψ is greater than zero for these modes with $h = 90$ km. For $m \le 8$, $\psi < 0$ near the antipode at night, and we may then use the following formula:

$$C_m(\rho) = 20 \log_{10} (R_a/\pi a) - (20/3) \log_{10} m + (40/3) \log_{10} f_{kc}$$

$$+ 10 \log_{10} [J_o(2\pi \rho/\lambda)]^2 + 44.422 \qquad (\psi \le 0) \tag{20}$$

In (19) and (20), R_a denotes the ray distance to the antipode. If a horizontal magnetic dipole is used for reception of the field radiated from the vertical electric dipole, then the J_o in (19) and (20) is to be replaced by J_1; here J_o and J_1 are Bessel functions. Very near $\psi = 0$, the values of $C_m(R)$ determined by (16) will exceed those given by (18), particularly at the lower frequencies, and in this region a smooth curve may be drawn between the values for $\psi >> 0$ and the values given by (18); similarly, at the antipode the values of $C_m(\rho)$ given by (19) will exceed those given by (20), and a smooth curve may be drawn between the values for $\psi >> 0$ and those given by (20). Fig. 26 gives examples of $C_m(R)$ calculated in this way for m = 1, 2 and 9 for day-time propagation (h = 70 km), for a smooth ionosphere, and typical refraction conditions.

It is clear from Fig. 25 that this focusing will be fully realized in practice only to the extent that the ionosphere presents a smooth surface to the radio waves. A discussion is presented in Appendix I which indicates how allowance may be made for ionospheric roughness. It is shown that an individual ionospheric mode of propagation consists of a steady specularly-reflected component plus a random Rayleigh distributed component. If we let k^2 denote the ratio of the power in the random component relative to that in the specularly-reflected component, then we may estimate the convergence $C_m(R, p)$ exceeded 100 p% of the time in terms of the values of $k^2(1 - p)$ exceeded $100(1 - p)$% of the time:

$$C_m(R, p) = 10 \log_{10} \left[\frac{c_m + k^2(1 - p)}{1 + k^2(1 - p)} \right] \tag{21}$$

Here c_m (see 16) denotes the ratio of the received power with and without focusing at a smooth ionosphere. As the probability varies from 0 to 1, $k^2(1 - p)$ will vary from zero for a smooth ionosphere to ∞ for a perfectly rough ionosphere, and $C_m(R, p)$ will vary from the values given by (16), (18), (19), and (20) for a smooth ionosphere to zero for a perfectly rough ionosphere. The transmission losses given in this report correspond to median values, i.e., p = 0.5. The random variable k^2 depends upon the radio frequency, angle of incidence, ϕ, and time of day.

As an illustration of the effects of focusing near the antipode and of the influence of ionospheric roughness, Fig. 27 shows the

CONVERGENCE FACTOR IN IONOSPHERIC PROPAGATION
h = 70 kilometers; N_s = 313 and h_s = 0 and $k^2(l)$ = 0

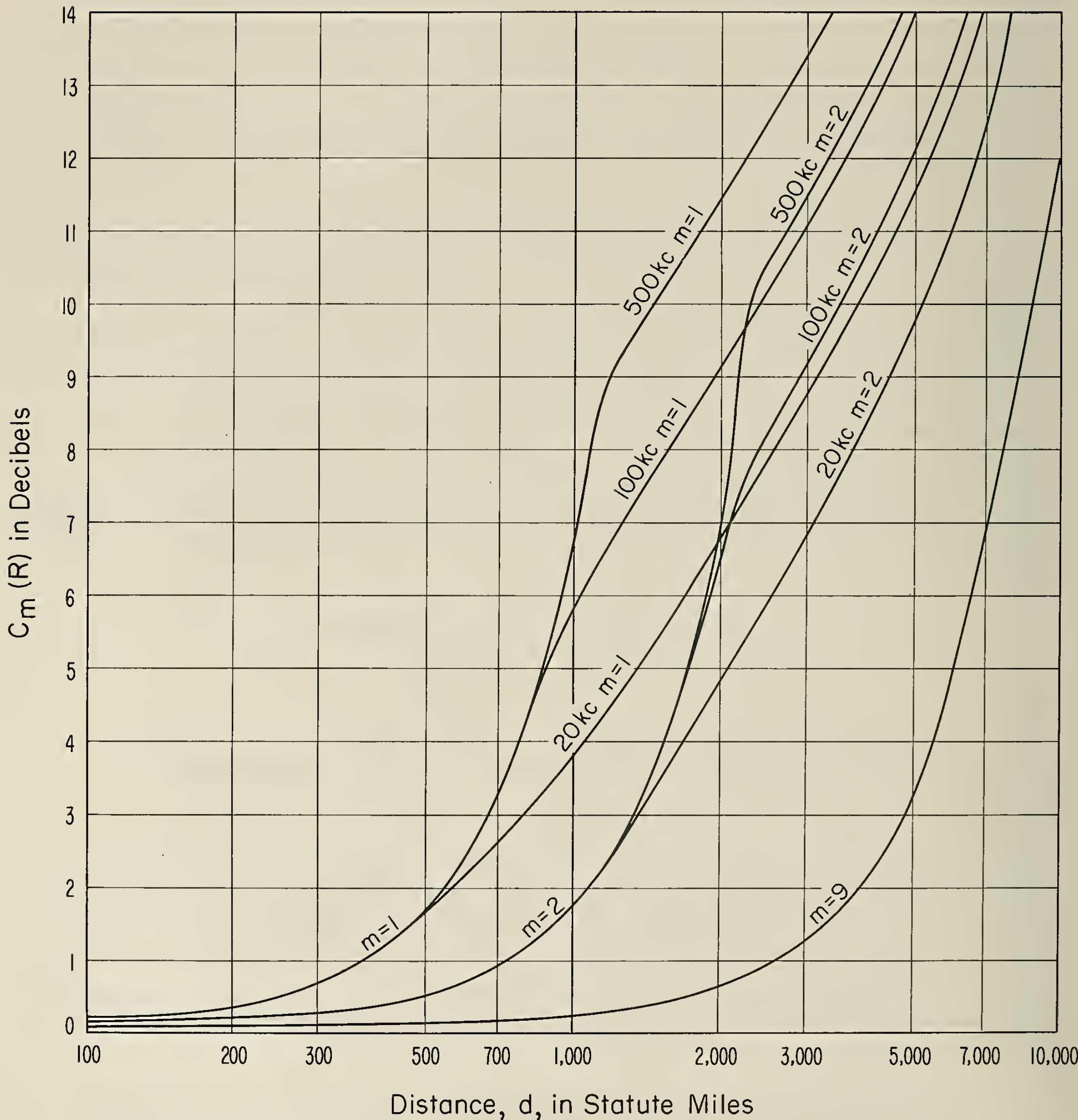

Figure 26

TRANSMISSION LOSS EXPECTED NEAR THE ANTIPODE AT NIGHT FOR 100 kc

Over Land = σ = 0.005 Mhos/meter, ϵ = 15

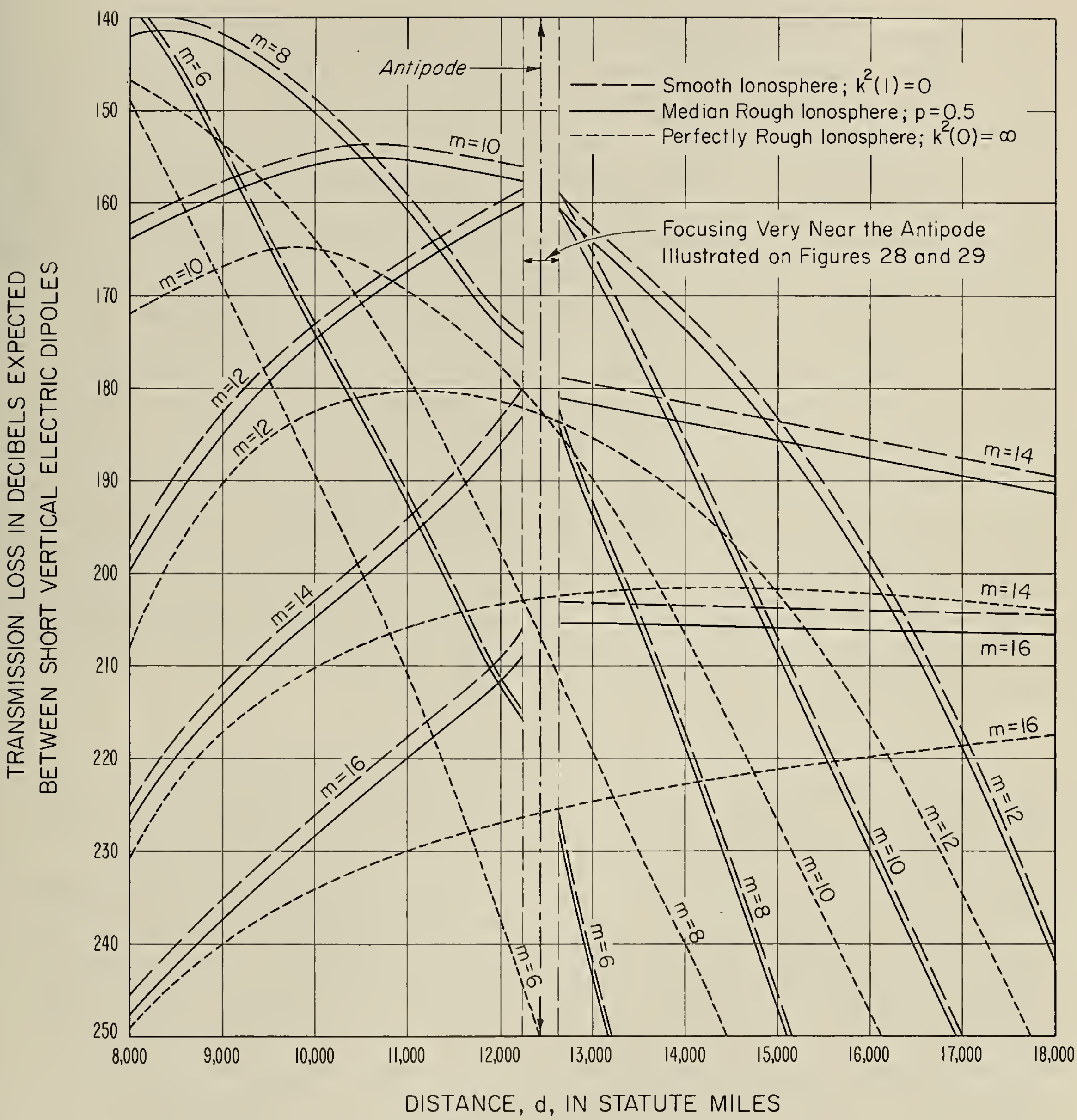

Figure 27

transmission loss expected between vertical electric dipoles in the range from 8,000 to 18,000 miles for 100 kc at night over land. Three values are shown for each of the modes m = 6, 8, 10, 12, 14, and 16 corresponding (a) to a smooth ionosphere ($p = 0$, $k^2(1) = 0$), (b) to an ionosphere of median roughness ($p = 0.5$), and (c) to a perfectly rough ionosphere ($p = 1$, $k^2(0) = \infty$).

In the immediate vicinity of the antipode, i.e., within a few wavelengths, the focusing for a smooth concentric ionosphere is very large. Thus Fig. 28 shows the value of $C_m(R_a, p)$ expected right at the antipode at night for a smooth, concentric ionosphere and for a rough, concentric ionosphere; the values expected for h = 70 km during the daytime would be only slightly different; Fig. 29 shows the rapid decrease of the focusing as we leave the antipode and, at distances greater than 100λ, the envelope will be just 6 db above the values of transmission loss shown on Fig. 27, i.e., the values shown on Fig. 27 correspond to the single wave expected from a directive transmitting antenna with an infinite front-to-back ratio. We see on Fig. 29 that the field expected from the non-directive dipole oscillates with increasing distance from the antipode; this oscillation is caused by the interference between the waves arriving at the receiving point along the short and long great circle paths. Thus there will be concentric rings around the antipode at which the expected field will be equal to zero. The radii of these concentric rings are the same for a concentric ionosphere, regardless of the number, m, of ionospheric reflections, and are determined by the zeros of the Bessel functions; for the electric field, the first two such rings have radii equal to 0.38λ and 0.88λ.

The actual ionosphere will never be concentric with the surface of the earth. In practice, as the sun rises and sets, or as the geomagnetic latitude of the reflection point is varied, the surface of the ionosphere will undoubtedly change in such a way that its radius of curvature and slope relative to a tangent plane on the earth will vary over appreciable ranges, and this will cause $C_m(R)$ to vary up and down relative to the values expected on the basis of the above analysis. However, except near the antipode, it seems plausible to assume that the median values of $C_m(R)$ may not be much influenced by such changes. The magnitude of the antipodal anomaly will be substantially reduced by these macroscopic perturbations of the spherical concentric shell model assumed for our calculations. Also, for the actual non-concentric ionosphere, the geographical location of the antipode may be expected to vary with time over a fairly large

EXPECTED FOCUSING AT THE ANTIPODE FOR A CONCENTRIC IONOSPHERE

h=90KM; N_s=324

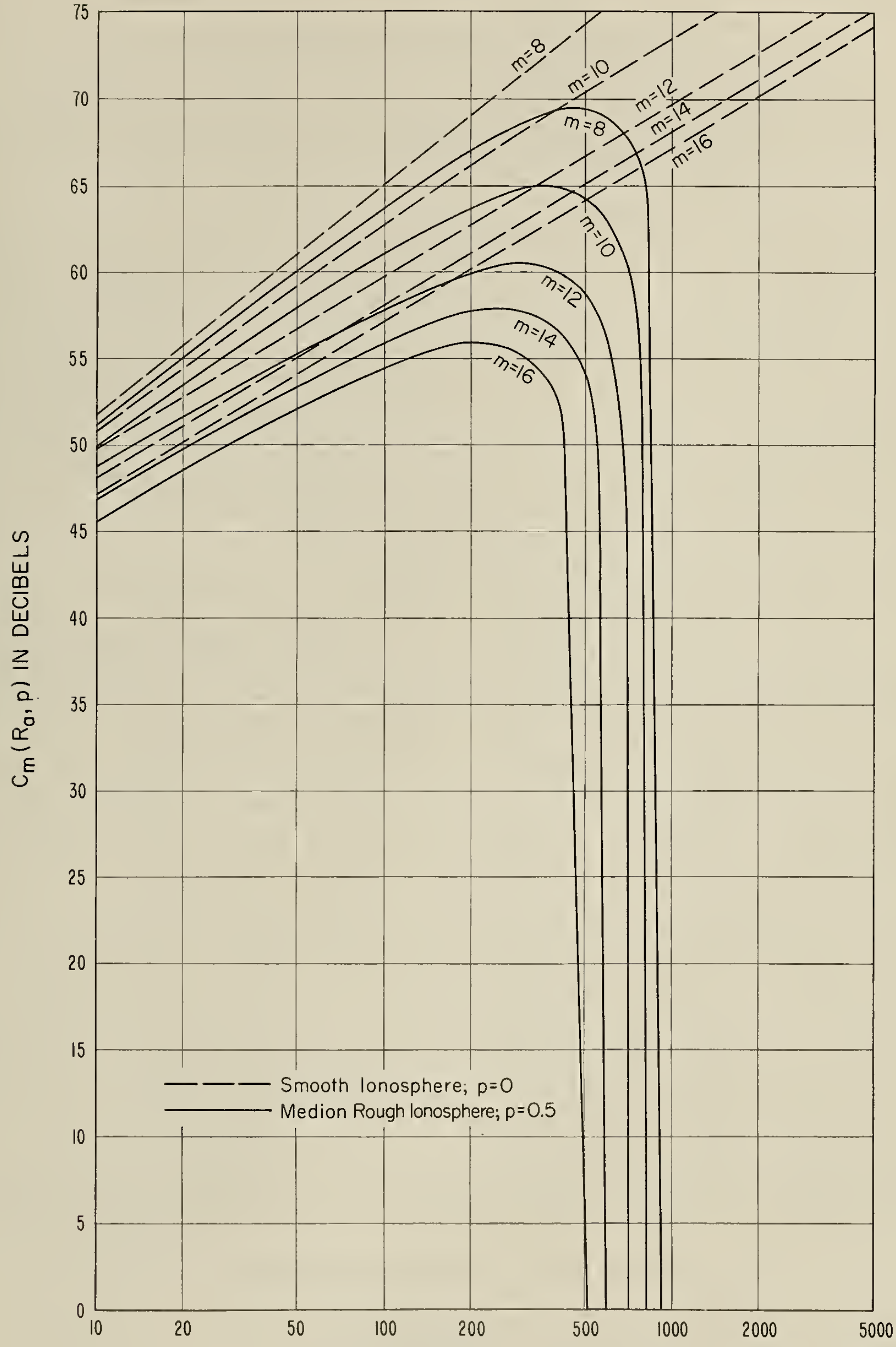

Figure 28

THE BEHAVIOR NEAR THE ANTIPODE OF THE CONVERGENCE FACTORS FOR THE RADIATION FROM A VERTICAL ELECTRIC DIPOLE FOR A CONCENTRIC IONOSPHERIC SHELL AROUND A SPHERICAL EARTH

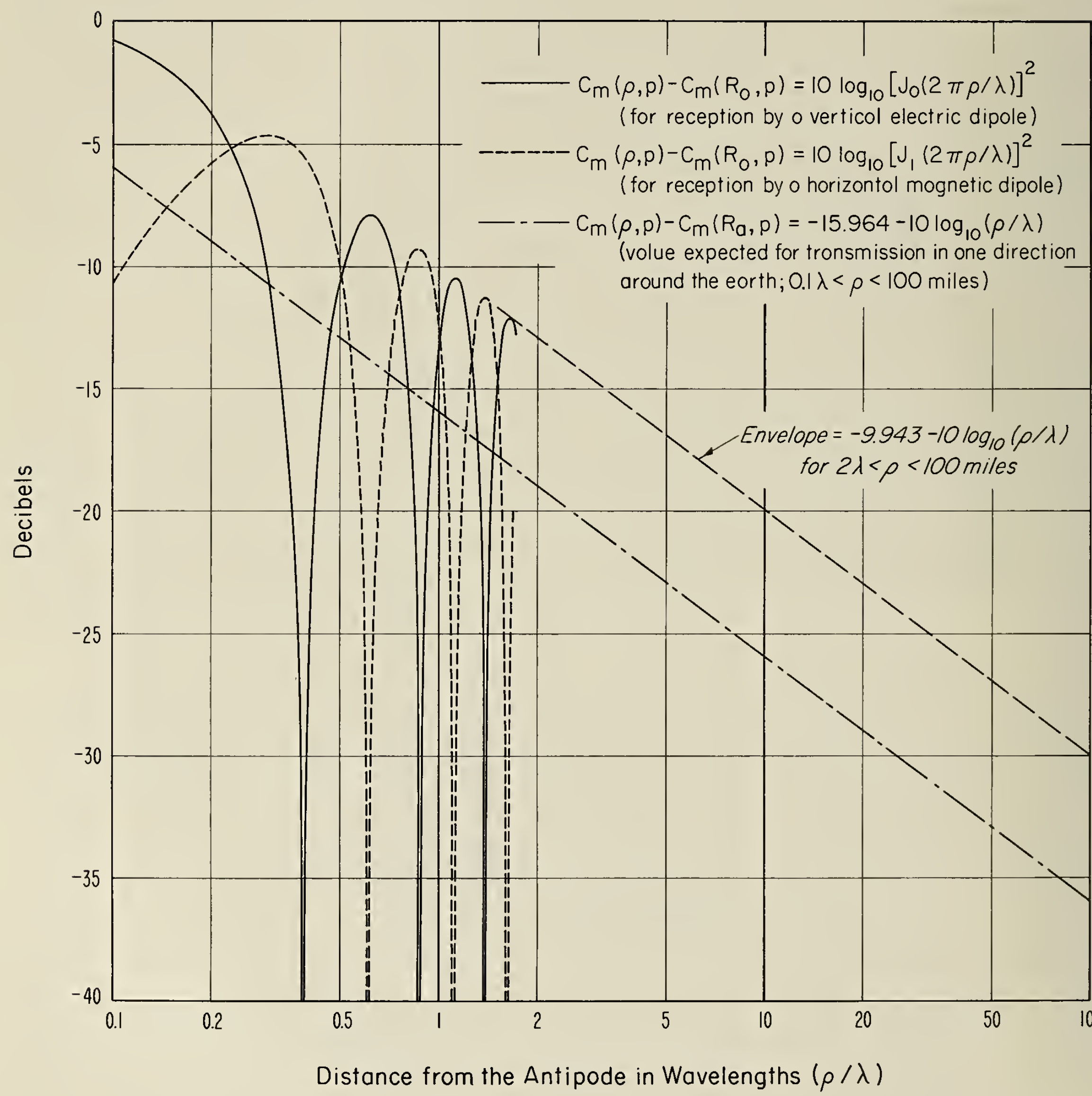

Figure 29

area, and this should result in a net increase in the fading range in this region. Furthermore, the antipodal locations may be expected at any given time to be different for the different modes, and thus the zeros predicted by (19) and (20) and shown on Fig. 29 are not likely to be observable unless some means is used to exploit the different times of arrival of the individual modes.

Consider next the loss, P, arising from the polarization characteristics of the downcoming ionospheric waves. An incident linearly-polarized wave will be reflected as two component waves, an ordinary and an extraordinary wave, each of which will be elliptically polarized. These two component waves, which will have roughly the same amplitudes except on frequencies near the gyrofrequency (near 1.5 Mc in the United States) will mutually interfere, and this causes the rapidly varying polarization characteristics of the observed downcoming waves. The polarization loss, P, arises from the fact that typical receiving antennas will respond to only one polarization. The amount of this loss will depend principally upon the transmission frequency, the penetration frequency for the layer involved, and the intensity and direction of the earth's magnetic field relative to the path; it can be calculated [13/34/43/] with some accuracy when these parameters are known. For more than one reflection at the ionosphere, the polarization loss becomes a very complex function of the reflection coefficients for the parallel and perpendicular components of the incident fields and is difficult to separate from the absorption loss, $A(\phi, 1 - p)$. All of the low frequency examples of ionospheric wave propagation in this report have been obtained using the empirical estimates described below for $P + A(\phi, 1 - p)$ which thus includes the polarization loss P; consequently we have calculated the total reflection loss as $m\{P + A(\phi, 1 - p)\} - (m - 1)P$ for $m > 1$. The calculations at $f = 100$ kc have been made in this report by setting $P = 3.01$ db, but this estimate is now believed to be substantially too large, except near vertical incidence. The calculations for all of the other frequencies from 20 kc to 1,000 kc were calculated with $P = 0$ for all values of m, although this assumption probably leads to somewhat more transmission loss than would be expected for $m > 1$ since the appropriate value of P probably lies between 0 and 3 db, approaching the latter value near vertical incidence; however, we are usually more interested in the values near oblique incidence for our applications, and this latter assumption should yield more nearly correct results for the solution of these problems.

Finally we will consider the loss, $A(\phi, 1 - p)$, on reflection at the ionosphere, exceeded for $100(1 - p)\%$ of the time; this depends

MEDIAN LOSS FOR ONE REFLECTION AT THE IONOSPHERE

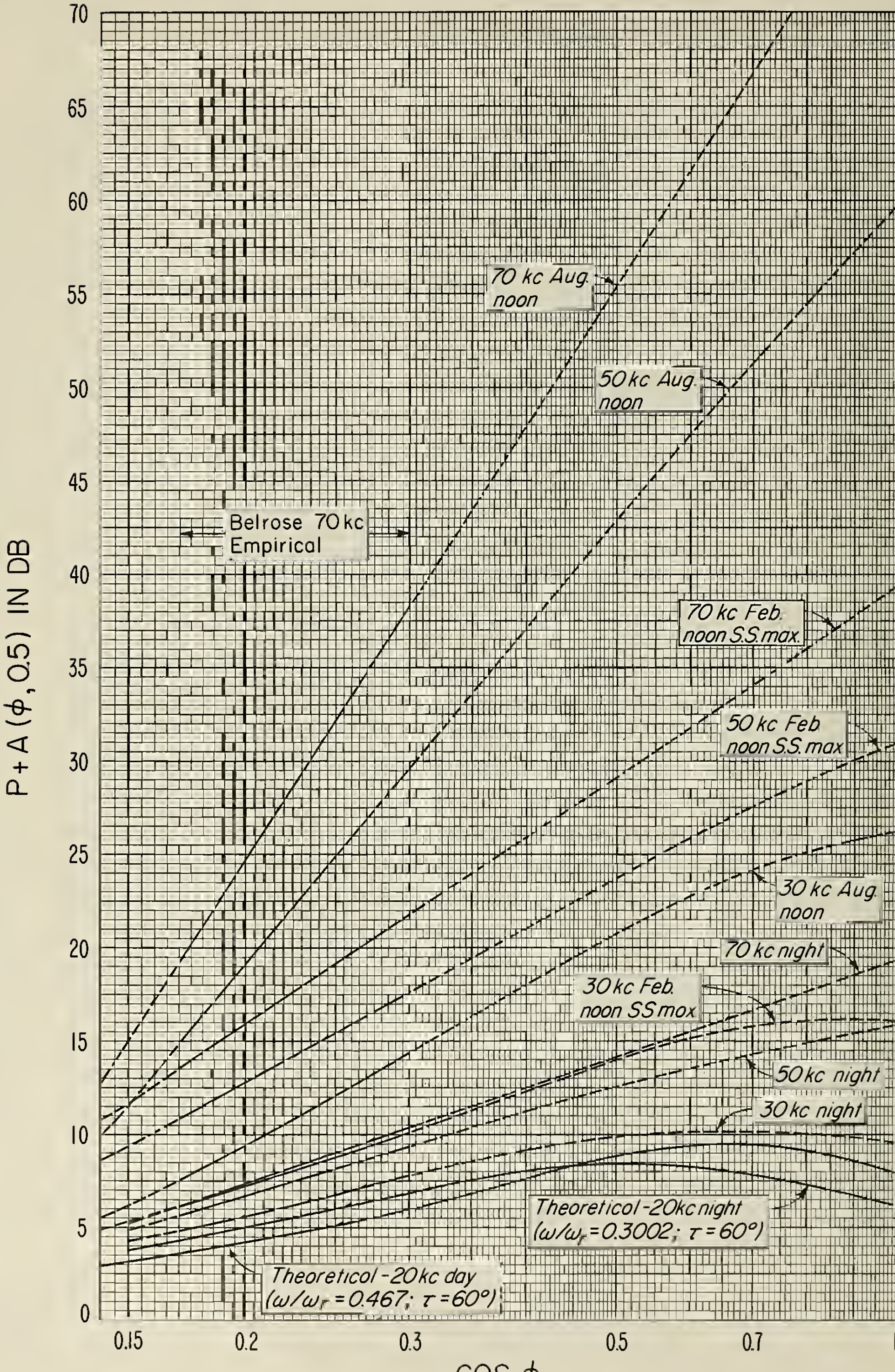

Figure 30

on the angle of incidence, ϕ, at the ionosphere, the radio frequency, time of day, season of the year, phase of the sunspot cycle and the geomagnetic latitude of the reflection point. For the examples developed in this report, we have used some empirical evaluations of $P + A(\phi, 1 - p)$ made by Belrose [45] on transmission paths between stations in England, the Scandinavian countries, and Germany. Using the results in his doctoral thesis, we may express the median values of $P + A(\phi, 0.5)$ as follows:

$$P + A(\phi, 0.5) = 17.2 \log_{10} (f_{kc} \cos \phi) - 12.4 \qquad (70 < f_{kc} < f_D) \qquad (22)$$
(NIGHT)

$$P + A(\phi, 0.5) = 30.8 \log_{10} (f_{kc} \cos \phi) - 22.6 \qquad (70 < f_{kc} < f_D) \qquad (23)$$
(FEB., NOON, SUNSPOT MINIMUM)

$$P + A(\phi, 0.5) = 33.6 \log_{10} (f_{kc} \cos \phi) - 22.6 \qquad (70 < f_{kc} < f_D) \qquad (24)$$
(FEB., NOON, SUNSPOT MAXIMUM)

$$P + A(\phi, 0.5) = 77.3 \log_{10} (f_{kc} \cos \phi) - 64.0 \qquad (70 < f_{kc} < f_D) \qquad (25)$$
(AUG., NOON)

The above formulas were determined empirically from data extending only over the range of frequencies from 70 - 250 kc and the range of distances from 350 to 900 miles; a recent analysis of lower frequency data by Watt, Maxwell and Whelan [46] indicates that the absorption is greater at frequencies less than 70 kc than would be predicted by the above formulas. Consequently, as shown on Fig. 30, we have used the theoretical results of Wait and Murphy [34] at 20 kc and then interpolated linearly on a logarithmic frequency scale to obtain values for intermediate frequencies; the same ionospheric parameters $L/H = 0.1$ by day (i.e., $\omega/\omega_r = 0.467$) and $L/H = 0.05$ at night (i.e., $\omega/\omega_r = 0.3002$) were used in these calculations at $f = 20$ kc as for those leading to Figs. 16 to 19, but the index τ for the earth's magnetic field was set equal to 60° in the present calculations, whereas τ was set equal to zero in the calculations leading to Figs. 16 to 19.

Figs. 31 to 36 give the median transmission loss expected in accordance with the above methods of calculation at 20, 50, and 200 kc in over-land and over-sea propagation and for day and night conditions.

MEDIAN TRANSMISSION LOSS OVER LAND AT 50 kc

$\sigma = 0.005$ Mhos/meter; $\epsilon = 15$; $h_t = h_r = 30$ feet

Day h = 70 km; Night h = 90 km

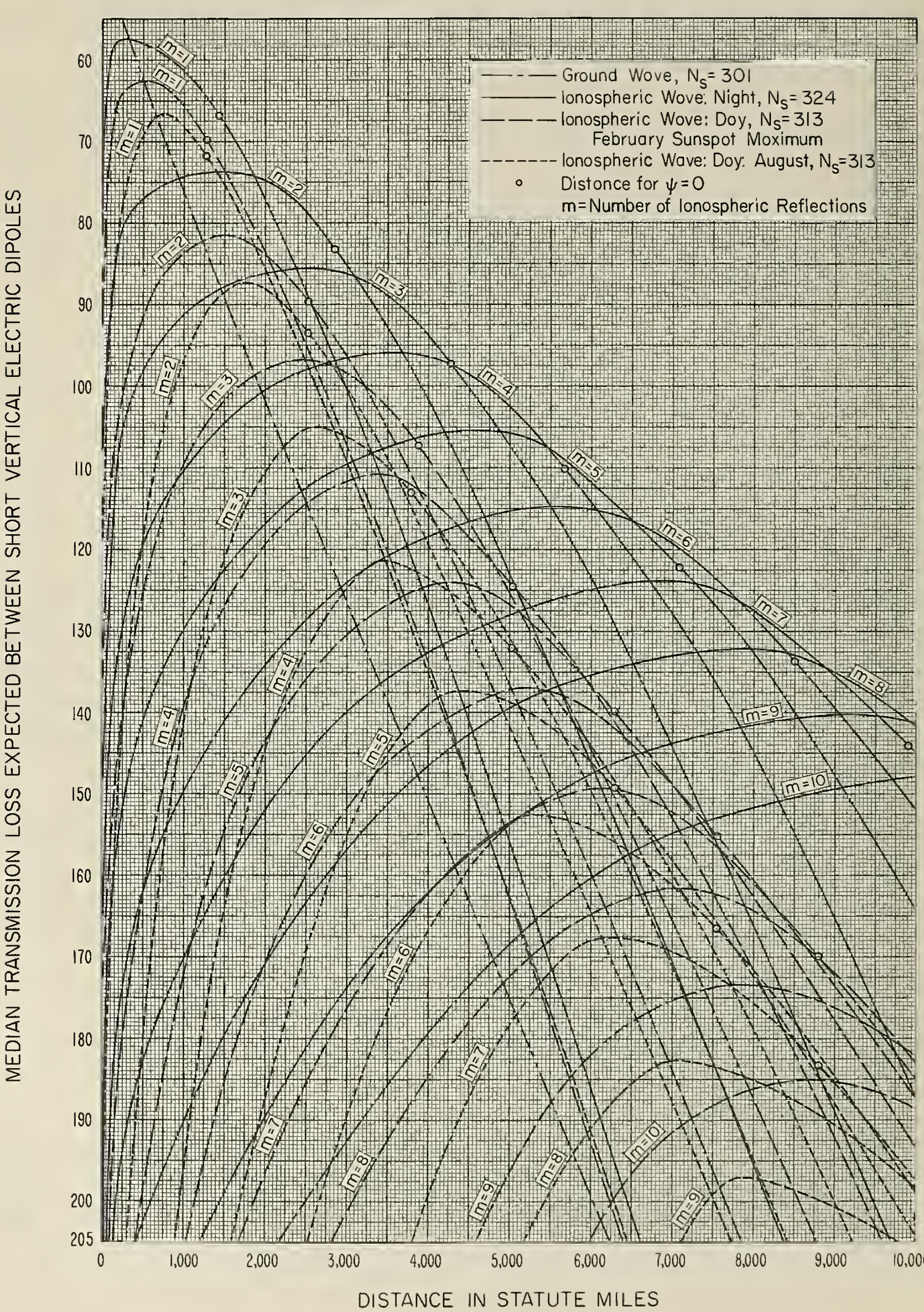

Figure 33

MEDIAN TRANSMISSION LOSS OVER SEA AT 50 kc

$\sigma = 5$ Mhos/meter; $\epsilon = 80$; $h_t = h_r = 30$ feet
Day $h = 70$ km; Night $h = 90$ km

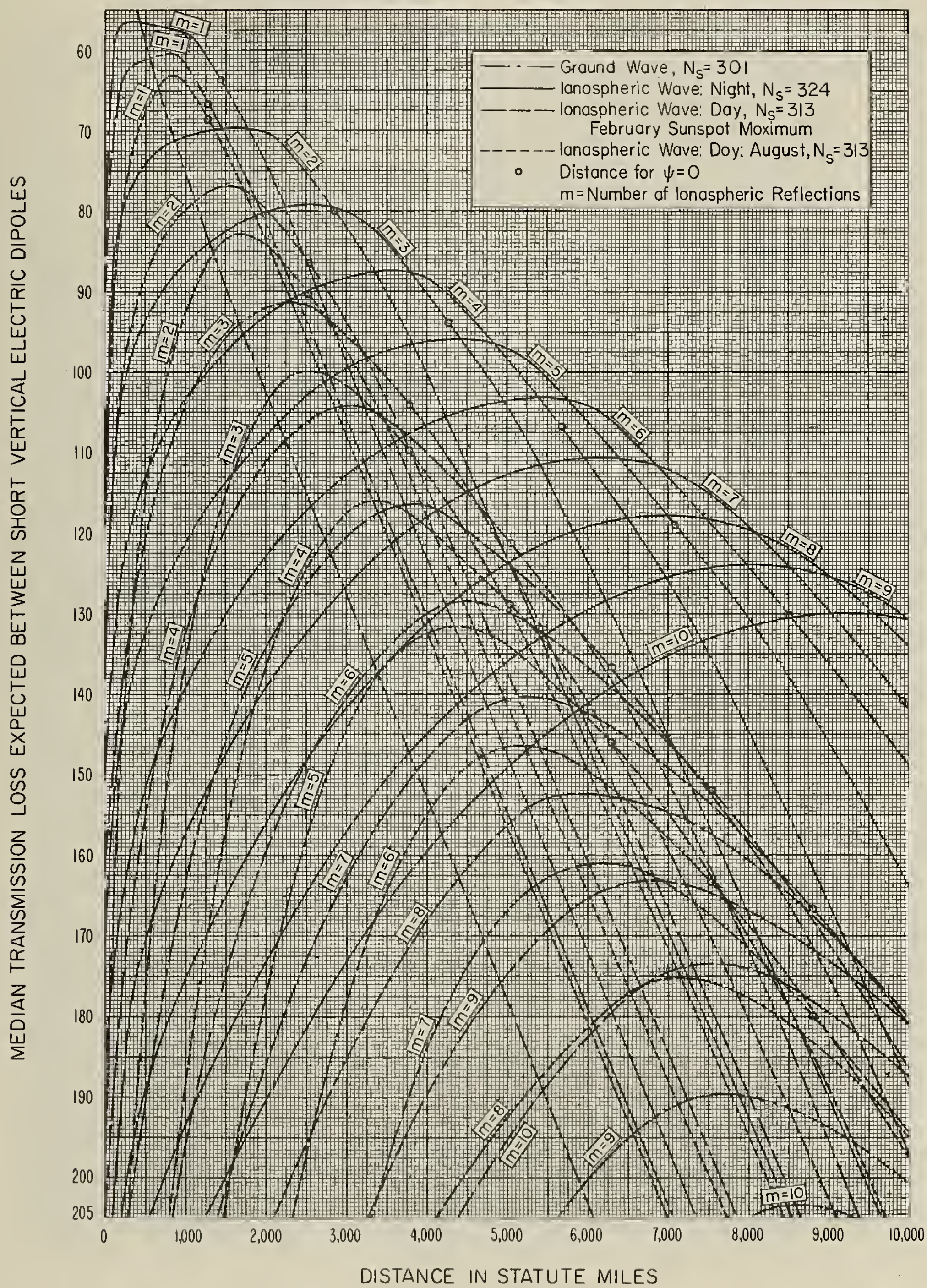

Figure 34

MEDIAN TRANSMISSION LOSS OVER LAND AT 200 kc

σ = 0.005 Mhos/meter, ϵ = 15; $h_t = h_r$ = 30 feet

Day h = 70 km; Night h = 90 km

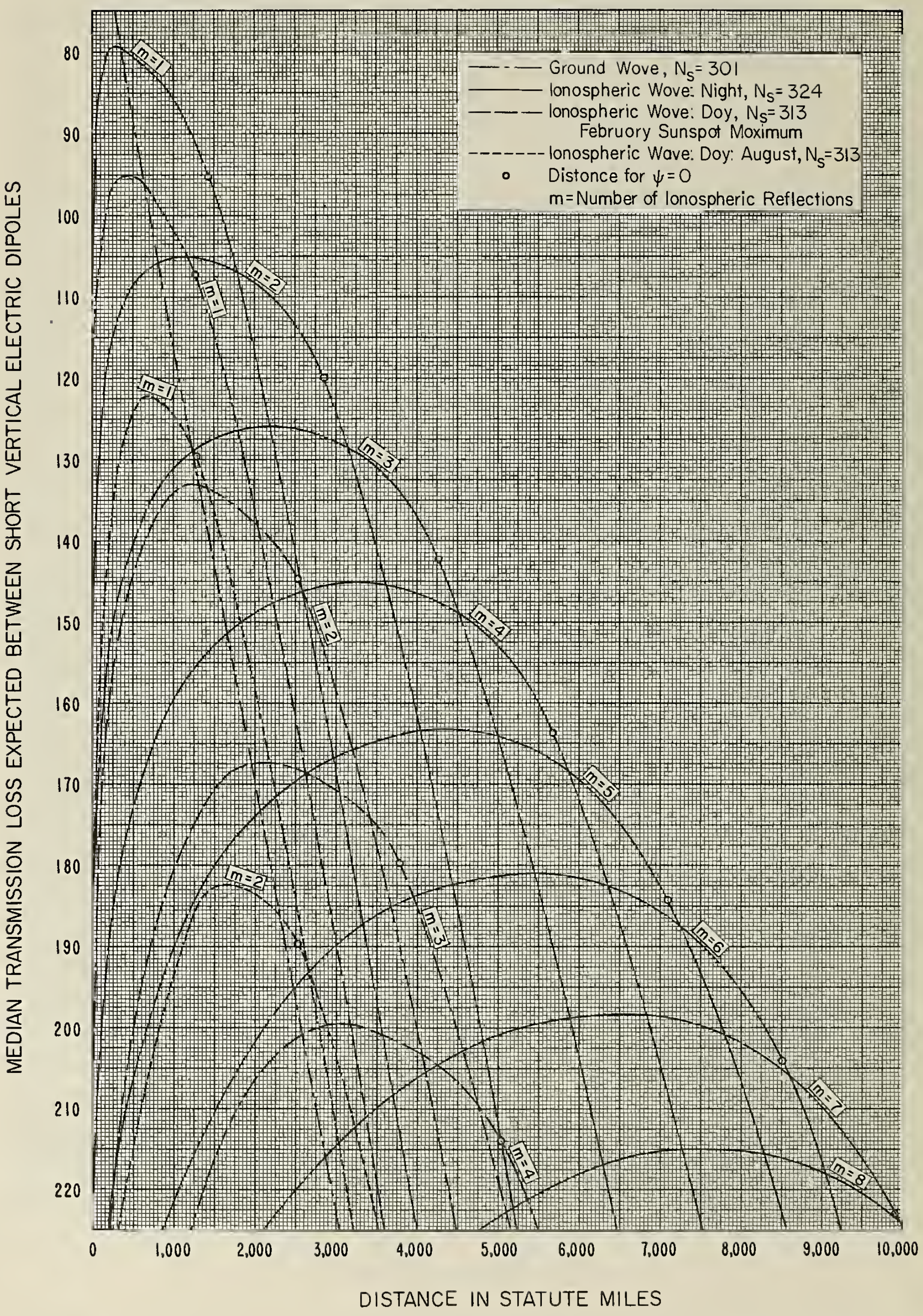

Figure 35

MEDIAN TRANSMISSION LOSS OVER SEA AT 200 kc

$\sigma = 5$ Mhos/meter; $\epsilon = 80$; $h_t = h_r = 30$ feet

Day $h = 70$ km; Night $h = 90$ km

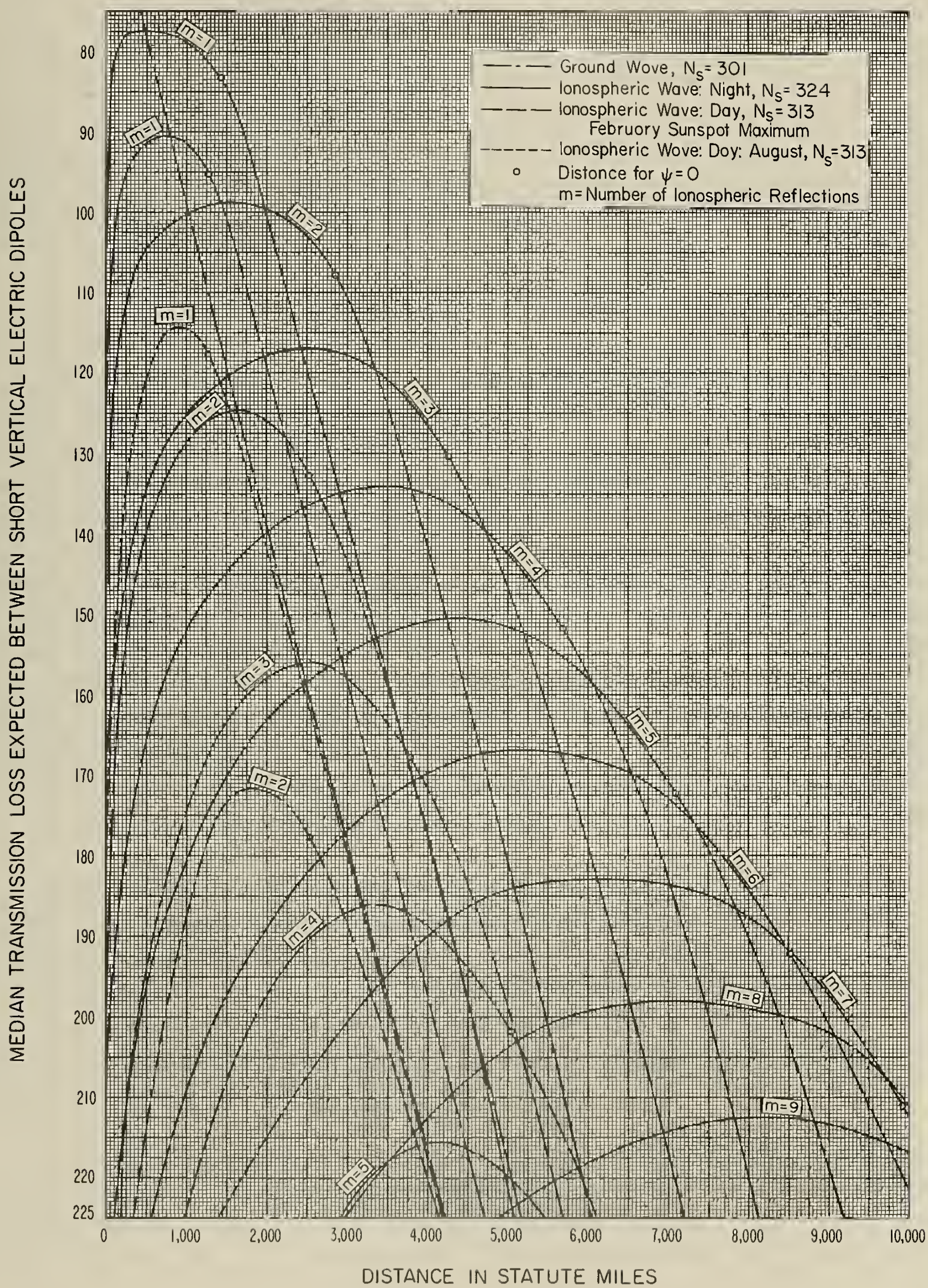

Figure 36

Figs. 31 and 32 show the large decrease in the transmission loss near the antipode, and illustrate the fact that each mode of propagation has two important branches at points somewhat removed from the antipode, corresponding to propagation via the short and long great circle paths, respectively; actually there are still other branches for each mode corresponding to propagation more than once around the earth, but these are not shown. The decrease in transmission loss shown at the antipode is the value for an idealized concentric ionosphere and will, in practice, undoubtedly be somewhat smaller. Transmission loss curves for the separate modes are not given at 20 kc for sea water since they differ so little from those for overland. It should be noted that the curves on Figs. 16 and 17 for 20 kc will be more useful for most applications than those on Fig. 31 since they combine the separate modes with proper relative phases.

Throughout this section the formulas and graphs refer to the median values of transmission loss for individual modes of propagation. This form of presentation was used since it is more useful in applications such as the design of navigation systems or of systems to avoid multipath distortion. To determine the expected median transmission loss for a continuous wave transmission, it is necessary to convert the transmission losses for the individual modes to power ratios, and then add these power ratios; at 500 kc, and possibly even as low as 50 kc, it is reasonable to assume that the several ionospheric modes will have random relative phases so that the median power of the resultant will be equal to the sum of the median powers of the individual modes. For example, if there were two modes with equal median transmission losses, the median transmission loss for the sum of these two modes would be 3 db less, and for three equal modes the sum would have 4.77 db less transmission loss than each individual mode.

The author has studied the behavior of $P + A(\phi, 0.5)$ at night in the United States for frequencies in the standard broadcast band from 500 to 1,500 kc over a very wide range of distances, and has found the following semi-empirical formula:

$$P + A(\phi, 0.5) = \frac{26 \cos \phi}{(f_{mc} \cos \phi)^{0.4}} \tag{26}$$

(NIGHT)

Note that (22) indicates an increasing loss with increasing frequency, presumably because of a deeper penetration of the D layer as the frequency is increased, while (26) indicates that the loss decreases with increasing frequency. At the higher frequencies where (26) was established, the waves penetrated the D layer and, as shown by Martyn[47] this behavior of $P + (\phi, 0.5)$ with frequency and angle of incidence is to be expected. By virtue of the method used for its determination, (26) includes the polarization loss P; since the extraordinary waves are much weaker than the ordinary waves in this frequency range, there will be additional polarization loss at each reflection from the ionosphere. With the above discussion in mind, it seems appropriate to assume that the penetration frequency of the D layer at night is effectively defined by the following relation:

$$P + A(\phi, 0.5)_{(26)} = P + A(\phi, 0.5)_{(22)} \tag{27}$$

(At the D layer penetration frequency, f_D, at night)

As determined in this way, the D layer penetration frequency at night varies from about 500 kc at vertical incidence to about 250 kc with $\cos\phi = 0.164$, the minimum value expected for a 90 km layer height; the anomalous behavior of this penetration frequency suggests that neither of our empirical absorption formulas are very dependable in this intermediate range of frequencies. Since nothing better is readily available, it was decided to calculate the transmission loss at night at frequencies greater than the above-defined D layer penetration frequency by using $m\ 26 \cos\phi/(f_{Mc} \cos\phi)^{0.4}$ as the total loss on reflection; the reflection height was assumed to be 110 km at night, but the value of $\cos\phi$ to be used in the absorption equation was determined on the assumption that the absorption takes place at a height of 100 km.

Figs. 37 to 40 give the median transmission loss expected between short vertical electric dipoles at 500 kc and at 1,000 kc in over-land and over-sea propagation and for day and night conditions. The absorption at night was determined by (26) as described above, but, in the daytime, (24) and (25) were used since radio waves in this frequency range are then presumably reflected and absorbed by the D layer at an assumed height of 70 km.

At still higher frequencies during the daytime, the radio waves will penetrate the D layer and be reflected by the E layer at a height of about 110 km. The ionospheric absorption is so great during the daytime in the range of frequencies from, say 500 kc to 4 Mc, and

MEDIAN TRANSMISSION LOSS OVER LAND AT 500 kc

$\sigma = 0.005$ Mhos/meter, $\epsilon = 15$; $h_t = h_r = 30$ feet

Day h = 70 km ; Night h = 110 km

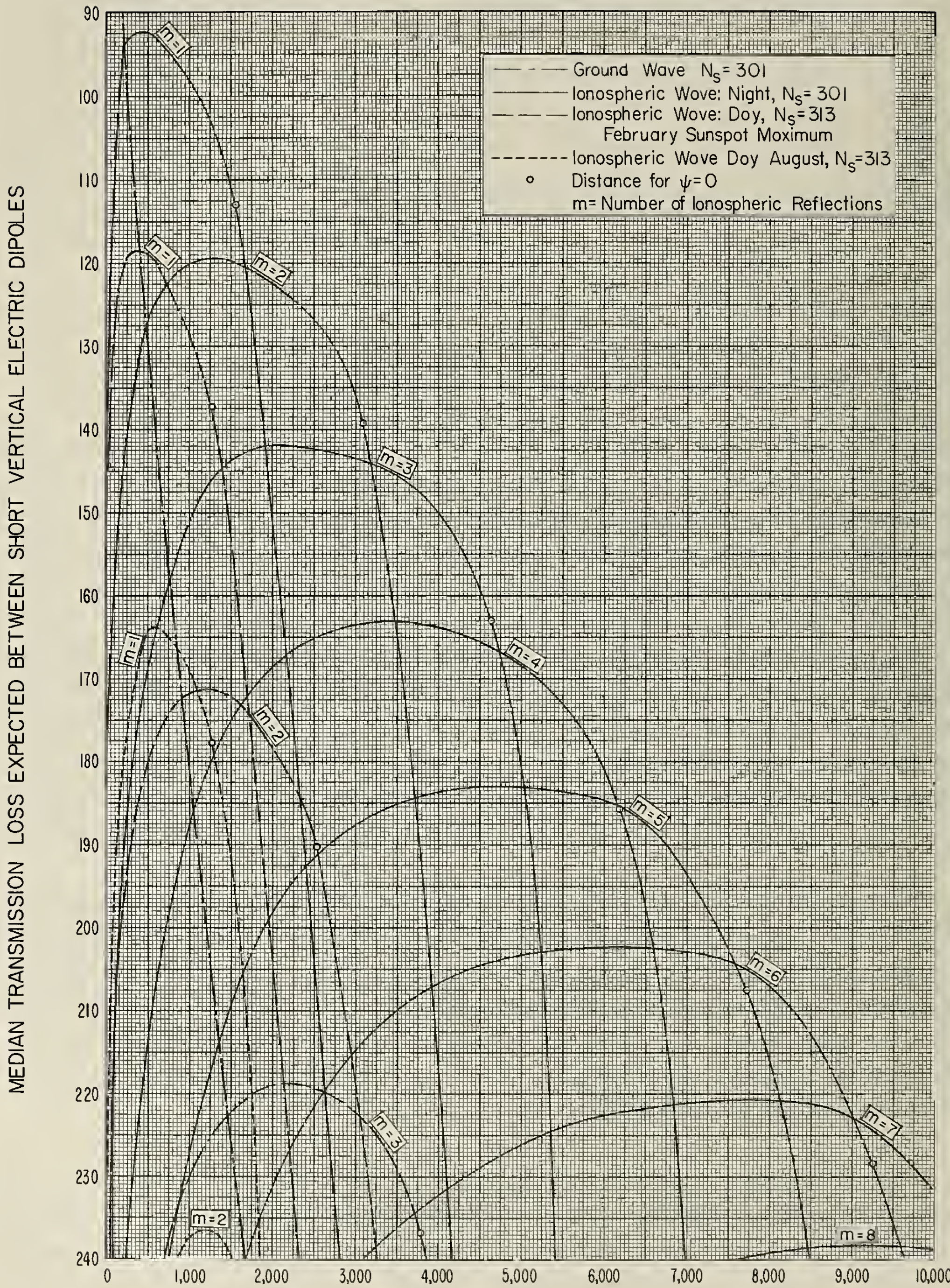

Figure 37

MEDIAN TRANSMISSION LOSS OVER SEA AT 500 kc

$\sigma = 5$ Mhos/meter, $\epsilon = 80$, h = h = 30 feet

Day h = 70 km ; Night h = 110 km

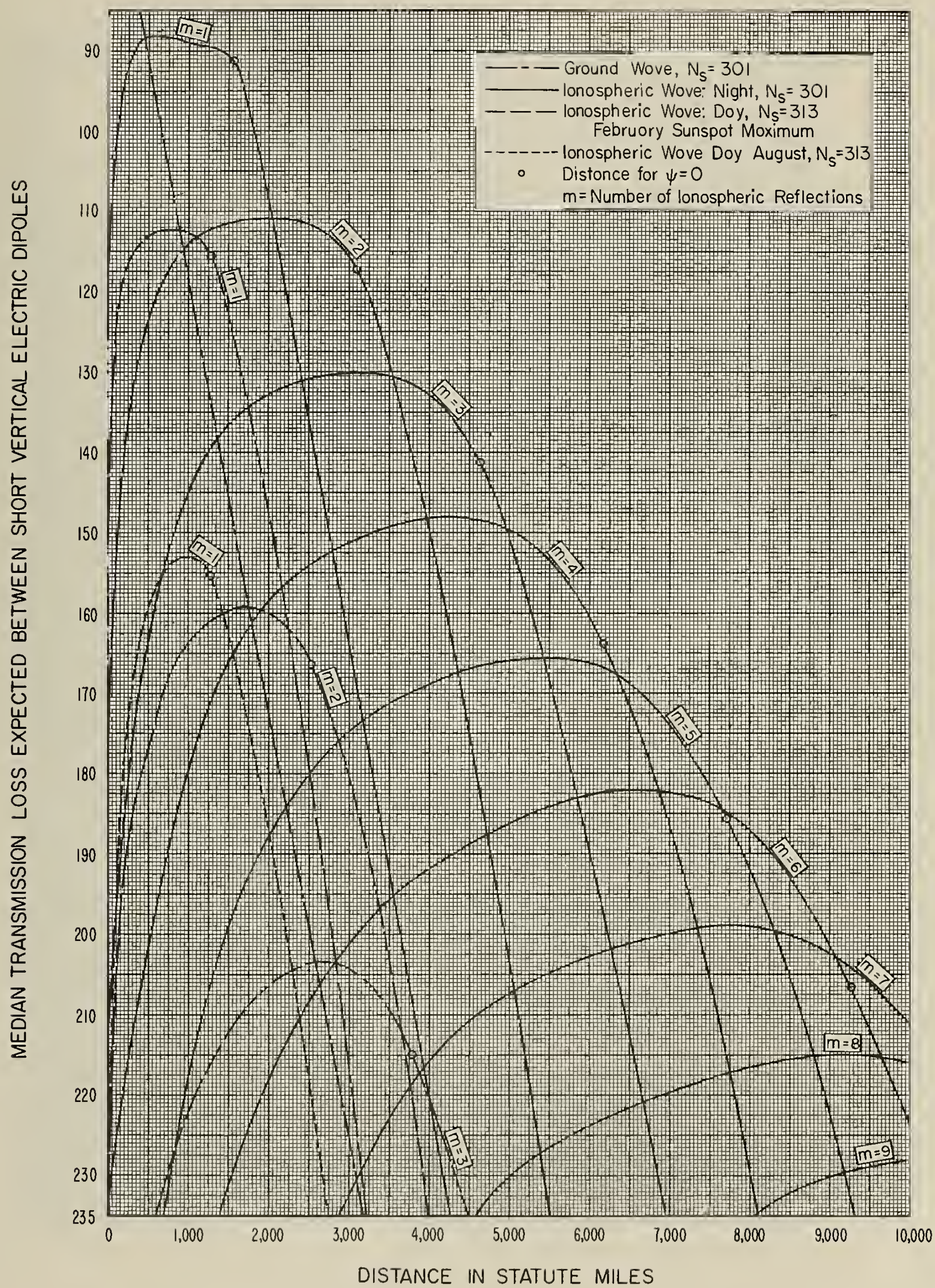

Figure 38

MEDIAN TRANSMISSION LOSS OVER LAND AT 1000 kc

σ = 0.005 Mhos/meter, ϵ = 15; $h_t = h_r$ = 30 feet

Day h = 70 km ; Night h = 110 km

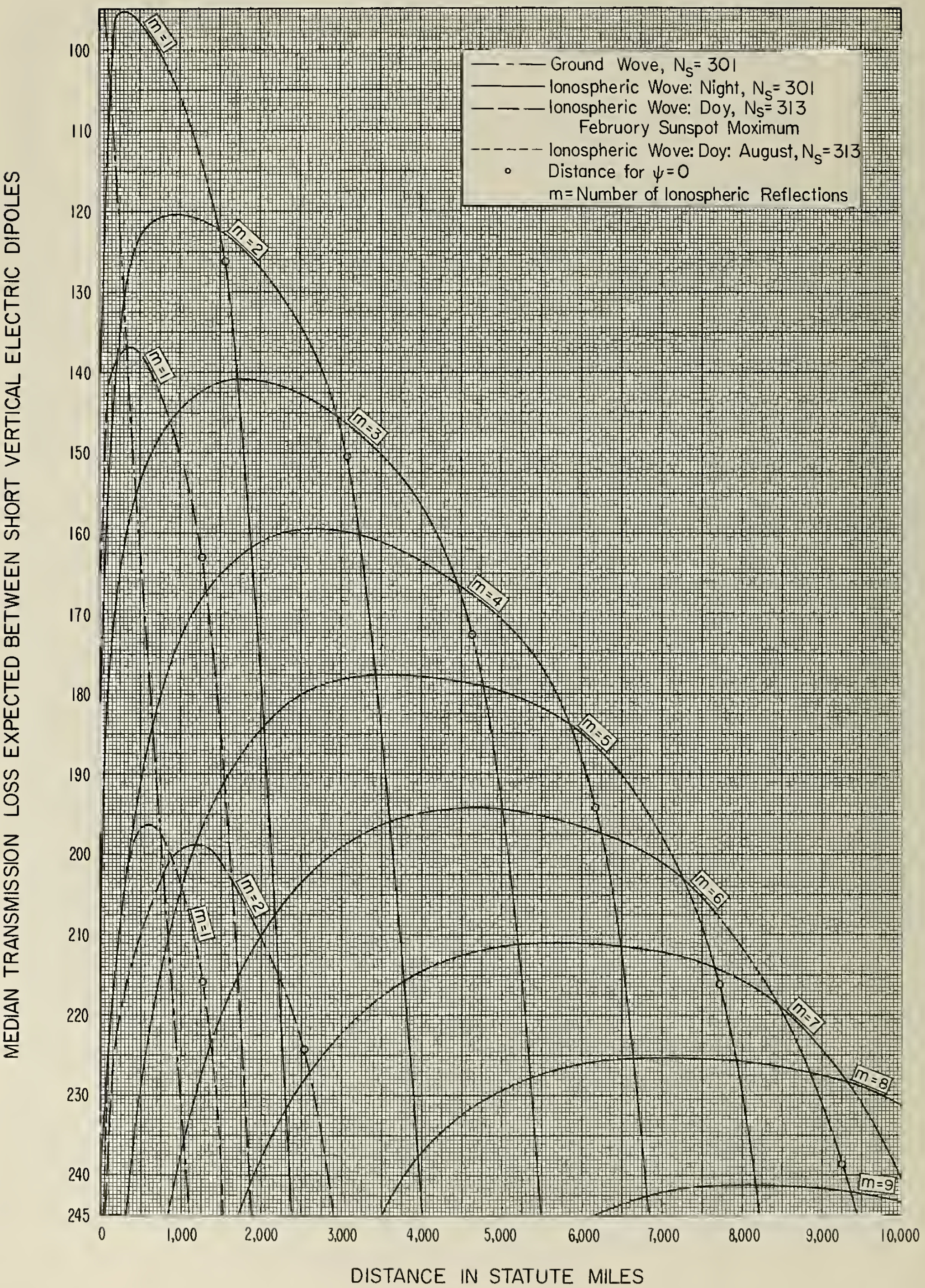

Figure 39

MEDIAN TRANSMISSION LOSS OVER SEA AT 1000kc

σ = 5 Mhos/meter; ϵ = 80, $h_t = h_r$ = 30 feet

Day h = 70 km ; Night h = 110 km

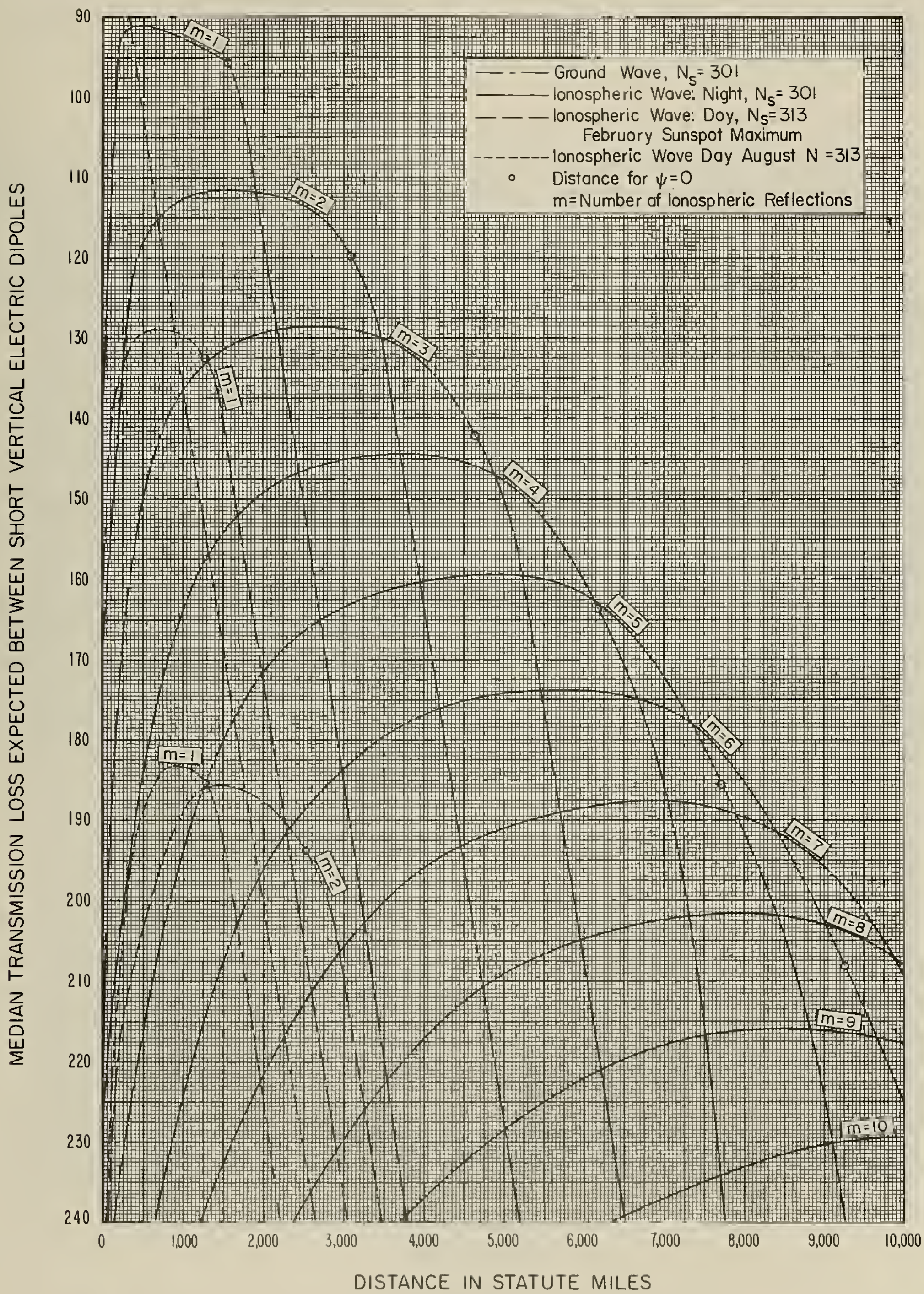

Figure 40

the reflection phenomena so complex, with reflections taking place sometimes at the D layer, sometimes at the E layer and sometimes at the F layer, that useful, simple absorption formulas are not available. For this reason the calculations of transmission loss given in this report for this range of frequencies have been made by extrapolating (23), (24) and (25) to higher frequencies, and by extrapolating to lower frequencies the absorption formulas applicable to the high frequency band as discussed in the next section.

Figs. 41 to 45 give transmission losses for propagation over land, based on the above-described methods of computation and on the methods described in following sections, and are designed to show more clearly the effect of radio frequency for day and night, for two seasons and for minimum and maximum sunspot conditions. Only one set of curves are presented for propagation at night since the seasonal and sunspot cycle effects on the transmission loss are comparatively small at night. The curves on these figures give the transmission loss expected between short electric dipole antennas, oriented vertically at frequencies less than 5 Mc and horizontally for frequencies greater than 5 Mc, for the ground wave and for the particular sky wave mode with a minimum transmission loss at the distances 200, 500, 1,000, 2,000, 5,000 and 10,000 miles. At each distance we have shown only the value expected for the single sky wave mode with the minimum transmission loss; with continuous wave transmission, the losses would be several db less than these values, particularly at the larger distances where several sky wave modes with comparable intensities are expected. Note that ground proximity losses L_a and L_b, as discussed in Appendix III, have been omitted in calculating the values shown on Figs. 41 to 45.

MEDIAN TRANSMISSION LOSS FOR MIDNIGHT AT THE RECEIVING ANTENNA

February; Sunspot Maximium; σ =0.005 Mhos/meter; ϵ =15; $h_t = h_r$ = 30 feet
West to East Transmission Path with Washington, D.C. at the Midpoint

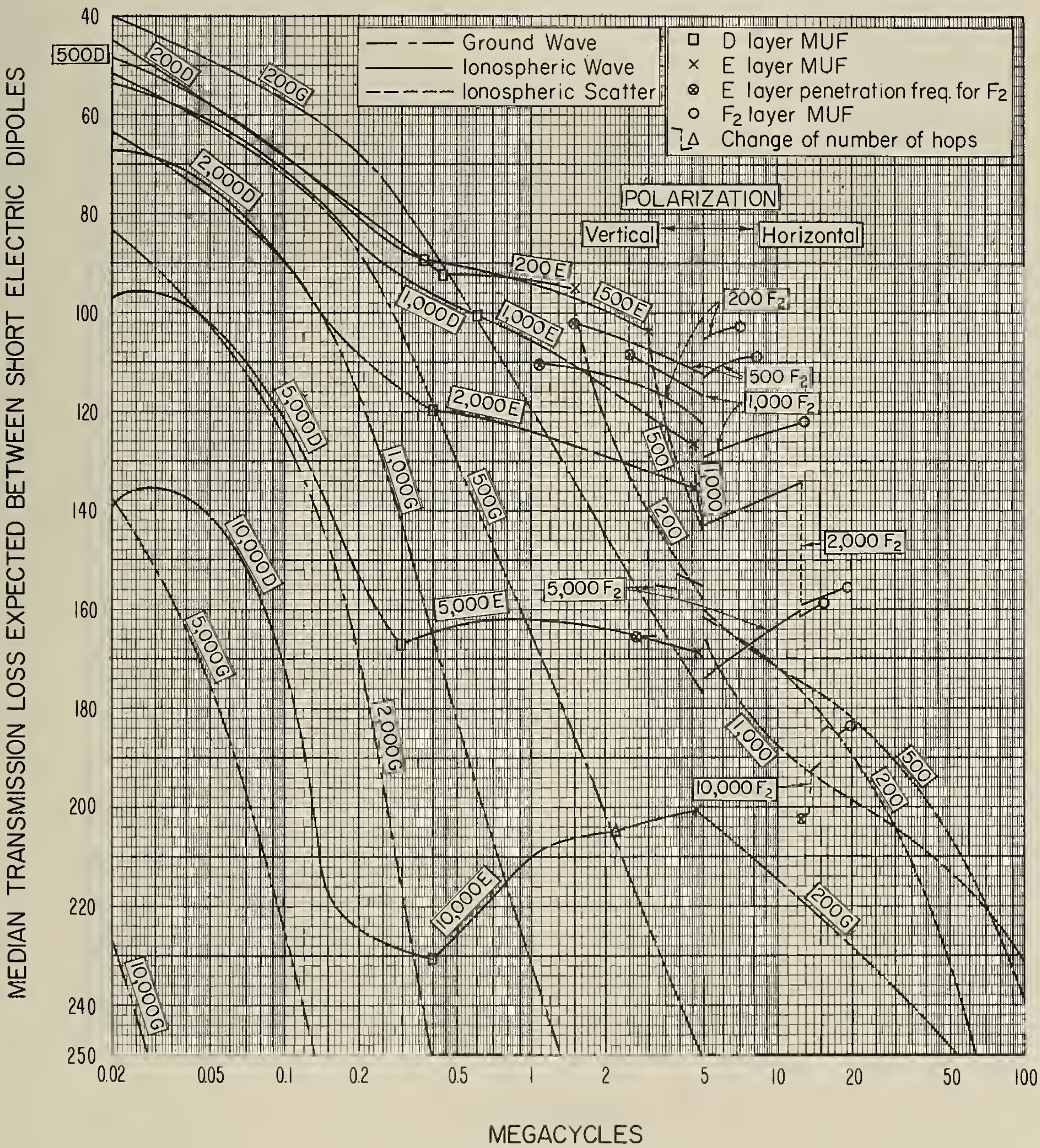

Figure 41

MEDIAN TRANSMISSION LOSS FOR NOON AT THE RECEIVING ANTENNA

February; Sunspot Minimum; σ=0.005 Mhos/meter; ϵ=15; $h_t=h_r$=30 feet
West to East Transmission Path with Washington, D.C. at the Midpoint

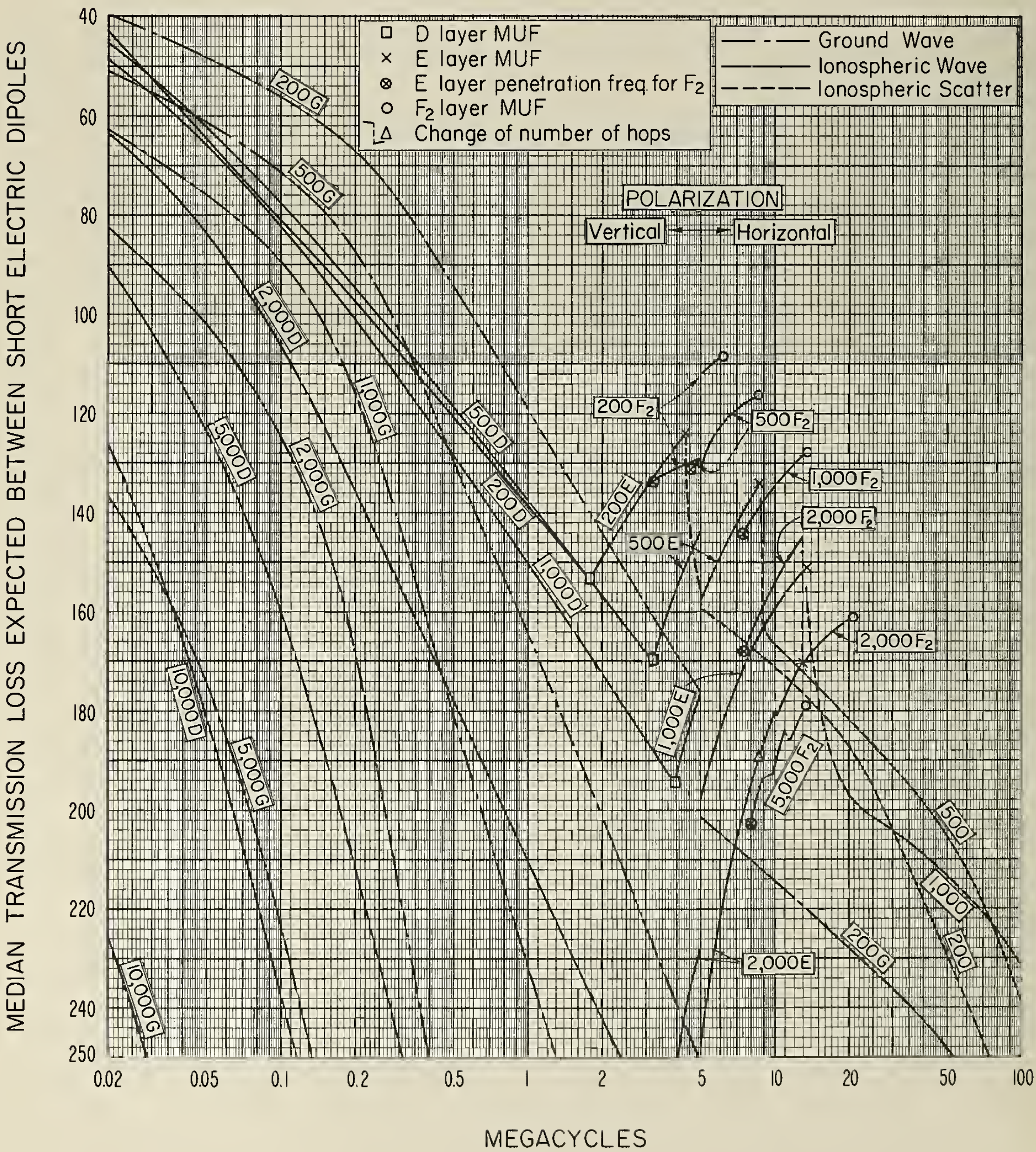

Figure 42

MEDIAN TRANSMISSION LOSS FOR NOON AT THE RECEIVING ANTENNA

February ; Sunspot Maximium ; $\sigma = 0.005$ Mhos/meter , $\epsilon = 15$; $h_t = h_r = 30$ feet

West to East Transmission Path with Washington, D.C. at the Midpoint

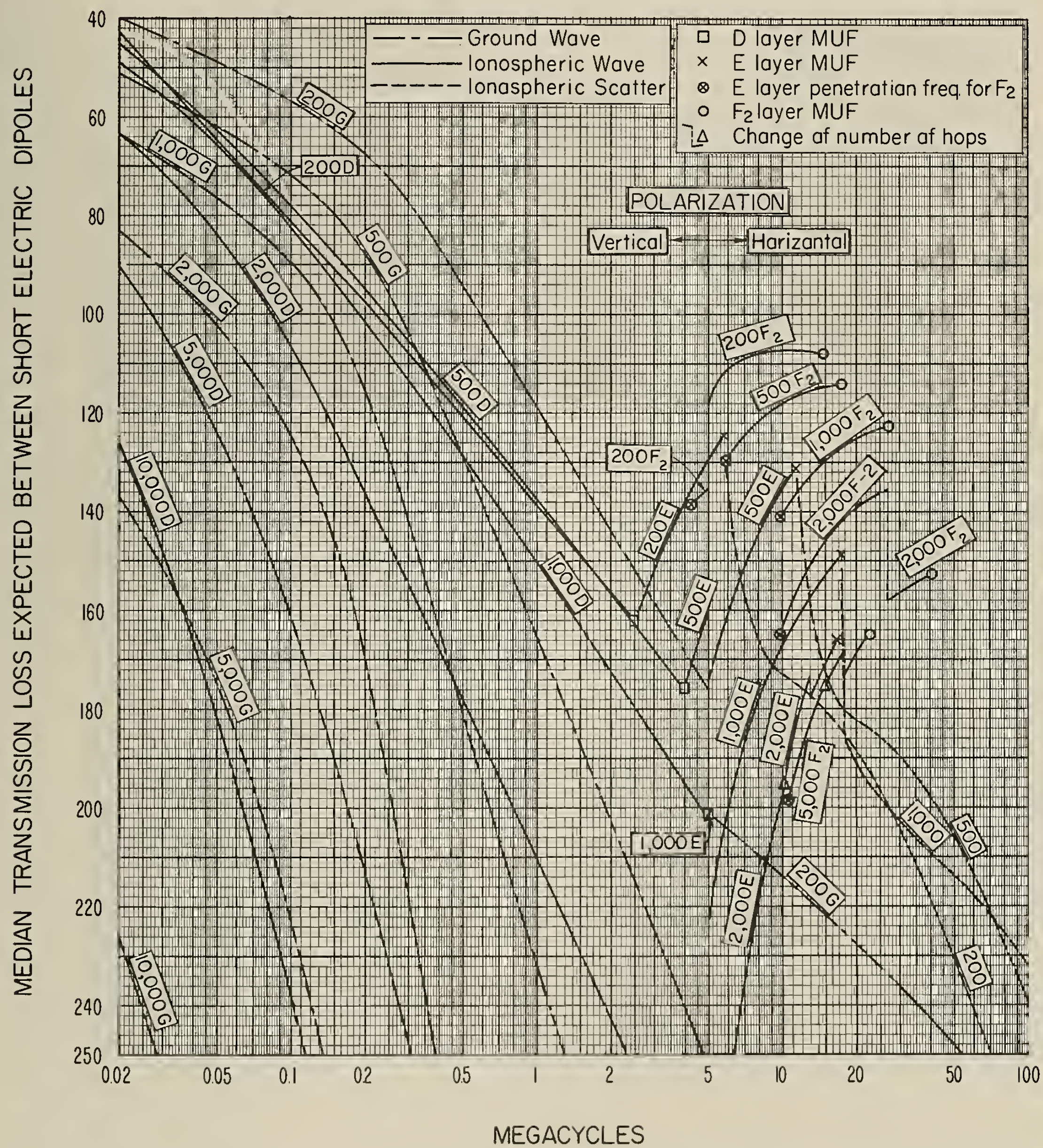

Figure 43

MEDIAN TRANSMISSION LOSS FOR NOON AT THE RECEIVING ANTENNA
August ; Sunspot Minimum ; $\sigma = 0.005$ Mhos/meter ; $\epsilon = 15$; $h_t = h_r = 30$ feet
West to East Transmission Path with Washington, D.C. at the Midpoint

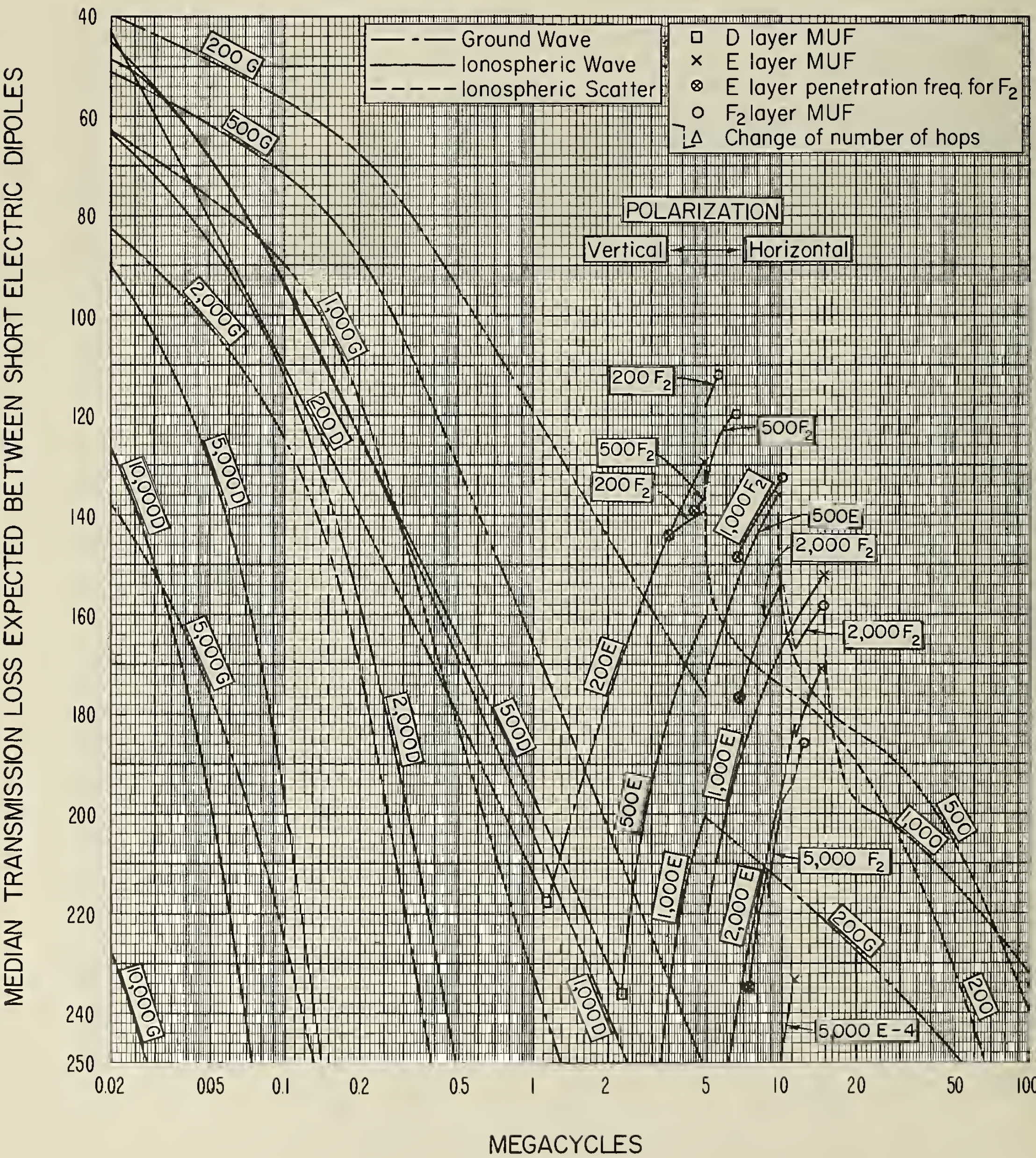

Figure 44

MEDIAN TRANSMISSION LOSS FOR NOON AT THE RECEIVING ANTENNA

August; Sunspot Maximum; σ=0.005 Mhos/meter; ϵ=15; h_t=h_r=30 feet

West to East Transmission Path with Washington, D.C. at the Midpoint

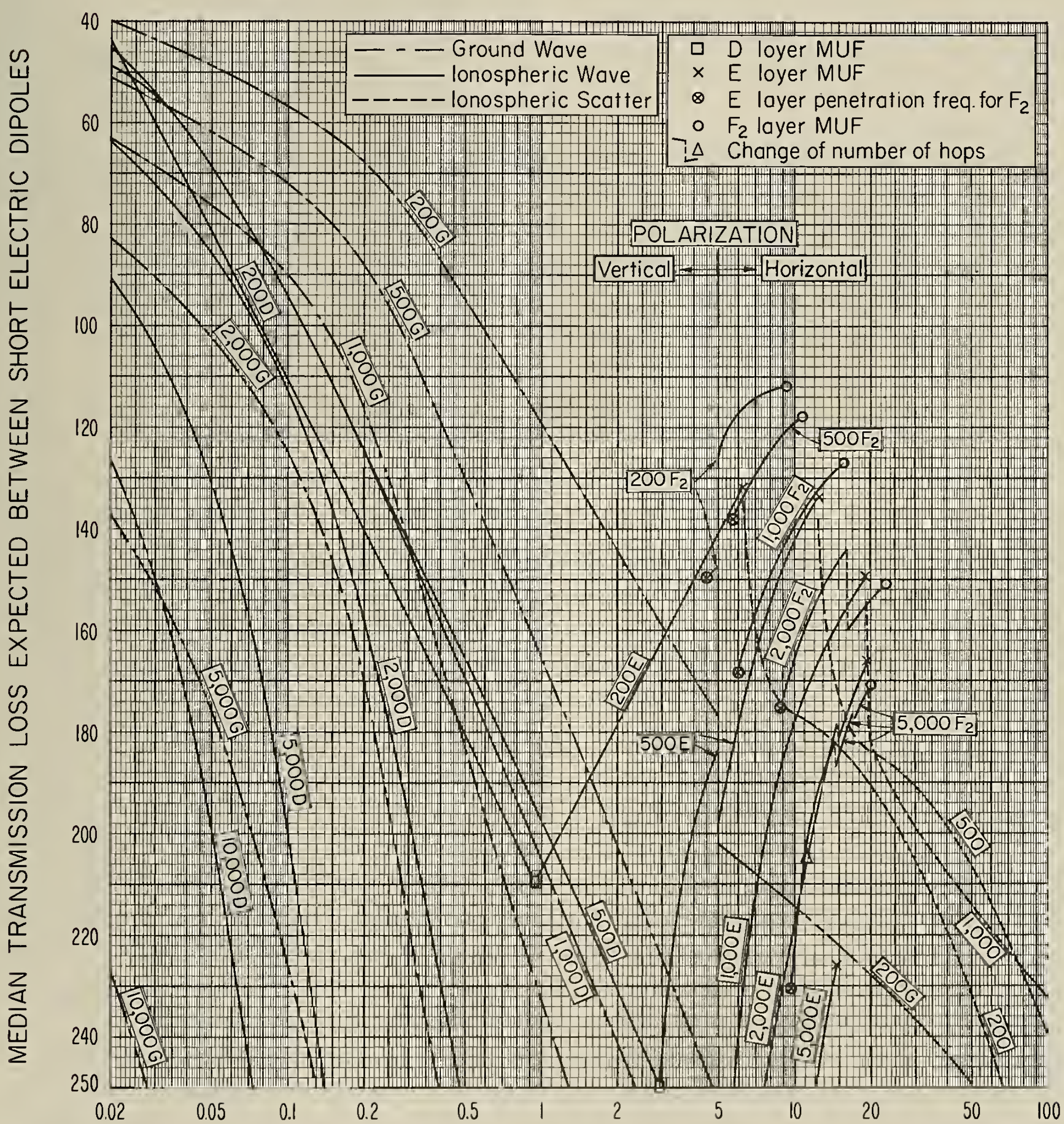

Figure 45

4.3 High Frequency Ionospheric Propagation

We see on Figs. 41 to 45 that the variation of transmission loss with frequency changes as the various layers of the ionosphere are penetrated. The method of determining the D layer penetration frequency was described in the preceding section, and the penetration frequencies for the higher layers were determined by the methods described in references 24 and 25; for this purpose the propagation path was assumed to be from West to East with its midpoint at Washington, D. C., and with either noon or midnight at the eastern end of the path.

During the daytime the polarization and absorption losses in the high frequency band have been calculated by the methods described in a Signal Corps report. 48/ Thus the constant attenuation of 8.9 db found in their analysis has been somewhat arbitrarily attributed to a polarization loss P, and the following semi-empirical formula used for calculating the daytime absorption:

$$A(\phi,\ 0.5) = \frac{615.5\,\{\cos\,(0.881\,\chi)\}^{1.3}\,(1 + 0.0037\,s)}{(f_{Mc} + f_H)^{1.98}\,\cos\,\phi} \qquad \text{(DAY)} \qquad (28)$$

In this formula χ denotes the zenith angle of the sun at the reflection point, and s denotes the smoothed Zurich sunspot number; for sunspot minimum, s was set equal to 10, and for sunspot maximum, s was set equal to 150. The gyrofrequency, $f_H = 1.5$ Mc, on the average in the United States. The angle of incidence, ϕ, to be used in (28) refers to the value this angle will have at the absorption level, and this angle will be systematically larger, for a given angle of elevation ψ, than the angles of incidence at the higher layers where the reflections take place. The Signal Corps analysis was based on the assumption that the absorption takes place at a height of 100 km and this same height was used in our calculations. In the Signal Corps report, convenient graphical methods are given for determining many of the factors involved in calculating (28). Prof. A. Kazantsev 49/ 50/ has proposed a method for calculating $A(\phi,\ 0.5)$ which, in essence, involves the replacement of the numerator of (28) by a constant times the square of the penetration frequency of the E layer at vertical incidence; this method appears to have considerable merit, but a critical determination of its accuracy compared to that of the Signal Corps method has not yet been published.

Thus, during the daytime we have used (9) for calculating the median transmission loss in the high frequency band with $P = 8.9$ db and $A(\phi, 0.5)$ determined by (28). Note that the focusing is probably negligible in this frequency range since the ionosphere will very likely appear rough to these radio waves most of the time; in the absence of quantitative information on ionospheric roughness at these higher frequencies, we have arbitrarily set $C_m(R, 0.5) = 0$ at all distances for $f \geq 2$ Mc both day and night.

At night the absorption in the high frequency band is quite small; it has been estimated in this report by means of (26). We have already noted, however, that (26) includes a polarization loss, P, and the Signal Corps report indicates, in effect, that the absorption plus the polarization loss at night is equal to 8.9 db; thus it appears to be appropriate to use (9) for calculating the transmission loss with $P + A(\phi, 0.5)$ calculated by (26) for the lower frequencies where $m\{P + A(\phi, 0.5)\} > 8.9$ db and to set $m\{P + A(\phi, 0.5)\} = 8.9$ db for all higher frequencies. This is the method used for the examples presented in this report.

4.4 Ionospheric Scatter Propagation

At frequencies above the penetration frequency of the E layer, the radio waves are scattered forward with sufficient intensity to be usable for communications over distances of the order of 600 to 1,400 miles. 51/ 52/ 53/ The transmission losses shown on Figs. 41 to 45 for this mode of propagation are based on the measurements reported by Bailey, Bateman and Kirby 51/ for the Fargo, North Dakota to Churchill, Manitoba path as extrapolated to other distances and frequencies by means of a theory developed by Wheelon. 54/ 55/ 56/ Thus Wheelon attributes the scattering to turbulence in the D and E regions of the ionosphere and, on the assumptions (1) that the spectrum of this turbulence may be determined by the mixing in gradient hypothesis and (2) that the viscosity cut-off has a characteristic scale $\ell_s = 1.5$ meters, is able to develop a formula for the transmission loss expected with this mode of propagation.

Wheelon's analysis leads directly to the spectrum of the turbulence, but the turbulence may also be characterized in the range of wave numbers smaller than the viscosity cut-off by the correlation function $(r/\ell_o) K_1(r/\ell_o)$ which describes the degree of correlation in the fluctuations in electron density at points a distance r apart; K_1

denotes the modified Bessel function of the second kind and ℓ_o is a characteristic scale of the turbulence, set equal to 100 meters in our subsequent analysis. It is interesting to note that this same correlation function is applicable for describing tropospheric turbulence as well. 57/ 58/

The following formula gives the median transmission loss expected for the ionospheric scatter mode of propagation, i.e., on frequencies above the effective maximum usable frequency, f_{MUF}, of the scattering region:

$$L_{ms} = L_{bf}(R) + A_t(\psi) + A_r(\psi) - S(0.5) - 10 \log_{10} \sec \phi$$

$$+ B(k^2, \ell_o, \ell_s) + P + A(\phi, 0.5) \qquad (f_{Mc} \geq f_{MUF}) \qquad (29)$$

In the above, $L_{bf}(R)$ denotes the free space transmission loss for waves traveling a distance corresponding to an average scatter path of length R; this path length has been determined in this report on the assumption that the mean layer height h = 87 km both day and night. For horizontally polarized waves the following formula may be used to estimate the median value for the sum of the space wave radiation factors:

$$A_t(\psi) + A_r(\psi) = - 20 \log_{10}[2 \sin (2\pi h_t \sin \psi / \lambda)]$$

$$- 20 \log_{10} [2 \sin(2\pi h_r \sin \psi/\lambda)] - G_p(0.5) \quad \text{(Horizontal polarization)} \qquad (30)$$

In the above, h_t and h_r denote the heights of the transmitting and receiving antennas above the local terrain, and $G_p(0.5)$ denotes the median path antenna gain. For the high gain antennas normally used for communication by scatter, there will usually be a substantial "loss in gain" relative to the value G_p would be expected to have for communication between similar antennas in free space. For example, on the Fargo to Churchill path, G_p as determined for successive half-hour periods of time, was found to be a random approximately normally distributed variable with a median value $G_p(0.5)$ = 25.7 db and a standard deviation of 5.85 db; the sum of the free space gains in this case was about 40 db. It has been found that some of this "loss in gain" can be recovered by directing the antenna towards the better scattering regions. The values of transmission loss shown on Figs. 41 to 45 are for propagation between short horizontal electric dipoles, and in this case $G_p = 3.52$ db. The antenna heights, h_t and h_r, were taken to be 30 feet except at the higher frequencies where somewhat lower values of h_t and h_r were chosen so that $4 h_{t,r} \sin \psi/\lambda = 1$; this choice of h_t and h_r effectively minimized the loss and in this case $A_t(\psi) + A_r(\psi) = -12.041 - G_p$. Near the maximum effective range for ionospheric scatter, 53/ the transmission loss increases so rapidly with increasing distance that it is useful in some cases to use very large antenna heights so as to increase the range slightly by the amounts indicated by (12).

The factor S involves the intensity and scales of the turbulence and, together with G_p, exhibits most of the variability of the transmission loss. The median value S(0.5) undoubtedly varies somewhat diurnally, seasonally, and with the sunspot cycle but, since such changes are not large with a probable extreme range of the monthly medians at a given time of day of less than 20 db, we have calculated all of the examples in this report by setting S(0.5) = - 8.4 db, the value obtained for the Fargo-Churchill path. An analysis is presented in Appendix II which shows that this value of S(0.5) is not inconsistent with what is presently known about ionospheric turbulence.

The factor $10 \log_{10} \sec \phi$ provides a measure of the size of the effective scattering volume for transmission paths of various lengths.

The transmission loss factor $B(k^2, \ell_o, \ell_s)$ may be expressed:

$$B(k^2, \ell_o, \ell_s) = 25 \log_{10} [1 + k^2 \ell_o^2] + 20 \log_{10} [1 + (k^2 \ell_s^2)^{2/3}] + (40/3 \log_{10} [1 + (k^2 \ell_s^2)^2] \tag{31}$$

Although the characteristic scale lengths, ℓ_o and ℓ_s, are likely to be somewhat variable diurnally and seasonally, we have, for the purpose of the calculations in this report, taken them to be equal to the constant values ℓ_o = 100 meters and ℓ_s = 1.5 meters; k^2 is defined as follows:

$$k^2 = \left[\frac{4\pi}{\lambda} \cos \phi \right]^2 \left(1 - \frac{f_{MUF}^2}{f^2} \right) \tag{32}$$

When f is equal to the maximum usable frequency, f_{MUF}, $k^2 = 0$, the wavelength in the medium increases without limit, and the scattering is no longer directed forward, but occurs uniformly in all directions. In this limiting case, $B(k^2, \ell_o, \ell_s) = 0$ and (29) indicates a scatter loss exceeding that predicted by (9) for normal E layer propagation at the MUF by only $(8.4 - 10 \log_{10} \sec \phi)$ decibels. For the calculations in this report, we have somewhat arbitrarily used the median E layer MUF as a measure of the MUF of the scattering region.

For ionospheric scatter, we have taken P = 3 db for both day and night propagation conditions. During the day, the absorption term $A(\phi, 0.5)$ was computed by (28), but at night $P + A(\phi, 0.5)$ was determined by (26) up to frequencies for which the resulting value is greater than 3 db, and at higher frequencies $P + A(\phi, 0.5)$ is set equal to 3 db.

There is no present evidence for the existence of F layer ionospheric scatter or for multi-hop E layer scatter and, for this reason, the transmission loss curves for d = 2,000, 5,000, and 10,000 miles stop abruptly at the MUF; the transmission loss is expected to increase very rapidly indeed at frequencies just above the F layer MUF.

5. The Bending of Radio Waves by the Troposphere

Since the density as well as the absolute humidity of the air decrease with the height, h, above sea level, the refractive index, n, also usually decreases with h, and this causes radio waves leaving an antenna at a given angle, ψ, to bend down towards the earth, the amount of this bending being larger, the smaller the value of ψ. This is illustrated on Fig. 46 which shows the total bending, τ, of a radio wave traveling entirely through the troposphere and subsequently being reflected at an ionospheric layer.

Since the refractive index, n, departs from unity by only a few parts in 10^{-4}, it is convenient to describe n in terms of the refractivity, N, which is defined:

$$N = (n - 1) \times 10^6 \tag{33}$$

If the value of N were known as a function of time at every point in the atmosphere between two radio antennas, it should be possible, in principle, to predict the instantaneous behavior of the transmission

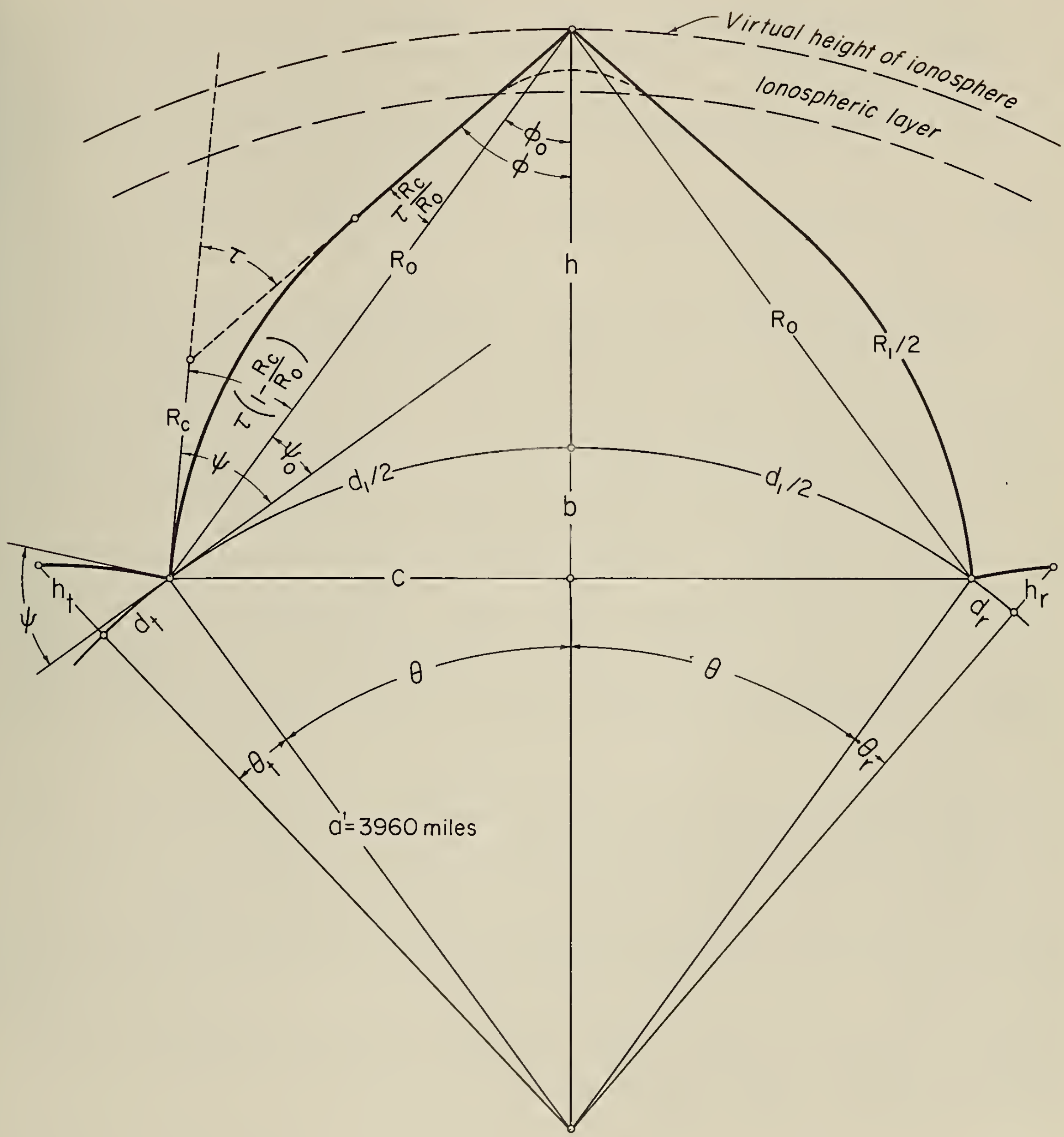
Virtual height of ionosphere
Ionospheric layer
ϕ_o
ϕ
$\tau \frac{Rc}{Ro}$
τ
R_o
h
R_o
$R_1/2$
$\tau\left(1-\frac{Rc}{Ro}\right)$
R_c
ψ
ψ_o
$d_1/2$
$d_1/2$
b
c
h_t
d_t
ψ
d_r
h_r
θ
θ
θ_t
θ_r
a'=3960 miles

Figure 46

loss in propagation between these antennas. Actually, of course, this is not feasible because of the complexity of the solution of such an electromagnetic problem. Furthermore, even if the engineer could be provided with this instantaneous information, he would normally be forced to describe it in some statistical terms before he could use it effectively in the design or use of radio systems. Consequently, we are led to the description of N in statistical terms, with the hope that these statistical characteristics of N may be used for the prediction of the more important statistical parameters describing the transmission loss. At a given instant N will vary considerably with height above the surface, and, to a lesser extent, with distance along the path. If, however, we average the values of N over a period of an hour, then $\overline{N}$ will, on typical propagation paths, be more nearly constant along the path at a given height, but will normally decrease monotonically with increasing height above the surface. For the solution of most radio prediction problems, it is permissible and, indeed, desirable to average $\overline{N}$ over still longer periods of time in order to obtain mean conditions useful in radio systems design. Thus, for predicting the diurnal, seasonal, or geographical variations of the median transmission loss, we may further average the values of $\overline{N}$ as determined from day to day over a period of many years for a particular hour of the day, month of the year and geographical location. The resulting values $\overline{\overline{N}}$ will vary still less along the path and, on most paths, $\overline{\overline{N}}$, for a given time of day and season of the year, may be taken to be a function only of the height, $h - h_s$, above the earth's surface where h represents the height, expressed in kilometers, above sea level, while h_s represents the height of the surface above sea level. There will be some paths for which $\overline{\overline{N}}$ will also vary appreciably in the horizontal plane; examples are paths with one terminal over land and the other over the sea, and these will undoubtedly require special treatment. Since the average values $\overline{\overline{N}}$ tend for most paths to be very nearly horizontally homogeneous, it should only be necessary to know the vertical profile of $\overline{\overline{N}}$ at one point along the path for a successful prediction of the median transmission loss at a particular time of day and season of the year. For very long paths on which $\overline{\overline{N}}$ does vary appreciably along the path, we may base our radio predictions on the two $\overline{\overline{N}}$ profiles at the intersections of the two radio horizons with the great circle path.

From the above discussion it appears to be desirable to study these $\overline{\overline{N}}$ profiles, and it will be convenient in the following analysis to omit the superscripts and simply let N(h) denote these long-term average values. The most generally reliable single parameter for the description of the profile as it affects radio propagation is the difference, ΔN, in the values, N_1, at a height of one kilometer above the surface and N_s the value at the surface:

$$\Delta N \equiv N(h_s + 1) - N(h_s) \equiv N_1 - N_s \tag{34}$$

Note that ΔN is a negative quantity. Most of the diurnal, seasonal, and geographical variations in propagation between antennas at heights of less than one kilometer above the surface may be predicted on the assumption that N(h) decreases linearly with height above the surface up to a height of one kilometer:

$$N(h) = N_s + \Delta N(h - h_s) \qquad [h_s \leq h \leq h_s + 1] \tag{35}$$

For radio propagation predictions at the higher frequencies above, say, 50 Mc, the above assumption of linearity for the initial decrease of N(h) with height is not adequate for some times of the day or for some geographical locations; in some of these special cases there may be ducting with a resulting substantial increase 59/ in the transmission loss for paths just short of the radio horizon, and a very large decrease 60/ in the transmission loss on paths just beyond the radio horizon. Since these appreciably non-linear profiles occur in only a very small percentage of all cases, 61/ we will not consider them further in this survey report. Furthermore, although the principles of duct propagation are well understood, 62/ 63/ 64/ there are nevertheless no very satisfactory formulas for predicting the transmission loss for the large variety of non-linear profiles typically encountered in practice.

The assumption of a linear profile makes possible the introduction of a great simplification in radio propagation predictions. Thus it has been shown 65/ that the behavior of radio waves in an atmosphere with a linear gradient is the same as that expected with no atmosphere for an earth with effective radius $a \equiv ka'$ where a' denotes the actual earth's radius, expressed in kilometers, and a is defined by:

$$\frac{1}{a} = \frac{1}{ka'} = \frac{1}{a'} + \frac{\Delta N}{(1 + N_s \cdot 10^{-6})} \tag{36}$$

Bean and Meaney 66/ demonstrate that there is a high correlation between the monthly median transmission loss and the monthly median values of ΔN, and give maps of the monthly median values of ΔN for the United States for several months of the year. The values of ΔN

must be determined from radio-sonde observations and are, as a consequence, not as readily available at all hours of the day nor for as many geographical locations as the surface values, N_s. Fortunately, ΔN may be predicted [67] with quite good accuracy from N_s and, in the absence of observations of ΔN, the following empirical formula may be used to determine the predicted value $\Delta N'$:

$$\Delta N' = -7.32 \exp\{0.005577\, N_s\} \tag{37}$$

If now we combine (35) and (37), we have the following expression for the initial behavior of N(h) in what will be referred to as the CRPL Standard Radio Refractivity Atmosphere as recently proposed and studied by Bean and Thayer: [67]

$$N(h) = N_s - (h - h_s)\, 7.32 \exp\{0.005577\, N_s\} \qquad [h_s \le h \le h_s + 1] \tag{38}$$

Note that the only parameters in (38) are the surface refractivity, N_s, and the height, h_s, of the surface above sea level.

Note that (37) may also be used to predict N_s in terms of known values of ΔN:

$$N_s' = 412.87 \log_{10}(-\Delta N) - 356.93 \tag{39}$$

When values of ΔN and of N_s are both available, and when the actual value of N_s differs from the value predicted by (39), it is better to use N_s' for predictions when $\psi < 3°$ rather than the actual value of N_s; in other words, ΔN is slightly better than N_s as a predictor of propagation conditions for small values of ψ. On the other hand, it is at present easier and usually also more accurate to predict N_s for some particular time of day, season of the year and geographical location, and then use (37) for determining $\Delta N'$, than it is to use the available maps [66] directly for the prediction of ΔN. It should also be noted that, even when ΔN is available, N_s is a better predictor [67] of the bending at high elevation angles: $\psi > 3°$. It is expected that the recent study program [68] proposed by the International Radio Consultative Committee (CCIR) will tend to expedite the gathering of the data on ΔN required for the development of suitable prediction methods; however, it is unfortunate that emphasis was given in that proposal to the gathering of data at only two hours of the day, 0200 and 1400 U. T., since it is precisely the large diurnal variation of ΔN, occurring at many locations, which is most difficult at present to predict with adequate accuracy.

The effect on N_s of the height of the surface above sea level may be determined from the relation:

$$N_s = N_o \exp(-c_s h_s) \tag{40}$$

where c_s = 0.1057/kilometer = 0.1701/statute mile = 0.03222/thousand feet. Bean and Horn 69/ give maps which may be used to estimate the value of N_o averaged throughout the day for the months of February and August at any geographical location in the world, together with a map of the annual range of N_s. A comprehensive climatological study of N_s for the United States is in preparation at C. R. P. L.; this study will make available charts useful for the prediction of N_o (and thus of N_s by means of (40) above) at 0200, 0800, 1400 and 2000 for February, May, August and November and, in addition, gives the detailed statistical characteristics of N_s at several representative weather stations in the United States.

Summarizing the above, we see that the average value of N up to a height of one kilometer above the surface may be predicted preferably, when ψ is small, in terms of a measured mean gradient, ΔN, or, alternatively and with only slightly less accuracy, in terms of the mean value of the surface refractivity, N_s. Above one kilometer, N decreases exponentially with height, and Bean and Thayer 67/ give the following formulas for N(h) in this range:

$$N(h) = N_1 \exp[-c_i(h - h_s - 1)] \qquad (h_s + 1 \leq h \leq 9 \text{ km}) \tag{41}$$

$$c_i = \frac{1}{8 - h_s} \log_e (N_1/105) \tag{42}$$

$$N(h) = 105 \exp[-0.1424 (h - 9)] \qquad h \geq 9 \text{ km} \tag{43}$$

Since the constant c_i depends only on N_s and h_s (see Table 5.1 below), it appears that the mean atmosphere may be described in most cases in terms of these two parameters or, alternatively, in terms of h_s and N_s' when ΔN is known. Note that h_s influences the description of the atmosphere [see (42)] only in the range from one kilometer above the surface to 9 km above sea level, and then only slightly for the range of values of h_s normally encountered in practice; consequently, we may, for practical purposes, consider that the atmosphere is well defined by the single parameter N_s. The success of this model in

Table 5.1

Constants for the CRPL Reference Atmospheres

N_s	h_s feet	a' MILES	$-\Delta N'$	k	a MILES	c_i per kilometer
0	0	3960	0	1	3960.00	0
200	10,000	3961.8939	22.3318	1.16599	4619.53	0.106211
250	5,000	3960.9470	29.5124	1.23165	4878.50	0.114559
301	1,000	3960.1894	39.2320	1.33327	5280.00	0.118710
313	700	3960.1324	41.9388	1.36479	5404.57	0.121796
350	0	3960	51.5530	1.48905	5896.66	0.130579
400	0	3960	68.1295	1.76684	6996.67	0.143848
450	0	3960	90.0406	2.34506	9286.44	0.154004

predicting the bending of radio waves has been examined by Bean and Thayer [67] and leaves little to be desired except in the small percentage of cases involving non-linear profiles.

For some mathematical analyses of radio propagation, the above-described CRPL Model Radio Refractivity Atmospheres* have the undesirable characteristic of having discontinuities in the gradient at one kilometer above the surface and at 9 km above sea level. The following exponential model is free of this defect and, although it does not fit the meteorological data above one kilometer as well as the CRPL Model Radio Refractivity Atmospheres, it does nevertheless provide a representation useful for many applications:

$$N(h) = N_s \exp[-c_e(h - h_s)] \tag{44}$$

---

* The CRPL Model Radio Refractivity Atmospheres have arbitrary values of N_s, h_s, and ΔN; in the CRPL Standard Radio Refractivity Atmospheres N_s and ΔN are related by (37) and (39), but h_s is arbitrary; and in the CRPL Reference Radio Refractivity Atmospheres N_s, ΔN, and h_s have the values given in Table 5.1.

The constant c_e is defined in terms of ΔN and N_s:

$$\exp(-c_e) = 1 + \frac{\Delta N}{N_s} \tag{45}$$

Table 5.2 gives the values of c_e for several values of ΔN for the particular case in which N_s' is determined by (39); the value $N_s = 313$ represents the average of the observed values of N_s in the United States.

Table 5.2

Typical Constants c_e for CRPL

Standard Exponential Radio Refractivity Atmospheres

$$N(h) = N_s \exp[-c_e(h - h_s)]$$

ΔN	N_s'	c_e per kilometer
0	0	0
22.3318	200	0.118400
29.5124	250.0	0.125625
30	252.9	0.126255
39.2320	301.0	0.139632
41.9388	313.0	0.143859
50	344.5	0.156805
51.5530	350.0	0.159336
60	377.2	0.173233
68.1295	400.0	0.186720
70	404.9	0.189829
90.0406	450.0	0.223256

COMPARISON OF RAYS IN THE CRPL REFERENCE REFRACTIVITY ATMOSPHERES—1958 AND THE 4/3 EARTH ATMOSPHERE

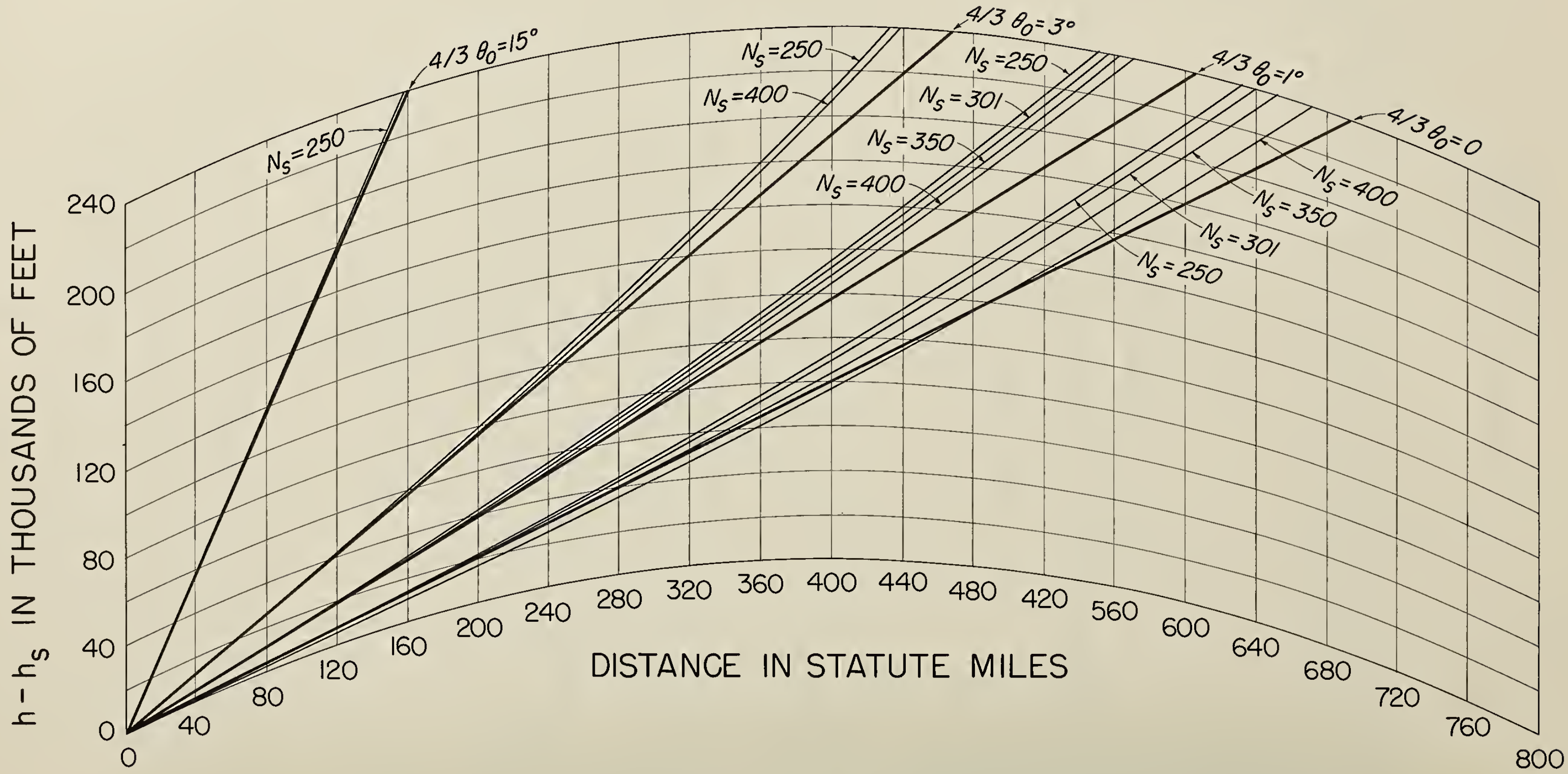

Figure 47

Fig. 47 compares the paths followed by radio rays leaving the earth at several selected elevation angles, ψ, for several of the CRPL reference atmospheres with the paths expected in a four-thirds earth atmosphere. Thus, the graph paper used for tracing these rays was so designed that they are straight lines for the linear gradient atmosphere corresponding to an effective earth's radius of 5,280 statute miles, i.e., $(4/3) \cdot 3{,}960$ miles. Note the very large departures at large heights of the rays in all of these representative atmospheres from the rays in the usually assumed four-thirds' earth atmosphere. Note that there are large departures from the four-thirds' earth atmosphere at large heights for $N_s = 301$, even though the bending in this atmosphere is correct for heights $h - h_s$ less than one kilometer. An appropriate allowance for this difference in bending is made in the tropospheric curves presented in subsequent sections of this report, but no such allowance was made in preparing Figs. 3, 4 and 6. A good estimate of the correction which should be made to the altitudes of the contours on Figs. 3 and 4 is simply the difference in heights, at the appropriate range, between the 4/3 earth rays and the N_s atmosphere rays. For a detailed discussion of such corrections with appropriate graphs, see a recent report by Rice, Longley and Norton.[70]

The Bean and Thayer report gives the elevation angle error $\epsilon \equiv \psi - \psi_o$ as a function of electrical path length, R_e, for rays in the reference atmospheres as well as $\Delta R_e \equiv R_e - R_o$.

$$R_e = \int_0^{(R_1/2)} n\,dR = c\,t_e \tag{46}$$

where c is the velocity of light in a vacuum and t_e is the time of transit along the ray path.

5.1 The Influence of Tropospheric Bending on Ionospheric Propagation

The bending of the radio waves by the troposphere has the effect of extending the range of ionospheric propagation and, although the effect is small, it is not negligible near oblique incidence. Table 5.3 shows the influence of N_s on R_1, d_1, and $\cos\phi$ for ionosphere heights h = 70, 90, 110, 225, 350, and 475 km. The calculations were made by tracing rays in the CRPL reference atmospheres with $N_s = 0$, 301 and 400. Since the variations with N_s are comparatively small, it would

Table 5.3: h = 70 km

	$N_s = 0$			$N_s = 301$			$N_s = 400$		
ψ m.r.	$R_1/2$ miles	d_1 miles	cos ϕ	$R_1/2$ miles	d_1 miles	cos ϕ	$R_1/2$ miles	d_1 miles	cos ϕ
0.0	588558 53*	116852 54	.147007	628625 53	124865 54	.144985	658709 53	130881 54	.144319
0.5	586581 53	116457 54	.147007	625995 53	124339 54	.144986	655233 53	130186 54	.144320
1.0	584611 53	116063 54	.147010	623384 53	123816 54	.144989	651804 53	129500 54	.144323
2.0	580691 53	115279 54	.147020	618219 53	122783 54	.144999	645083 53	128156 54	.144333
3.0	576797 53	114500 54	.147036	613131 53	121766 54	.145016	638543 53	126848 54	.144350
4.0	572930 53	113727 54	.147060	608118 53	120763 54	.145039	632178 53	125575 54	.144374
5.0	569090 53	112959 54	.147090	603179 53	119776 54	.145070	625984 53	124336 54	.144404
6.0	565277 53	112196 54	.147126	598313 53	118802 54	.145107	619952 53	123130 54	.144441
7.0	561490 53	111439 54	.147169	593518 53	117843 54	.145151	614075 53	121954 54	.144486
8.0	557729 53	110687 54	.147219	588791 53	116898 54	.145201	608345 53	120809 54	.144536
9.0	553996 53	109940 54	.147276	584132 53	115966 54	.145259	602754 53	119690 54	.144594
10.0	550288 53	109198 54	.147339	579538 53	115047 54	.145323	597294 53	118599 54	.144658
12.0	542953 53	107731 54	.147485	570537 53	113247 54	.145471	586737 53	116487 54	.144807
15.0	532148 53	105570 54	.147753	557475 53	110635 54	.145743	571708 53	113482 54	.145081
20.0	514666 53	102073 54	.148331	536771 53	106494 54	.146329	548453 53	108831 54	.145670
25.0	497832 53	987062 53	.149071	517255 53	102591 54	.147080	527018 53	104544 54	.146424
30.0	481640 53	954666 53	.149971	498799 53	988990 53	.147992	507075 53	100554 54	.147340
40.0	451128 53	893608 53	.152235	464702 53	920770 53	.150287	470841 53	933056 53	.149646
50.0	423022 53	837342 53	.155096	433914 53	859148 53	.153187	438614 53	868558 53	.152558
65.0	385085 53	761346 53	.160433	393083 53	777370 53	.158591	396365 53	783948 53	.157985
80.0	351773 53	694550 53	.166911	357770 53	706578 53	.165145	360147 53	711348 53	.164564
100.0	313660 53	618020 53	.177094	317856 53	626450 53	.175437	319468 53	629690 53	.174892
150.0	242840 53	475288 53	.208471	244755 53	479160 53	.207082	245461 53	480588 53	.206627
200.0	195780 53	379728 53	.245413	196770 53	381746 53	.244255	197128 53	382478 53	.243876
300.0	139660 53	263992 53	.327194	140003 53	264710 53	.326370	140125 53	264968 53	.326100
400.0	108492 53	197703 53	.412287	108642 53	198029 53	.411679	108695 53	198145 53	.411481
600.0	761588 52	124352 53	.577531	762006 52	124453 53	.577183	762154 52	124489 53	.577069
900.0	553385 52	680510 52	.788639	553476 52	680800 52	.788494	553508 52	680906 52	.788447

* 588558 53 is to be read 0.588558×10^3 = 588.558 miles

Table 5.3: $h = 90$ km

	$N_s = 0$			$N_s = 301$			$N_s = 400$		
ψ m.r	$R_1/2$ miles	d_1 miles	cos ϕ	$R_1/2$ miles	d_1 miles	cos ϕ	$R_1/2$ miles	d_1 miles	cos ϕ
0.0	667884 53*	132327 54	.166304	708924 53	140534 54	.164530	739332 53	146615 54	.163948
0.5	665906 53	131931 54	.166304	706293 53	140007 54	.164530	735857 53	145920 54	.163948
1.0	663935 53	131537 54	.166306	703681 53	139485 54	.164533	732426 53	145234 54	.163951
2.0	660010 53	130752 54	.166315	698511 53	138451 54	.164542	725700 53	143888 54	.163960
3.0	656109 53	129972 54	.166330	693415 53	137432 54	.164556	719151 53	142579 54	.163974
4.0	652231 53	129196 54	.166350	688390 53	136427 54	.164577	712775 53	141304 54	.163995
5.0	648377 53	128425 54	.166377	683437 53	135436 54	.164604	706565 53	140062 54	.164022
6.0	644546 53	127659 54	.166409	678553 53	134459 54	.164636	700515 53	138852 54	.164054
7.0	640738 53	126898 54	.166447	673736 53	133496 54	.164675	694617 53	137672 54	.164093
8.0	636954 53	126141 54	.166491	668985 53	132546 54	.164719	688862 53	136521 54	.164137
9.0	633194 53	125389 54	.166540	664298 53	131609 54	.164769	683243 53	135398 54	.164188
10.0	629456 53	124641 54	.166596	659673 53	130684 54	.164825	677752 53	134299 54	.164244
12.0	622052 53	123160 54	.166724	650600 53	128869 54	.164955	667122 53	132174 54	.164374
15.0	611121 53	120974 54	.166960	637407 53	126231 54	.165194	651960 53	129141 54	.164614
20.0	593366 53	117423 54	.167469	616421 53	122033 54	.165708	628420 53	124433 54	.165130
25.0	576188 53	113986 54	.168120	596546 53	118058 54	.166367	606622 53	120074 54	.165792
30.0	559579 53	110663 54	.168913	577659 53	114280 54	.167169	586242 53	115997 54	.166596
40.0	528039 53	104352 54	.170915	542496 53	107245 54	.169192	548930 53	108532 54	.168627
50.0	498669 53	984726 53	.173452	510401 53	100821 54	.171757	515380 53	101818 54	.171200
65.0	458477 53	904212 53	.178211	467239 53	921768 53	.176564	470775 53	928856 53	.176024
80.0	422594 53	832262 53	.184029	429274 53	845662 53	.182438	431879 53	850888 53	.181916
100.0	380770 53	748280 53	.193256	385544 53	757870 53	.191747	387348 53	761498 53	.191253
150.0	300551 53	586604 53	.222196	302828 53	591206 53	.220901	303653 53	592876 53	.220478
200.0	245253 53	474312 53	.256972	246466 53	476786 53	.255873	246897 53	477668 53	.255514
300.0	177164 53	333886 53	.335520	177599 53	334796 53	.334721	177752 53	335116 53	.334460
400.0	138410 53	251460 53	.418461	138604 53	251880 53	.417866	138671 53	252026 53	.417671
600.0	976108 52	158890 53	.581086	976655 52	159022 53	.580741	976845 52	159068 53	.580629

* 667884 53 is to be read $0.667884 \times 10^3 = 667.884$ miles

Table 5.3 : h = 110 km

	$N_s = 0$			$N_s = 301$			$N_s = 400$		
ψ m.r.	$R_1/2$ miles	d_1	cos ϕ	$R_1/2$ miles	d_1 miles	cos ϕ	$R_1/2$ miles	d_1 miles	cos ϕ
0.0	738948 53*	146104 54	.183431	780680 53	154449 54	.181833	811318 53	160577 54	.181311
0.5	736971 53	145709 54	.183432	778049 53	153923 54	.181834	807842 53	159881 54	.181312
1.0	734999 53	145314 54	.183434	775436 53	153400 54	.181836	804411 53	159195 54	.181314
2.0	731071 53	144529 54	.183442	770263 53	152366 54	.181844	797682 53	157849 54	.181322
3.0	727164 53	143747 54	.183455	765161 53	151345 54	.181857	791127 53	156538 54	.181335
4.0	723278 53	142970 54	.183473	760128 53	150339 54	.181876	784742 53	155261 54	.181354
5.0	719413 53	142197 54	.183497	755164 53	149346 54	.181900	778522 53	154017 54	.181378
6.0	715570 53	141429 54	.183526	750267 53	148367 54	.181929	772459 53	152805 54	.181407
7.0	711748 53	140664 54	.183560	745436 53	147401 54	.181964	766546 53	151622 54	.181442
8.0	707947 53	139904 54	.183600	740667 53	146447 54	.182004	760773 53	150468 54	.181482
9.0	704167 53	139148 54	.183644	735960 53	145506 54	.182049	755135 53	149340 54	.181527
10.0	700409 53	138396 54	.183694	731313 53	144576 54	.182099	749621 53	148238 54	.181578
12.0	692955 53	136906 54	.183810	722189 53	142751 54	.182216	738940 53	146102 54	.181695
15.0	681933 53	134701 54	.184023	708903 53	140094 54	.182431	723684 53	143050 54	.181910
20.0	663984 53	131111 54	.184482	687717 53	135857 54	.182894	699940 53	138302 54	.182375
25.0	646557 53	127625 54	.185070	667587 53	131831 54	.183487	677885 53	133891 54	.182970
30.0	629649 53	124242 54	.185786	648391 53	127991 54	.184210	657194 53	129752 54	.183695
40.0	597364 53	117781 54	.187596	612462 53	120802 54	.186037	619108 53	122132 54	.185527
50.0	567071 53	111717 54	.189897	579417 53	114188 54	.188358	584600 53	115226 54	.187855
65.0	525210 53	103331 54	.194227	534541 53	105201 54	.192725	538266 53	105947 54	.192234
80.0	487390 53	957482 53	.199546	494590 53	971920 53	.198087	497366 53	977492 53	.197611
100.0	442705 53	867754 53	.208034	447930 53	878252 53	.206641	449883 53	882178 53	.206186
150.0	354913 53	690810 53	.235005	357490 53	696020 53	.233788	358414 53	697892 53	.233391
200.0	292603 53	564280 53	.267934	294010 53	567150 53	.266886	294506 53	568162 53	.266544
300.0	213764 53	401672 53	.343570	214284 53	402760 53	.342795	214465 53	403140 53	.342542
400.0	167896 53	304110 53	.424489	168130 53	304620 53	.423906	168211 53	304796 53	.423716
600.0	118933 53	193007 53	.584586	119000 53	193169 53	.584246	119023 53	193226 53	.584135
900.0	867957 52	106078 53	.791582	868105 52	106125 53	.791440	868156 52	106142 53	.791393

* 738948 53 is to be read 0.738948×10^3 = 738.948 miles

Table 5.3: h = 225 km

	$N_s = 0$			$N_s = 301$			$N_s = 400$		
ψ m.r.	$R_1/2$ miles	d_1 miles	cos ϕ	$R_1/2$ miles	d_1 miles	cos ϕ	$R_1/2$ miles	d_1 miles	cos ϕ
0.0	106179 54*	207428 54	.258920	110549 54	216166 54	.257826	113678 54	222422 54	.257474
0.5	105981 54	207032 54	.258920	110286 54	215640 54	.257827	113330 54	221728 54	.257475
1.0	105783 54	206638 54	.258922	110024 54	215116 54	.257828	112987 54	221040 54	.257476
2.0	105390 54	205850 54	.258927	109506 54	214080 54	.257834	112313 54	219692 54	.257481
3.0	104997 54	205066 54	.258936	108994 54	213056 54	.257843	111656 54	218378 54	.257490
4.0	104607 54	204284 54	.258949	108489 54	212046 54	.257855	111015 54	217096 54	.257503
5.0	104217 54	203504 54	.258965	107989 54	211046 54	.257872	110390 54	215846 54	.257519
6.0	103829 54	202728 54	.258985	107496 54	210060 54	.257892	109780 54	214628 54	.257539
7.0	103443 54	201956 54	.259008	107009 54	209086 54	.257915	109184 54	213436 54	.257563
8.0	103058 54	201186 54	.259035	106527 54	208122 54	.257942	108602 54	212272 54	.257590
9.0	102674 54	200420 54	.259066	106051 54	207170 54	.257973	108032 54	211132 54	.257621
10.0	102292 54	199655 54	.259100	105580 54	206228 54	.258007	107475 54	210018 54	.257655
12.0	101533 54	198136 54	.259179	104653 54	204374 54	.258087	106392 54	207852 54	.257735
15.0	100405 54	195879 54	.259325	103298 54	201664 54	.258233	104840 54	204748 54	.257882
20.0	985538 53	192177 54	.259639	101122 54	197312 54	.258549	102408 54	199885 54	.258198
25.0	967396 53	188549 54	.260043	990359 53	193140 54	.258955	100129 54	195327 54	.258605
30.0	949620 53	184993 54	.260536	970279 53	189124 54	.259450	979709 53	191011 54	.259100
40.0	915160 53	178098 54	.261785	932132 53	181493 54	.260705	939392 53	182946 54	.260358
50.0	882139 53	171488 54	.263382	896308 53	174324 54	.262310	902087 53	175481 54	.261964
65.0	835250 53	162098 54	.266413	846311 53	164313 54	.265355	850602 53	165173 54	.265014
80.0	791441 53	153316 54	.270181	800264 53	155085 54	.269140	803572 53	155748 54	.268805
100.0	737602 53	142508 54	.276293	744298 53	143853 54	.275279	746732 53	144342 54	.274953
150.0	623696 53	119559 54	.296436	627364 53	120300 54	.295502	628644 53	120559 54	.295202
200.0	534648 53	101482 54	.322278	536832 53	101927 54	.321435	537580 53	102080 54	.321163
300.0	409770 53	757298 53	.385379	410680 53	759200 53	.384709	410987 53	759844 53	.384494
400.0	330065 53	587778 53	.456640	330504 53	588730 53	.456115	330651 53	589050 53	.455946
600.0	239192 53	381496 53	.603728	239326 53	381820 53	.603409	239370 53	381930 53	.603306
900.0	176605 53	212096 53	.799691	176636 53	212194 53	.799554	176646 53	212226 53	.799510

* 106179 54 is to be read 0. 106179 $\times 10^4$ = 1061. 79 miles

Table 5.3: h = 350 km

	$N_s = 0$			$N_s = 301$			$N_s = 400$		
ψ m.r.	$R_1/2$ miles	d_1 miles	cos ϕ	$R_1/2$ miles	d_1 miles	cos ϕ	$R_1/2$ miles	d_1 miles	cos ϕ
0.0	133071 54*	256682 54	.318449	137533 54	265602 54	.317591	140690 54	271916 54	.317318
0.5	132873 54	256286 54	.318449	137269 54	265076 54	.317591	140343 54	271222 54	.317318
1.0	132676 54	255890 54	.318450	137008 54	264552 54	.317592	139999 54	270534 54	.317319
2.0	132281 54	255102 54	.318455	136489 54	263514 54	.317596	139325 54	269186 54	.317324
3.0	131888 54	254316 54	.318462	135976 54	262490 54	.317603	138667 54	267870 54	.317331
4.0	131496 54	253532 54	.318472	135470 54	261476 54	.317613	138025 54	266586 54	.317341
5.0	131106 54	252750 54	.318484	134969 54	260474 54	.317626	137399 54	265334 54	.317353
6.0	130716 54	251972 54	.318500	134474 54	259484 54	.317642	136787 54	264110 54	.317369
7.0	130328 54	251196 54	.318518	133985 54	258506 54	.317660	136189 54	262916 54	.317387
8.0	129941 54	250420 54	.318539	133500 54	257538 54	.317681	135605 54	261746 54	.317409
9.0	129555 54	249648 54	.318563	133022 54	256580 54	.317705	135033 54	260602 54	.317433
10.0	129170 54	248880 54	.318590	132548 54	255632 54	.317732	134472 54	259482 54	.317460
12.0	128404 54	247348 54	.318652	131614 54	253766 54	.317794	133383 54	257304 54	.317522
15.0	127263 54	245066 54	.318766	130247 54	251032 54	.317909	131818 54	254174 54	.317637
20.0	125386 54	241312 54	.319013	128045 54	246628 54	.318156	129360 54	249258 54	.317884
25.0	123539 54	237618 54	.319329	125925 54	242388 54	.318474	127047 54	244634 54	.318202
30.0	121721 54	233980 54	.319716	123876 54	238290 54	.318862	124848 54	240234 54	.318590
40.0	118172 54	226880 54	.320697	119958 54	230452 54	.319846	120713 54	231962 54	.319576
50.0	114740 54	220012 54	.321954	116245 54	223022 54	.321107	116851 54	224234 54	.320838
65.0	109808 54	210134 54	.324347	110999 54	212518 54	.323508	111455 54	213434 54	.323241
80.0	105130 54	200758 54	.327335	106094 54	202690 54	.326506	106451 54	203406 54	.326242
100.0	992777 53	189010 54	.332213	100024 54	190509 54	.331399	100292 54	191048 54	.331140
150.0	864457 53	163158 54	.348535	868760 53	164027 54	.347769	870245 53	164328 54	.347525
200.0	758979 53	141748 54	.369968	761667 53	142296 54	.369259	762577 53	142481 54	.369034
300.0	601625 53	109296 54	.424129	602833 53	109548 54	.423541	603235 53	109633 54	.423355
400.0	494569 53	865258 53	.487522	495183 53	866586 53	.487047	495386 53	867028 53	.486896
600.0	365833 53	572904 53	.622816	366031 53	573382 53	.622517	366096 53	573540 53	.622422
900.0	273231 53	322086 53	.807951	273277 53	322234 53	.807821	273293 53	322284 53	.807780

* 133071 54 is to be read $0.133071 \times 10^4 = 1330.71$ miles

Table 5.3: h = 475 km

	$N_s = 0$			$N_s = 301$			$N_s = 400$		
ψ m.r.	$R_1/2$ miles	d_1 miles	cos φ	$R_1/2$ miles	d_1 miles	cos φ	$R_1/2$ miles	d_1 miles	cos φ
0.0	155762 54*	296720 54	.365944	160276 54	305746 54	.365222	163450 54	312094 54	.364996
0.5	155564 54	296324 54	.365944	160012 54	305220 54	.365223	163102 54	311398 54	.364996
1.0	155366 54	295930 54	.365945	159751 54	304696 54	.365224	162759 54	310712 54	.364997
2.0	154972 54	295140 54	.365949	159232 54	303658 54	.365227	162084 54	309362 54	.365001
3.0	154578 54	294354 54	.365955	158719 54	302632 54	.365233	161426 54	308046 54	.365007
4.0	154186 54	293568 54	.365963	158211 54	301618 54	.365241	160783 54	306760 54	.365015
5.0	153794 54	292786 54	.365974	157710 54	300614 54	.365252	160156 54	305506 54	.365026
6.0	153404 54	292004 54	.365987	157214 54	299622 54	.365265	159544 54	304282 54	.365039
7.0	153014 54	291226 54	.366002	156723 54	298642 54	.365281	158945 54	303084 54	.365054
8.0	152626 54	290448 54	.366020	156238 54	297670 54	.365298	158359 54	301912 54	.365072
9.0	152238 54	289674 54	.366040	155758 54	296710 54	.365319	157785 54	300766 54	.365092
10.0	151852 54	288902 54	.366062	155282 54	295760 54	.365341	157223 54	299642 54	.365115
12.0	151082 54	287362 54	.366114	154345 54	293886 54	.365393	156130 54	297456 54	.365167
15.0	149935 54	285068 54	.366210	152971 54	291136 54	.365489	154559 54	294312 54	.365263
20.0	148043 54	281284 54	.366417	150753 54	286702 54	.365697	152085 54	289366 54	.365471
25.0	146176 54	277550 54	.366683	148614 54	282424 54	.365963	149753 54	284702 54	.365737
30.0	144334 54	273866 54	.367007	146542 54	278280 54	.366288	147530 54	280256 54	.366063
40.0	140727 54	266648 54	.367832	142564 54	270322 54	.367115	143335 54	271864 54	.366890
50.0	137219 54	259628 54	.368888	138774 54	262738 54	.368174	139396 54	263984 54	.367950
65.0	132145 54	249466 54	.370903	133385 54	251950 54	.370194	133857 54	252896 54	.369972
80.0	127291 54	239738 54	.373425	128304 54	241766 54	.372722	128676 54	242514 54	.372502
100.0	121158 54	227426 54	.377554	121951 54	229018 54	.376862	122233 54	229586 54	.376644
150.0	107432 54	199773 54	.391480	107903 54	200724 54	.390820	108064 54	201050 54	.390613
200.0	958097 53	176182 54	.409999	961124 53	176799 54	.409380	962142 53	177007 54	.409186
300.0	777739 53	138983 54	.457769	779170 53	139282 54	.457242	779643 53	139381 54	.457077
400.0	649497 53	111704 54	.515028	650251 53	111867 54	.514593	650499 53	111921 54	.514457
600.0	488805 53	751980 53	.640345	489059 53	752594 53	.640064	489141 53	752796 53	.639976
900.0	368904 53	427016 53	.815687	368966 53	427214 53	.815562	368986 53	427280 53	.815523

* 155762 54 is to be read $0.155762 \times 10^4 = 1557.62$ miles

Table 5.4: h = 70 km: N_s = 301

ψ m.r.	c_1 / c_{11}	c_2 / c_{12}	c_3 / c_{13}	c_4 / c_{14}	c_5 / c_{15}	c_6 / c_{16}	c_7 / c_{17}	c_8 / c_{18}	c_9 / c_{19}	c_{10} / c_{20}
.5	24508 53	25768 53	28079 53	31842 53	37845 53	47734 53	65429 53	10280 54	21931 54	40469 56
	27115 54	15500 54	12184 54	11151 54	11353 54	12721 54	15868 54	23072 54	46036 54	40467 56
1.0	12321 53	12949 53	14100 53	15971 53	18950 53	23841 53	32545 53	50745 53	10597 54	25172 55
	14217 54	79361 53	61791 53	56187 53	56864 53	63283 53	78210 53	11192 54	21425 54	25175 55
2.0	61999 52	65103 52	70784 52	79996 52	94600 52	11842 53	16038 53	24642 53	49488 53	45994 54
	78319 53	41486 53	31671 53	28424 53	28428 53	31223 53	37916 53	52705 53	94002 53	46033 54
3.0	41598 52	43645 52	47386 52	53435 52	62985 52	78468 52	10546 53	15982 53	30990 53	18851 54
	58110 53	28993 53	21679 53	19200 53	18980 53	20584 53	24588 53	33295 53	56024 53	18893 54
4.0	31400 52	32919 52	35690 52	40160 52	47189 52	58516 52	78079 52	11679 53	21939 53	10245 54
	49105 53	22859 53	16721 53	14610 53	14277 53	15296 53	17991 53	23791 53	38115 53	10289 54
5.0	25282 52	26484 52	28674 52	32197 52	37717 52	46561 52	61695 52	91158 52	16638 53	64461 53
	44946 53	19280 53	13778 53	11874 53	11472 53	12146 53	14079 53	18218 53	27986 53	64905 53
6.0	21202 52	22193 52	23996 52	26890 52	31406 52	38602 52	50808 52	74203 52	13192 53	44376 53
	43713 53	16993 53	11844 53	10064 53	96147 52	10063 53	11504 53	14592 53	21613 53	44825 53
7.0	18286 52	19127 52	20654 52	23098 52	26900 52	32925 52	43057 52	62194 52	10794 53	32470 53
	44916 53	15459 53	10489 53	87855 52	82981 52	85889 52	96902 52	12067 53	17307 53	32922 53
8.0	16098 52	16826 52	18146 52	20254 52	23522 52	28673 52	37264 52	53267 52	90420 52	24829 53
	48951 53	14410 53	94980 52	78375 52	73194 52	74936 52	83487 52	10220 53	14245 53	25283 53
9.0	14394 52	15034 52	16193 52	18040 52	20894 52	25369 52	32774 52	46385 52	77140 52	19630 53
	57516 53	13704 53	87515 52	71108 52	65658 52	66506 52	73207 52	88197 52	11981 53	20085 53
10.0	13078 52	13650 52	14685 52	16330 52	18863 52	22815 52	29306 52	41086 52	67039 52	15990 53
	76308 53	13309 53	82097 52	65645 52	59924 52	60064 52	65352 52	77562 52	10294 53	16448 53
12.0	11051 52	11519 52	12363 52	13699 52	15743 52	18903 52	24019 52	33084 52	52165 52	11205 53
	85170 54	13083 53	74412 52	57496 52	51281 52	50352 52	53592 52	61878 52	78854 52	11665 53
15.0	90180 51	93817 51	10035 52	11064 52	12624 52	15003 52	18780 52	25263 52	38131 52	72940 52
	39945 53	14258 53	68663 52	50032 52	43027 52	40986 52	42303 52	47096 52	57076 52	77588 52
20.0	68980 51	71552 51	76147 51	83313 51	94031 51	11006 52	13477 52	17533 52	24975 52	41920 52
	11045 53	25794 53	68677 52	43962 52	35316 52	31970 52	31467 52	33260 52	37757 52	46611 52
25.0	56154 51	58092 51	61538 51	66869 51	74743 51	86321 51	10373 52	13125 52	17873 52	27474 52
	54971 52	52439 53	83406 52	43181 52	31852 52	27294 52	25665 52	25924 52	27943 52	32248 52
30.0	47905 51	49439 51	52153 51	56319 51	62408 51	71224 51	84198 51	10406 52	13668 52	19712 52
	33882 52	98466 52	14694 53	47729 52	31251 52	25123 52	22540 52	21824 52	22507 52	24655 52
40.0	36953 51	37975 51	39769 51	42487 51	46386 51	51888 51	59699 51	71071 51	88395 51	11683 52
	16986 52	29675 52	93230 52	10525 53	37660 52	24916 52	19966 52	17735 52	16907 52	17062 52
50.0	30523 51	31256 51	32533 51	34448 51	37153 51	40892 51	46053 51	53282 51	63717 51	79532 51
	10544 52	15379 52	27046 52	88308 52	87711 52	32484 52	21492 52	17104 52	15027 52	14113 52
65.0	24503 51	24982 51	25812 51	27040 51	28743 51	31040 51	34111 51	38232 51	43849 51	51716 51
	63200 51	81051 51	11171 52	17452 52	36598 52	89830 54	41834 52	22530 52	16368 52	13531 52
80.0	20886 51	21223 51	21801 51	22649 51	23810 51	25346 51	27351 51	29961 51	33381 51	37928 51
	44118 51	52842 51	65777 51	86467 51	12392 52	20960 52	58219 52	95433 52	28647 52	17908 52
100.0	17965 51	18192 51	18579 51	19142 51	19901 51	20888 51	22146 51	23737 51	25748 51	28301 51
	31581 51	35865 51	41599 51	49536 51	61055 51	78972 51	11005 52	17565 52	39645 52	25566 53
150.0	14187 51	14292 51	14468 51	14721 51	15054 51	15477 51	15998 51	16631 51	17392 51	18303 51
	19392 51	20695 51	22261 51	24157 51	26471 51	29332 51	32925 51	37530 51	43588 51	51839 51
200.0	12648 51	12707 51	12806 51	12947 51	13131 51	13361 51	13640 51	13973 51	14364 51	14819 51
	15347 51	15957 51	16659 51	17469 51	18404 51	19486 51	20743 51	22212 51	23939 51	25987 51
300.0	11345 51	11370 51	11413 51	11472 51	11550 51	11646 51	11761 51	11895 51	12050 51	12227 51
	12426 51	12650 51	12899 51	13177 51	13485 51	13825 51	14201 51	14616 51	15074 51	15580 51
400.0	10889 51	10902 51	10925 51	10957 51	10998 51	11049 51	11109 51	11180 51	11260 51	11351 51
	11453 51	11566 51	11690 51	11827 51	11976 51	12138 51	12315 51	12506 51	12712 51	12935 51
600.0	10524 51	10529 51	10538 51	10550 51	10566 51	10585 51	10608 51	10634 51	10664 51	10698 51
•	10735 51	10776 51	10821 51	10870 51	10922 51	10979 51	11040 51	11105 51	11175 51	11249 51

Table 5.4: h = 90 km: N_s = 301

ψ m.r.	c_1 / c_{11}	c_2 / c_{12}	c_3 / c_{13}	c_4 / c_{14}	c_5 / c_{15}	c_6 / c_{16}	c_7 / c_{17}	c_8 / c_{18}	c_9 / c_{19}	c_{10} / c_{20}
.5	27821 53	29656 53	33114 53	39007 53	49111 53	67810 53	10901 54	25004 54	21543 55	25104 54
	15589 54	12964 54	12607 54	13873 54	17396 54	26283 54	60726 54	21561 55	43519 54	27185 54
1.0	13989 53	14904 53	16628 53	19560 53	24574 53	33811 53	53990 53	12133 54	15308 55	12991 54
	79357 53	65489 53	63303 53	69214 53	86035 53	12798 54	28176 54	15314 55	23058 54	13993 54
2.0	70409 52	74943 52	83467 52	97920 52	12250 53	16740 53	26383 53	57092 53	44467 55	69480 53
	40981 53	33293 53	31797 53	34332 53	41971 53	60661 53	12299 54	44468 55	13029 54	74086 53
3.0	47253 52	50249 52	55870 52	65373 52	81455 52	11057 53	17212 53	35989 53	79118 54	49778 53
	28262 53	22593 53	21321 53	22742 53	27367 53	38532 53	73001 53	79132 54	99951 53	52594 53
4.0	35677 52	37904 52	42076 52	49106 52	60945 52	82208 52	12646 53	25627 53	26380 54	40332 53
	21962 53	17267 53	16102 53	16972 53	20121 53	27658 53	49488 53	26402 54	88301 53	42262 53
5.0	28731 52	30497 52	33799 52	39348 52	48648 52	65218 52	99204 52	19534 53	13637 54	35066 53
	18232 53	14091 53	12984 53	13528 53	15811 53	21260 53	36221 53	13664 54	85917 53	36469 53
6.0	24099 52	25558 52	28281 52	32844 52	40455 52	53913 52	81134 52	15559 53	84261 53	31978 53
	15792 53	11990 53	10916 53	11245 53	12966 53	17082 53	27889 53	84572 53	91271 53	33035 53
7.0	20788 52	22028 52	24338 52	28197 52	34605 52	45854 52	68304 52	12783 53	57555 53	30240 53
	14093 53	10503 53	94486 52	96262 52	10955 53	14161 53	22270 53	57891 53	10765 54	31053 53
8.0	18302 52	19378 52	21378 52	24710 52	30220 52	39821 52	58740 52	10747 53	41959 53	29480 53
	12861 53	94014 52	83553 52	84200 52	94638 52	12017 53	18279 53	42312 53	15032 54	30113 53
9.0	16367 52	17314 52	19074 52	21997 52	26809 52	35138 52	51349 52	91987 52	32027 53	29548 53
	11945 53	85564 52	75117 52	74890 52	83167 52	10386 53	15333 53	32394 53	32638 54	30043 53
10.0	14872 52	15720 52	17293 52	19899 52	24171 52	31516 52	45646 52	80175 52	25393 53	30560 53
	11298 53	79217 52	68687 52	67757 52	74375 52	91441 52	13138 53	25772 53	68898 54	30947 53
12.0	12568 52	13264 52	14551 52	16672 52	20122 52	25978 52	36997 52	62701 52	17116 53	35781 53
	10422 53	69744 52	58953 52	56951 52	61141 52	73029 52	10008 53	17512 53	76209 53	36009 53
15.0	10255 52	10799 52	11800 52	13438 52	16073 52	20466 52	28487 52	46102 52	10733 53	70031 53
	99128 52	61076 52	49582 52	46435 52	48321 52	55541 52	71819 52	11146 53	27139 53	70105 53
20.0	78422 51	82298 51	89385 51	10085 52	11898 52	14841 52	19987 52	30397 52	59469 52	39613 53
	10655 53	54059 52	40648 52	36126 52	35823 52	38979 52	46760 52	63741 52	10880 53	39685 53
25.0	63799 51	66742 51	72091 51	80660 51	93996 51	11515 52	15080 52	21836 52	38098 52	11728 53
	15021 53	53272 52	36372 52	30564 52	28942 52	30031 52	33981 52	42488 52	61360 52	11881 53
30.0	54364 51	56709 51	60945 51	67670 51	77993 51	94038 51	12022 52	16726 52	26883 52	61131 52
	52036 53	58791 52	35115 52	27685 52	25027 52	24866 52	26800 52	31427 52	40965 52	63188 52
40.0	41819 51	43400 51	46230 51	50650 51	57275 51	67220 51	82631 51	10811 52	15549 52	26631 52
	75966 52	12442 53	39315 52	25888 52	21083 52	19270 52	19130 52	20404 52	23415 52	29346 52
50.0	34408 51	35554 51	37587 51	40720 51	45324 51	52043 51	62039 51	77595 51	10378 52	15443 52
	28491 52	12029 53	67360 52	29579 52	20744 52	17273 52	15891 52	15730 52	16593 52	18657 52
65.0	27437 51	28198 51	29532 51	31555 51	34459 51	38556 51	44377 51	52857 51	65787 51	87048 51
	12679 52	22240 52	71250 52	75885 52	27701 52	18406 52	14780 52	13147 52	12548 52	12678 52
80.0	23207 51	23746 51	24685 51	26090 51	28068 51	30790 51	34526 51	39720 51	47138 51	58216 51
	75959 51	10783 52	17885 52	45466 52	11999 53	28972 52	17812 52	13706 52	11784 52	10879 52
100.0	19737 51	20104 51	20737 51	21672 51	22964 51	24697 51	26997 51	30057 51	34179 51	39862 51
	47983 51	60223 51	80247 51	11782 52	21035 52	75507 52	57236 52	22639 52	15030 52	11855 52
150.0	15215 51	15387 51	15678 51	16099 51	16664 51	17393 51	18315 51	19468 51	20905 51	22699 51
	24957 51	27832 51	31555 51	36493 51	43258 51	52951 51	67769 51	92804 51	14312 52	29160 52
200.0	13312 51	13410 51	13574 51	13808 51	14118 51	14510 51	14993 51	15580 51	16285 51	17129 51
	18136 51	19340 51	20786 51	22533 51	24662 51	27289 51	30580 51	34784 51	40292 51	47756 51
300.0	11693 51	11735 51	11805 51	11905 51	12034 51	12195 51	12390 51	12619 51	12887 51	13196 51
	13549 51	13952 51	14410 51	14928 51	15516 51	16181 51	16936 51	17794 51	18772 51	19891 51
400.0	11101 51	11124 51	11161 51	11214 51	11283 51	11368 51	11469 51	11587 51	11724 51	11879 51
	12053 51	12249 51	12466 51	12708 51	12974 51	13268 51	13592 51	13947 51	14337 51	14766 51
600.0	10636 51	10645 51	10659 51	10680 51	10705 51	10737 51	10775 51	10819 51	10869 51	10925 51
•	10987 51	11057 51	11132 51	11215 51	11305 51	11402 51	11507 51	11619 51	11740 51	11869 51

Table 5.4: h = 110 km: N_s = 301

ψ m.r.	c_1 / c_{11}	c_2 / c_{12}	c_3 / c_{13}	c_4 / c_{14}	c_5 / c_{15}	c_6 / c_{16}	c_7 / c_{17}	c_8 / c_{18}	c_9 / c_{19}	c_{10} / c_{20}
.5	30838 53	33323 53	38141 53	46752 53	62737 53	96854 53	20023 54	29060 55	30137 54	17234 54
	14188 54	14040 54	16117 54	21938 54	40050 54	29075 55	62344 54	32159 54	24893 54	23448 54
1.0	15507 53	16748 53	19151 53	23437 53	31367 53	48186 53	98345 53	10969 55	15605 54	87648 53
	71612 53	70439 53	80312 53	10819 54	19294 54	10979 55	33493 54	16580 54	12642 54	11783 54
2.0	78066 52	84223 52	96119 52	11725 53	15612 53	23755 53	47311 53	36860 54	83549 53	45168 53
	36339 53	35320 53	39741 53	52501 53	89706 53	36935 54	19560 54	88050 53	65055 53	59349 53
3.0	52401 52	56475 52	64330 52	78238 52	10364 53	15626 53	30420 53	18578 54	59918 53	31075 53
	24610 53	23639 53	26259 53	34057 53	56021 53	18645 54	15666 54	62679 53	44768 53	39967 53
4.0	39570 52	42603 52	48439 52	58735 52	77430 52	11571 53	22050 53	11237 54	48592 53	24082 53
	18766 53	17815 53	19545 53	24914 53	39606 53	11299 54	14694 54	50490 53	34763 53	30359 53
5.0	31871 52	34279 52	38905 52	47036 52	61714 52	91449 52	17081 53	75528 53	42282 53	19931 53
	15276 53	14333 53	15537 53	19482 53	30030 53	76118 53	15648 54	43667 53	28882 53	24660 53
6.0	26736 52	28728 52	32547 52	39238 52	51245 52	75318 52	13806 53	54386 53	38586 53	17205 53
	12963 53	12021 53	12879 53	15900 53	23829 53	54958 53	19406 54	39632 53	25074 53	20916 53
7.0	23065 52	24761 52	28004 52	33666 52	43772 52	63831 52	11494 53	41118 53	36512 53	15295 53
	11322 53	10378 53	10992 53	13371 53	19529 53	41677 53	32179 54	37319 53	22464 53	18291 53
8.0	20310 52	21782 52	24593 52	29486 52	38170 52	55241 52	97830 52	32234 53	35612 53	13899 53
	10101 53	91522 52	95860 52	11496 53	16398 53	32783 53	36774 55	36241 53	20617 53	16368 53
9.0	18163 52	19462 52	21938 52	26232 52	33815 52	48581 52	84684 52	25989 53	35707 53	12848 53
	91620 52	82041 52	84995 52	10056 53	14032 53	26529 53	29972 54	36200 53	19293 53	14915 53
10.0	16505 52	17670 52	19885 52	23715 52	30445 52	43431 52	74580 52	21506 53	36936 53	12089 53
	84506 52	74785 52	76649 52	89519 52	12238 53	22042 53	13037 54	37323 53	18422 53	13845 53
12.0	13950 52	14908 52	16724 52	19846 52	25276 52	35576 52	59417 52	15435 53	43231 53	11014 53
	73782 52	63753 52	63986 52	72918 52	96063 52	15963 53	54098 53	43459 53	17441 53	12311 53
15.0	11382 52	12134 52	13551 52	15966 52	20109 52	27782 52	44716 52	10291 53	84073 53	10223 53
	63652 52	53001 52	51594 52	56837 52	71373 52	10812 53	25195 53	84148 53	17657 53	11080 53
20.0	87030 51	92415 51	10249 52	11944 52	14791 52	19881 52	30384 52	60550 52	48748 53	10272 53
	54506 52	42439 52	39304 52	41152 52	48386 52	65661 52	11413 53	48820 53	23896 53	10716 53
25.0	70774 51	74886 51	82524 51	95222 51	11614 52	15242 52	22323 52	40185 52	14348 53	12419 53
	51181 52	36841 52	32438 52	32422 52	36107 52	45269 52	67286 52	14502 53	10530 54	12640 53
30.0	60263 51	63554 51	69628 51	79615 51	95796 51	12309 52	17394 52	29009 52	74654 52	21211 53
	52390 52	34184 52	28523 52	27274 52	28975 52	34154 52	45855 52	76724 52	25609 53	21298 53
40.0	46274 51	48514 51	52600 51	59192 51	69561 51	86274 51	11514 52	17232 52	32410 52	15265 53
	72027 52	33627 52	24620 52	21523 52	21043 52	22555 52	26544 52	35132 52	56385 52	15329 53
50.0	37978 51	39614 51	42568 51	47256 51	54451 51	65628 51	83858 51	11656 52	18701 52	42298 52
	39389 53	41385 52	24618 52	19375 52	17495 52	17364 52	18693 52	21890 52	28474 52	43748 52
65.0	30148 51	31244 51	33199 51	36240 51	40768 51	47502 51	57797 51	74473 51	10441 52	16973 52
	39988 52	20580 53	33539 52	20298 52	15899 52	14147 52	13719 52	14281 52	15923 52	19187 52
80.0	25365 51	26148 51	27532 51	29649 51	32728 51	37156 51	43611 51	53362 51	69049 51	97129 51
	15850 52	37875 52	16389 53	29742 52	17987 52	13948 52	12216 52	11593 52	11723 52	12566 52
100.0	21401 51	21938 51	22877 51	24289 51	26292 51	29079 51	32957 51	38451 51	46506 51	58993 51
	80177 51	12224 52	23932 52	17907 53	38395 52	19038 52	13611 52	11275 52	10184 52	97879 51
150.0	16202 51	16455 51	16890 51	17527 51	18396 51	19545 51	21038 51	22974 51	25498 51	28830 51
	33328 51	39593 51	48731 51	62995 51	87789 51	14007 52	31443 52	23197 53	27399 52	15528 52
200.0	13963 51	14107 51	14353 51	14707 51	15180 51	15788 51	16552 51	17501 51	18673 51	20122 51
	21922 51	24178 51	27044 51	30754 51	35677 51	42436 51	52159 51	67130 51	92748 51	14557 52
300.0	12042 51	12105 51	12210 51	12360 51	12556 51	12801 51	13100 51	13458 51	13880 51	14374 51
	14951 51	15620 51	16398 51	17303 51	18358 51	19593 51	21047 51	22772 51	24836 51	27334 51
400.0	11320 51	11354 51	11410 51	11489 51	11593 51	11721 51	11874 51	12055 51	12265 51	12506 51
	12780 51	13090 51	13439 51	13831 51	14271 51	14764 51	15315 51	15934 51	16627 51	17407 51
600.0	10756 51	10769 51	10790 51	10820 51	10859 51	10907 51	10963 51	11029 51	11105 51	11190 51
•	11285 51	11391 51	11507 51	11635 51	11774 51	11926 51	12090 51	12268 51	12460 51	12667 51

appear to be reasonable for most applications to use only the single value $N_s = 301$ in ionospheric calculations, and the remaining tables in this section give the convergence factor c_m for several angles, ψ, and for m = 1 to 20. The values of c_m are given since they involve the geometry in a rather complex way; however, since the ionosphere probably appears rough to the radio waves reflected at the higher layers, c_m is given only for h = 70, 90, and 110 km.

The results presented in this section were all obtained by ray tracing methods, and such methods yield reliable results only when the following two conditions are satisfied: (a) the index of refraction, n, must not change appreciably in a distance equal to a wavelength, and (b) the fractional change in the spacing between neighboring rays in a wavelength along the ray must be small compared with unity. Both of these conditions require that resort must be made to wave solutions of the problem at the lower frequencies. Condition (b) above is always violated at a caustic, and we have shown in Appendix I how such cases may be treated. It might be supposed, since n changes only from about 1.0003 to 1 for a 70 km change in h, that condition (a) would be well satisfied at frequencies even as low as 5 kc; however, it must be remembered that this small change in n actually causes appreciable bending when ψ is small, and we should, instead, require that $\Delta N/N < 0.1(2\pi/\lambda) = 0.002\, f_{kc}$ if we are to expect ray tracing to apply. This more stringent requirement is met for f > 65 kc for the $N_s = 301$ atmosphere, and it appears that a wave solution will be required at lower frequencies for a precise treatment of the bending. Until an adequate wave solution becomes available, it would seem that the ray tracing solution here given should be used even for frequencies as low as 10 kc since the alternate assumption of $N_s = 0$ would undoubtedly yield an even poorer approximation to the actual bending.

5.2 The Total Bending

Above a height of about 70 km, the troposphere no longer bends the radio waves appreciably, and the designation τ has been given to the total bending of radio waves passing entirely through it. Table 5.5 gives τ, the critical range, R_c, and $R_e - (R_1/2)$ as a function of ψ for the CRPL Reference Radio Refractivity Atmospheres. The results provide a convenient means for determining the true elevation angle ψ_o and true range R_o of a satellite at very high heights, say h > 70 km*,

* These results may actually be used without appreciable error whenever $R_e > 2\, R_c$.

Table 5.5

The Total Bending, τ, Critical Range, R_c, and R_e - (R_1/2) for the C.R.P.L. Reference Radio Refractivity Atmospheres

	N_s = 200.0	h_s = 10,000'		N_s = 250.0	h_s = 5,000'		N_s = 301.0	h_s = 1,000'	
ψ	τ	R_c	$R_e - (R_1/2)$	τ	R_c	$R_e - (R_1/2)$	τ	R_c	$R_e - (R_1/2)$
m.r.	m.r.	km.	meters	m.r.	km.	meters	m.r.	km.	meters
0.0	7.1845	200.400	62.2	9.4504	198.752	78.1	12.1522	196.588	95.40
0.5	7.1022	199.007	61.5	9.3356	197.274	77.1	11.9871	195.049	94.1
1.0	7.0211	197.632	60.8	9.2226	195.817	76.2	11.8252	193.537	92.9
2.0	6.8630	194.937	59.4	9.0025	192.966	74.3	11.5109	190.592	90.5
3.0	6.7100	192.309	58.1	8.7899	190.195	72.5	11.2090	187.744	88.3
4.0	6.5622	189.743	56.7	8.5848	187.498	70.8	10.9194	184.987	86.1
5.0	6.4193	187.235	55.4	8.3869	184.870	69.1	10.6416	182.313	83.9
6.0	6.2813	184.782	54.3	8.1962	182.308	67.6	10.3754	179.717	82.0
7.0	6.1480	182.381	53.1	8.0124	179.807	66.1	10.1202	177.190	80.0
8.0	6.0194	180.027	51.9	7.8353	177.363	64.7	9.8757	174.730	78.1
9.0	5.8951	177.719	50.8	7.6645	174.973	63.2	9.6413	172.331	76.3
10.0	5.7751	175.454	49.8	7.4999	172.635	61.9	9.4165	169.988	74.6
12.0	5.5470	171.046	47.8	7.1882	168.104	59.3	8.9940	165.461	71.4
15.0	5.2326	164.720	45.0	6.7602	161.641	55.7	8.4207	159.027	67.0
20.0	4.7721	154.868	40.97	6.1379	151.664	50.58	7.5998	149.131	60.57
25.0	4.3771	145.812	37.44	5.6086	142.576	46.11	6.9125	140.141	55.19
30.0	4.0352	137.488	34.54	5.1539	134.283	42.31	6.3292	131.954	50.52
40.0	3.4745	122.821	29.49	4.4155	119.781	36.33	5.3943	117.660	43.17
50.0	3.0364	110.443	25.80	3.8448	107.623	31.50	4.6808	105.694	37.39
65.0	2.5379	95.332	21.46	3.2016	92.847	26.22	3.8847	91.165	31.17
80.0	2.1689	83.422	18.30	2.7295	81.232	22.29	3.3051	79.749	26.50
100.0	1.8076	71.142	15.30	2.2702	69.270	18.55	2.7442	67.997	21.96
150.0	1.2606	51.401	10.68	1.5794	50.052	13.02	1.9053	49.122	15.39
200.0	0.9586	39.975	8.19	1.2000	38.928	9.97	1.4464	38.201	11.80
300.0	0.6379	27.600	5.59	0.7978	26.879	6.80	0.9611	26.375	8.03
400.0	0.4693	21.156	4.26	0.5868	20.604	5.19	0.7068	20.217	6.12
600.0	0.2912	14.699	2.94	0.3641	14.316	3.59	0.4384	14.047	4.25
900.0	0.1584	10.630	2.13	0.1980	10.354	2.59	0.2384	10.158	3.06

Table 5.5

The Total Bending, τ, Critical Range, R_c, and R_e - $(R_1/2)$ for the C. R. P. L. Reference Radio Refractivity Atmospheres

	N_s = 350.0	h_s = 0'		N_s = 400.0	h_s = 0'		N_s = 450.0	h_s = 0'	
ψ	τ	R_c	$R_e - (R_1/2)$	τ	R_c	$R_e - (R_1/2)$	τ	R_c	$R_e - (R_1/2)$
m.r.	m.r.	km	meters	m.r.	km	meters	m.r.	km	meters
0.0	15.6236	192.552	111.10	20.4292	189.878	128.70	27.5747	191.865	152.6
0.5	15.3818	190.840	109.40	20.0507	187.842	126.60	26.9134	189.128	149.3
1.0	15.1452	189.165	107.80	19.6822	185.861	124.30	26.2746	186.497	146.1
2.0	14.6878	185.921	104.80	18.9747	182.063	120.20	25.0635	181.540	140.2
3.0	14.2512	182.809	101.80	18.3060	178.467	116.40	23.9391	176.959	134.6
4.0	13.8349	179.818	99.00	17.6748	175.055	112.70	22.8975	172.716	129.4
5.0	13.4383	176.939	96.3	17.0798	171.811	109.3	21.9340	168.775	124.7
6.0	13.0605	174.163	93.8	16.5190	168.717	106.0	21.0429	165.099	120.3
7.0	12.7008	171.479	91.4	15.9905	165.759	103.0	20.2186	161.655	116.2
8.0	12.3583	168.881	89.1	15.4923	162.923	100.1	19.4552	158.414	112.4
9.0	12.0320	166.361	86.9	15.0224	160.199	97.2	18.7472	155.350	108.8
10.0	11.7210	163.914	84.8	14.5787	157.574	94.6	18.0892	152.443	105.5
12.0	11.1413	159.218	80.7	13.7626	152.593	89.8	16.9049	147.026	99.3
15.0	10.3651	152.608	75.4	12.6912	145.688	83.3	15.3978	139.701	91.4
20.0	9.2736	142.573	67.9	11.2232	135.398	74.3	13.4115	129.072	80.7
25.0	8.3768	133.571	61.49	10.0480	126.325	66.93	11.8776	119.907	72.17
30.0	7.6271	125.452	56.08	9.0849	118.249	60.80	10.6525	111.868	65.12
40.0	6.4460	111.434	47.70	7.6000	104.501	51.28	8.8124	98.383	54.48
50.0	5.5604	99.827	41.23	6.5103	93.278	44.12	7.4944	87.524	46.62
65.0	4.5872	85.861	34.05	5.3338	79.931	36.33	6.0979	74.749	38.22
80.0	3.8877	74.969	29.02	4.5005	69.621	30.82	5.1232	64.964	32.30
100.0	3.2172	63.818	24.05	3.7104	59.138	25.51	4.2089	55.077	26.79
150.0	2.2247	46.007	16.76	2.5542	42.519	17.71	2.8853	39.506	18.50
200.0	1.6860	35.747	12.83	1.9321	32.998	13.6	2.1789	30.628	14.13
300.0	1.1188	24.662	8.73	1.2803	22.745	9.21	1.4419	21.093	9.60
400.0	0.8224	18.899	6.65	0.9405	17.423	7.03	1.0588	16.153	7.33
600.0	0.5099	13.128	4.62	0.5830	12.100	4.86	0.6560	11.216	5.06
900.0	0.2772	9.494	3.33	0.3169	8.749	3.51	0.3566	8.108	3.66

in terms of its observed elevation angle ψ, its observed radio range R_e and the surface value, N_s, of refractivity at the observing point:

$$\psi_o = \psi - \tau[1 - (R_c/R_e)] \tag{47}$$

$$R_o = (R_1/2) - R_c \left[\frac{1}{3} - \frac{R_c}{2 R_e} \right] \sin^2 \tau \tag{48}$$

6. Tropospheric Scatter

The distance d_{Lt} to the radio horizon of a transmitting antenna of height, h_t, above a smooth spherical earth of radius a' and for a linear gradient atmosphere may be determined from:

$$d_{Lt} = \sqrt{2 k a' h_t} \tag{49}$$

where k is defined by (36). For the particular CRPL Reference N_s = 301 atmosphere, $k a'$ = 5,280 miles and, if h_t is expressed in feet and d_{Lt} in miles: $d_{Lt} = \sqrt{2 h_t}$. When h_t is greater than one kilometer, (49) no longer applies, and reference should then be made to the preceding section or to references 67 and 70; in particular, since the horizon is defined by the ray corresponding to $\psi = 0$, Fig. 47 shows the relation over a smooth earth between d_{Lt} and h_t at large heights and for several values of N_s. If we let h_r and d_{Lr} denote the height and distance to the radio horizon for the receiving antenna, then receiving antennas at a distance $d > d_{Lt} + d_{Lr}$ from the transmitting antenna lie below the horizon ray of the transmitting antenna, and it becomes convenient to calculate the transmission loss at such distances in terms of the angular distance, θ. [3/] Over a smooth, spherical earth and in a linear gradient atmosphere, θ may be determined by:

$$\theta = \frac{d - d_{Lt} - d_{Lr}}{ka'} \text{ radians} \tag{50}$$

The angular distance, θ, is a particularly convenient parameter for making appropriate allowance for the effects of irregularities in the terrain, and a detailed explanation of methods for calculating the cumulative distribution of transmission loss in propagation over irregular terrain and for a wide range of atmospheric conditions is given in a recent report by Rice, Longley, and Norton.[70] Thus it is shown in that report that the received field on these beyond-the-horizon paths may be considered to consist of diffracted and scattered components. The scattered component may be explained quantitatively for the winter afternoon hours in terms of scatter by a turbulent atmosphere using the mixing-in-gradient hypothesis as the basis for describing the turbulence, i.e., the $(r/\ell_0)K_1(r/\ell_0)$ correlation function may be used to describe the correlation in the variations of refractive index at points a distance r apart in the atmosphere.[57] Some direct experimental evidence for this description of atmospheric turbulence is given in a recent paper by the author.[58] The extension of these estimates of the transmission loss for winter afternoons to all-day, all-year values is then done empirically, using the angular distance as a parameter in this empirical analysis.

Fig. 48 shows the values of median basic transmission loss separately for the diffracted wave and for tropospheric scatter as calculated in the manner described in reference 70 for the range of frequencies from 10 to 10,000 Mc and for transmitting and receiving antennas both at a height of 30 feet. If we assume that the short term variations in the scatter fields are Rayleigh distributed, and that the diffracted waves are relatively steady, then we may determine the expected combined median basic transmission loss, L_{bm}, in terms of the diffracted wave transmission loss L_{bd} and the median basic scatter transmission loss, L_{bms} as follows:

$$L_{bm} = L_{bd} - R(0.5) \tag{51}$$

where $K = L_{bd} - L_{bms} + 1.592$ is the ratio in decibels of the average scattered power to the diffracted wave power, and R(0.5) is given graphically and in tables in reference 71. When K is less than -16.5 db, L_{bm} differs from L_{bd} by less than 0.1 db, and when K is greater than 19.5 db, L_{bm} differs from L_{bms} by less than 0.1 db.

Finally, to determine the expected values, $L_b(p)$, of basic transmission loss exceeded by (100 - p) per cent of the hourly medians during a year, we may simply subtract $V(p, \theta)$ as given on Fig. 49 from L_{bm} as calculated above from the values shown on Fig. 48.

Fig. 50 shows the influence on the median basic transmission loss at 100 Mc of changing one antenna height while keeping the other antenna height fixed at 30 feet. The values given are for a smooth

MEDIAN BASIC TRANSMISSION LOSS FOR
THE GROUND WAVE AND TROPOSPHERIC SCATTER
MODES OF PROPAGATION OVER A SMOOTH SPHERICAL EARTH

Over Land σ = 0.005 mhos/meter ϵ = 15
Polarization: Horizontal
Transmitting and Receiving Antennas Both 30 Feet Above the Surface

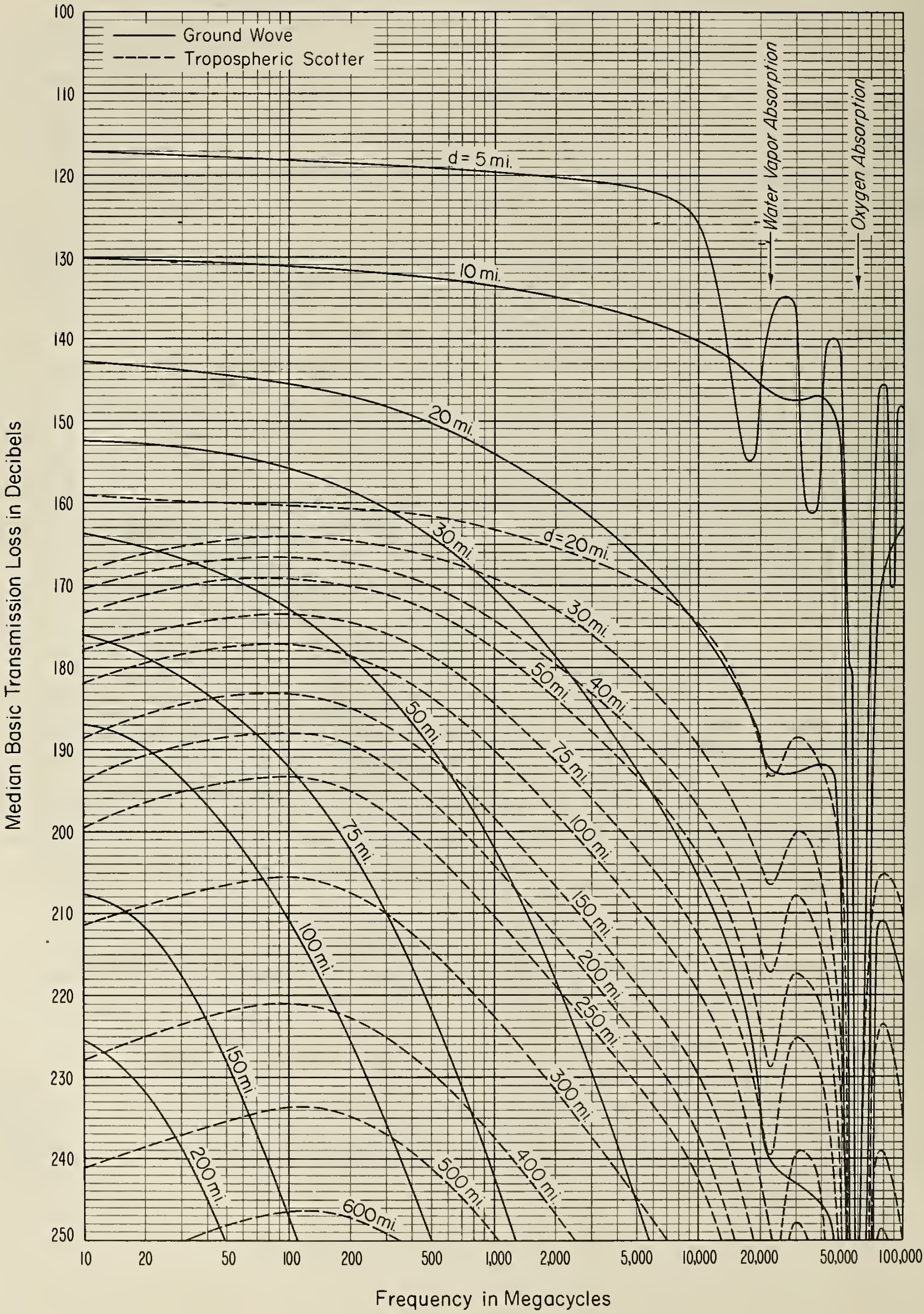

THE VARIANCE OF TRANSMISSION LOSS IN TROPOSPHERIC PROPAGATION

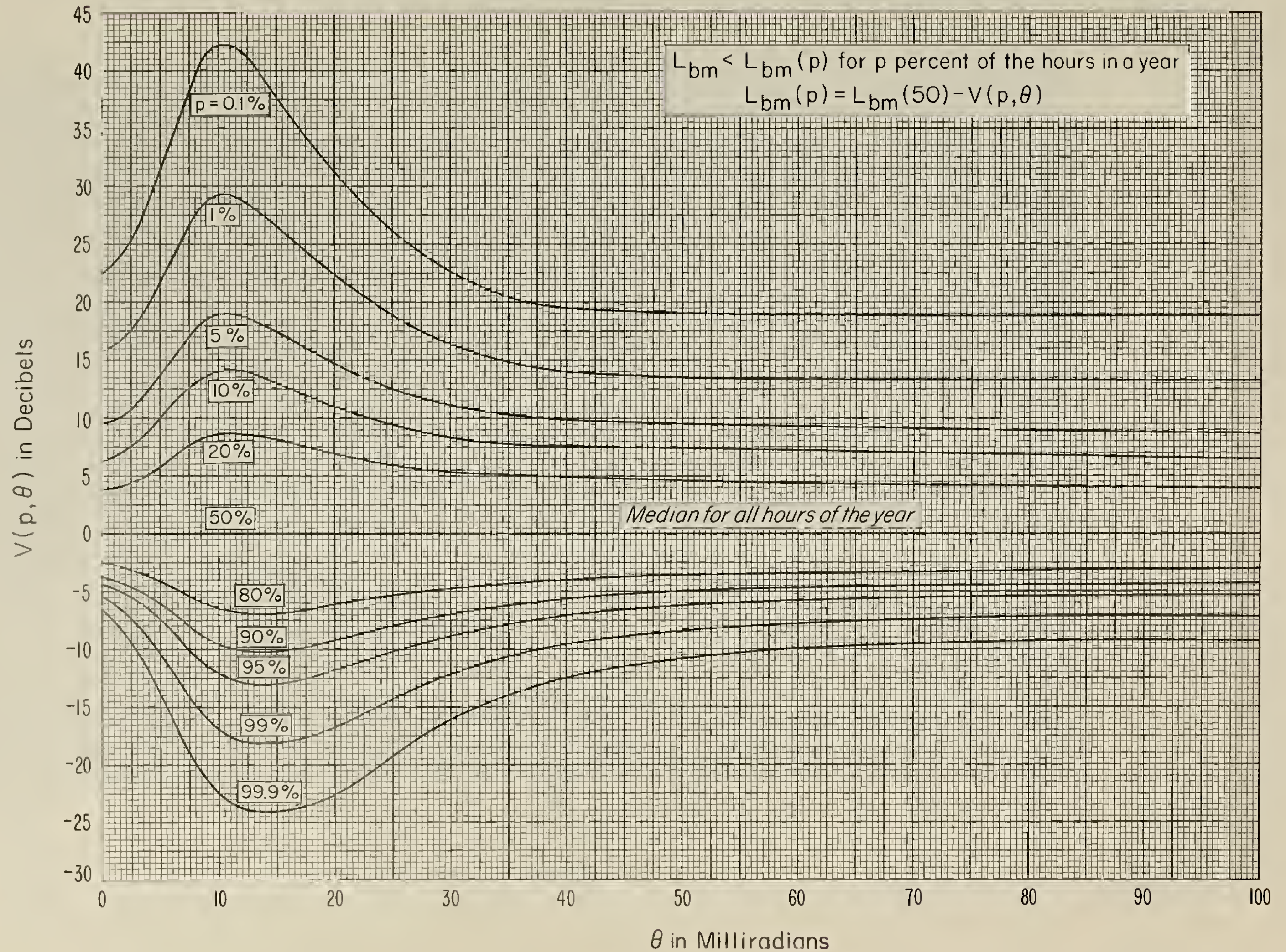

Figure 49

MEDIAN BASIC TRANSMISSION LOSS AT 100 MC

Smooth Spherical Earth and a CRPL Reference N_s=301 Atmosphere

Horizontal Polarization Over Land

One Antenna at 30 Feet and the Other Antenna at the Heights Indicated

∘ Location of Maximum Fields (minimum transmission losses)

——— (L_{bd}) Ground Wave

- - - - - (L_{bms}) Tropospheric Scatter for Winter Afternoon Hours

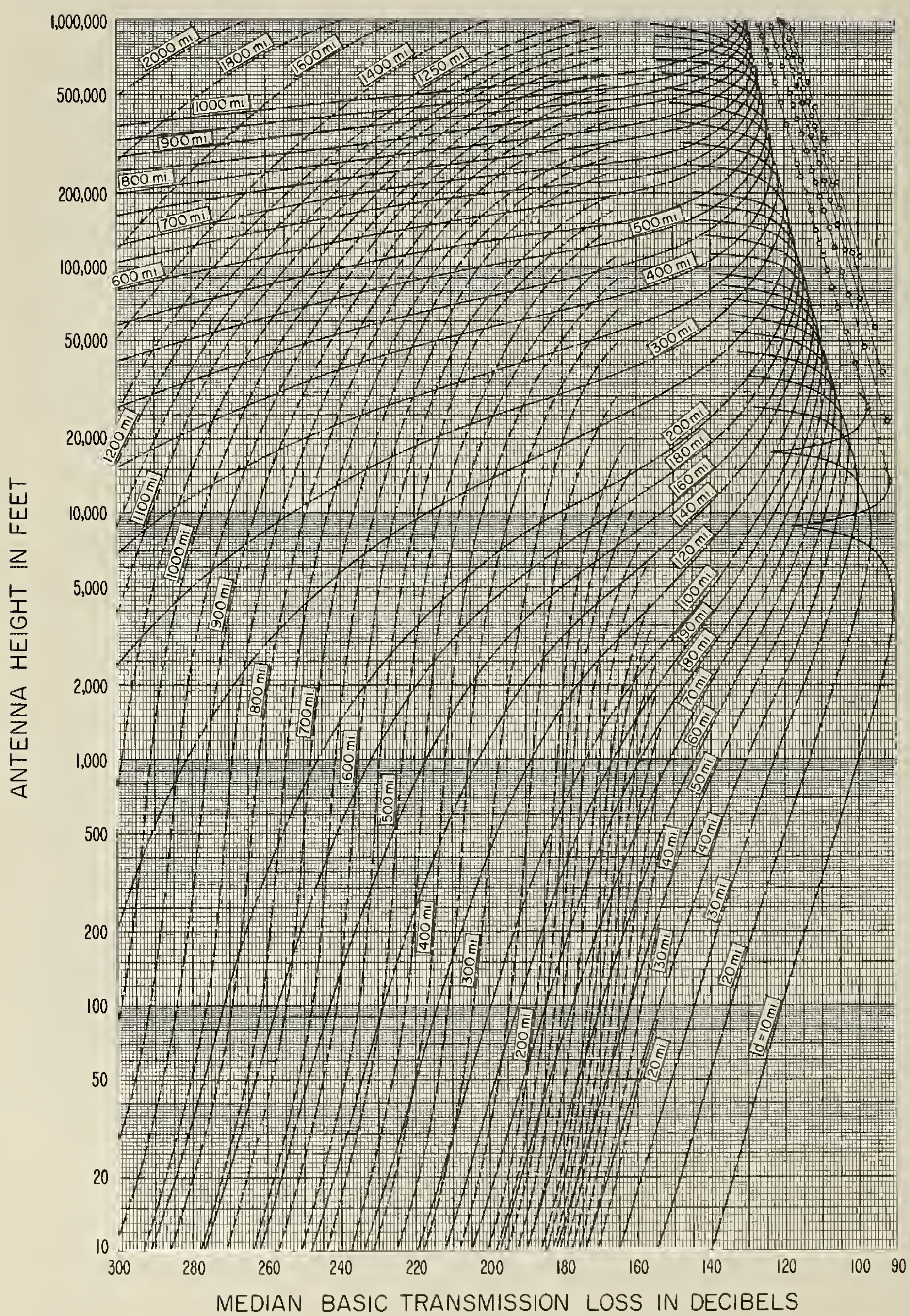

Figure 50

earth and a CRPL Reference $N_s = 301$ atmosphere. The first two oscillations of the field are shown for d = 10 and 20 miles, but for the other distances only one oscillation is shown. The six points of field maxima are shown for all of the distances as circled points. Note that the total number of maxima to be expected (as a function of range at a given height or as a function of height at a given range) for a particular antenna height is equal to the number of half wavelengths contained in this height; in the present case of 100 Mc, 30 feet represents 6 half-wavelengths; in this connection, see (8), page 11.

The scatter curves on Fig. 50 correspond to the winter afternoon hours, and the reader is referred to reference 70 for curves suitable for translating these values to transmission losses exceeded for several percentages of various periods of time. The scatter loss predictions on Fig. 50 are shown only up to heights just short of the radio horizon since the method of estimation given in reference 70 is not applicable to line-of-sight paths.

7. Point-to-Point Radio Relaying by Tropospheric Scatter

As an example of the method of using transmission loss in systems design, we will consider the problem of estimating the effective maximum range of a radio relay system using tropospheric scatter. As an illustration of typical ranges to be expected, we will assume that the terrain is smooth, and will base our predictions on a CRPL Reference Radio Refractivity Atmosphere with $N_s = 301$. We will assume that either two 28-foot or two 60-foot parabolic antennas are used at both ends of the path, with their centers 30 feet above the ground and connected in a quadruple diversity system. With these assumptions, we may use the methods described in reference 70 to determine the transmission loss, L(99), which we would expect one per cent of the actual hourly median transmission losses to exceed throughout a period of one year; the use of these one per cent losses implies that the specified service will be available for 99% of the hours. Tables 7.1 and 7.2 give for the 28' and 60' antennas the free space gains $G_t + G_r$, and the path antenna gains as a function of frequency and distance, while Tables 7.3 and 7.4 give L(99) as a function of frequency and distance.

The power required to provide a specified type and grade of service for 99% of the hours may now be obtained from the equation:

$$P_t = L_t + L(99) + R + F + B - 204 \tag{52}$$

Table 7.1

Path Antenna Gain in Decibels for 28-Foot Parabolic Antennas 30 Feet Above a Smooth Spherical Earth with a CRPL Model Radio Refractivity Atmosphere Corresponding to N_s = 301

f_{Mc}	$G_t + G_r$	G_p in Decibels						
	db	d = 100 mi.	150	200	300	500	700	1000
100	33.02	33.02	33.02	33.02	32.92	32.82	32.72	32.67
150	40.07	40.07	39.97	39.97	39.87	39.57	39.47	39.37
200	45.06	45.06	44.96	44.86	44.66	44.36	44.16	44.06
300	52.11	52.03	51.91	51.71	51.31	50.81	50.51	50.41
500	60.98	60.75	60.38	60.08	59.38	58.48	58.18	58.18
700	66.83	66.35	65.83	65.23	64.33	63.23	62.83	62.93
1000	73.02	72.12	71.22	70.42	69.22	67.92	67.32	67.22
1500	80.07	78.32	76.57	75.87	74.27	72.57	71.67	71.57
2000	85.06	82.48	80.66	79.26	77.16	75.46	74.36	73.86
3000	92.11	87.71	84.21	83.41	80.91	78.51	77.61	77.31
5000	100.98	93.28	90.18	87.68	84.68	82.18	81.28	80.98
7000	106.83	96.53	92.83	90.03	86.83	84.12	83.33	82.93
10000	113.02	99.32	95.22	92.52	89.02	86.02	85.22	84.92

Table 7.2

Path Antenna Gain in Decibels for 60-Foot Parabolic Antennas 30 Feet Above a Smooth Spherical Earth with a CRPL Model Radio Refractivity Atmosphere Corresponding to $N_s = 301$

f_{Mc}	$G_t + G_r$	G_p in Decibels						
	db	d = 100 mi.	150	200	300	500	700	1000
100	46.26	46.16	46.16	46.06	45.86	45.46	45.26	45.16
150	53.31	53.21	53.11	52.91	52.51	52.11	51.56	51.48
200	58.30	58.10	57.90	57.60	57.00	56.30	55.90	55.86
300	65.35	64.95	64.45	63.95	62.85	62.05	61.70	61.90
500	74.22	73.22	72.67	71.02	70.22	68.72	68.12	68.12
700	80.07	78.37	77.07	75.87	74.17	72.57	71.67	71.57
1000	86.26	83.46	81.46	79.96	77.86	76.26	75.01	74.66
1500	93.31	88.51	85.91	84.01	81.51	79.11	78.21	77.81
2000	98.30	91.70	88.80	86.60	83.70	81.10	80.20	79.80
3000	105.35	95.75	92.25	89.65	86.35	83.55	82.85	82.45
5000	114.22	100.02	95.62	92.92	89.52	86.52	85.62	85.42
7000	120.07	102.37	97.87	94.97	91.17	88.22	87.57	87.07
10000	126.26	104.56	99.96	96.66	93.06	90.06	89.26	88.76

Table 7.3

Transmission Loss L(99) (Corresponding to Fields Exceeded 99% of the time) Expected Between Two 28-Foot Parabolic Antennas at a Height of 30 Feet Above a Smooth Spherical Earth with a CRPL Model Radio Refractivity Atmosphere Corresponding to $N_s = 301$

L(99) in Decibels

f_{Mc}	d = 100 mi.	150	200	300	500	700	1000
100	160.21	164.33	166.95	182.31	207.79	233.29	276.57
150	154.20	158.56	161.57	176.52	200.95	225.91	269.52
200	150.24	154.72	157.92	173.08	197.38	221.76	265.56
300	145.32	150.27	153.55	169.33	192.88	217.45	260.36
500	140.10	145.87	149.64	165.94	189.74	214.13	255.99
700	137.39	143.81	147.98	164.83	188.55	213.08	254.05
1000	135.11	142.31	146.98	164.07	188.08	212.72	251.88
1500	133.32	141.88	146.32	164.50	188.91	213.41	254.20
2000	132.54	141.36	146.76	165.62	190.08	214.46	255.50
3000	132.70	143.69	148.71	168.01	193.39	217.50	257.99
5000	134.79	145.77	152.99	173.37	199.19	223.38	264.01
7000	137.37	149.86	158.13	179.75	206.98	231.32	272.13
10000	144.68	160.12	170.68	196.11	223.53	247.87	288.69

Table 7.4

Transmission Loss L(99) (Corresponding to Fields Exceeded 99% of the time) Expected Between Two 60-Foot Parabolic Antennas at a Height of 30 Feet Above a Smooth Spherical Earth with a CRPL Model Radio Refractivity Atmosphere Corresponding to $N_s = 301$

L(99) in Decibels

f_{Mc}	d = 100 mi.	150	200	300	500	700	1000
100	147.07	151.19	153.91	169.37	195.15	220.75	264.08
150	141.06	145.52	148.63	163.88	188.41	213.83	257.41
200	137.20	141.78	145.19	160.74	185.44	210.02	253.76
300	132.40	137.73	141.31	157.79	181.64	206.26	248.87
500	127.63	133.58	138.70	155.10	179.50	204.19	246.05
700	123.67	132.57	137.34	154.99	179.21	204.24	245.41
1000	123.77	132.07	137.44	155.43	179.74	205.03	244.44
1500	123.13	132.54	138.18	157.26	182.37	206.87	247.96
2000	123.32	133.22	139.43	159.08	184.45	208.62	249.56
3000	124.66	135.65	142.47	162.57	188.35	212.26	252.67
5000	128.05	140.34	147.75	168.53	194.85	219.04	259.57
7000	131.53	144.82	153.19	175.41	202.89	227.18	267.79
10000	139.44	155.38	166.54	192.07	219.49	243.83	284.85

Each of the terms in (52) is expressed in decibels; P_t is the transmitter power expressed in decibels above one watt; L_t is the loss in the transmitting antenna circuit and the transmitting antenna transmission line (this term is set equal to one db for the calculations in this report); R is the median pre-detection signal-to-r.m.s. noise ratio required for the specified grade of service; F is the effective receiver noise figure and includes the effects of the antenna noise as well as the receiver noise together with the receiving antenna circuit and transmission line loss;[1/] it is assumed that the receiver incorporates gain adequate to ensure that the first circuit noise is detectable; $B \equiv 10 \log_{10}(b_o + b_m)$ is the effective receiver bandwidth factor with b_o and b_m expressed in cycles per second; b_o allows for the drift between the transmitter and receiver oscillators, while b_m allows for the band occupied by the modulation; the constant term (-204) is $10 \log_{10} k\,T$ where k is Boltzmann's constant and the reference temperature is taken to be 288.44° Kelvin; this is just the noise power in a one cycle per second bandwidth in db relative to one watt.

For the calculations in this report, the transmitter and receiver oscillators were each assumed to have a stability of one part in 10^8 and to vary independently so that $b_o = \sqrt{2}\, f_{Mc} \cdot 10^{-2}$. Table 7.5 gives the values of b_m assumed for the various types of service considered. The effective receiver noise figure has been estimated as $F = 5 \log_{10} f_{Mc} - 5$. Table 7.5 also gives the values of R for the various kinds of service on the assumption that quadruple diversity is used. The value of R for the FM Multichannel system is expected to provide a service with less than an 0.01% teletype character error rate. The FM Multichannel System consists of 36 voice channels, each of which can accommodate sixteen 60 words per minute teletype circuits. The values of R given in Table 7.5 were determined by methods given in a recent report by Watt. [73/] The value of R for the FM Multichannel system corresponds to typical fading encountered at 1000 Mc, and this value of R may change by a few db with frequency as the fading changes, but such changes have so far not been evaluated quantitatively; furthermore, R will also change as the fading changes from hour to hour.

Table 7.6 gives as a function of frequency the maximum permissible hourly median transmission loss for a transmitter power of 10 kw: $L_M = 204 + P_t - L_t - R - F - B$ corresponding to the kinds of service described above. By combining the information in Tables 7.3, 7.4, and 7.6, we can estimate the maximum range for a quadruple diversity system with 10 kw transmitters. These ranges are shown on Fig. 51 as a function of the radio frequency.

Table 7.5

Type of Service	b_m cycles/sec.	R* decibels	Signal Bandwidth cycles/sec.	Post Detection Signal-to noise ratio decibels
Transmission Loss Measurement	0	0#	0	-
FM Multichannel System	3,750,000	9.5	36 Voice channels each capable of use for sixteen 60 words per min. teletype circuits	0.01% teletype character error rate
FM Music	150,000	26.5	15,000	50 **
U.S. Standard Television	3,750,000	32.7	3,750,000	30 **

* Ratio between the median intermediate frequency Rayleigh distributed signal and the r.m.s. Rayleigh distributed noise.

** This ratio will be exceeded with a quadruple diversity system for 99% of each hour for which the corresponding value of R is maintained in each receiver.

\# Diversity reception not involved in this case.

Table 7.6

Maximum Permissible Transmission Loss L_M for 10 KW Transmitters Using the Parameters of Table 7.5

f_{Mc}	Transmission loss Measurement	FM Multichannel	FM Music	U. S. Standard Television
100	236.50	162.76	159.74	139.56
150	233.85	161.88	158.86	138.68
200	231.98	161.26	158.23	138.06
300	229.34	160.37	157.35	137.17
500	226.01	159.27	156.25	136.07
700	223.82	158.54	155.51	135.34
1000	221.50	157.76	154.74	134.56
1500	218.85	156.88	153.86	133.68
2000	216.98	156.25	153.23	133.05
3000	214.34	155.37	152.35	132.17
5000	211.01	154.27	151.25	131.07
7000	208.82	153.53	150.51	130.33
10000	206.50	152.76	149.74	129.56

MAXIMUM DISTANCE AT WHICH SATISFACTORY SERVICE OF THE TYPES INDICATED MAY BE PROVIDED FOR 99% OF THE HOURS USING 10 KILOWATT TRANSMITTERS AND QUADRUPLE DIVERSITY

(Smooth Spherical Earth; $N_s = 301$; $h_t = h_r = 30$ feet)

Atmospheric Absorption and Rain Attenuation Typical of the Washington, D.C. Area

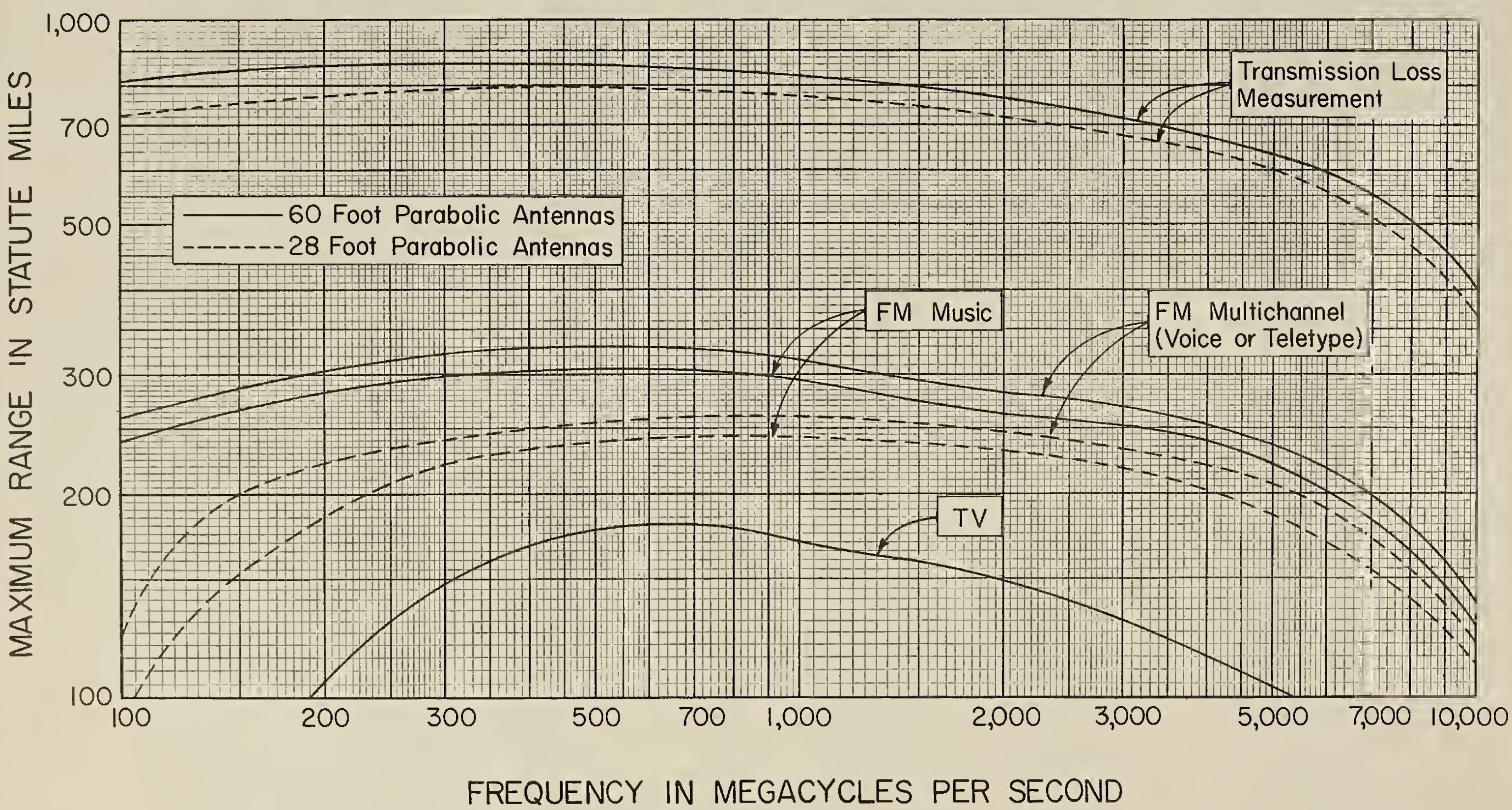

Figure 51

Acknowledgements: The author has had extensive assistance in preparing this report from many members of the Radio Propagation Engineering Division Staff. Acknowledgement of most of this assistance is given in the text or by reference, but in addition the following contributions should be mentioned. Don Watt assisted extensively with the theory of ionospheric roughness outlined in Appendix I. Anita Longley was largely responsible for the sky wave computations for Figs. 31 to 40, inclusive, while Peter Ratcliffe did most of the calculations for Figs. 41 to 45, inclusive. Lew Vogler calculated the diffracted fields shown on Fig. 50, while Anita Longley calculated the scattered fields. Ralph Johler calculated the values given in Table I-2. Gertrude Qvale typed the report, and John Harman drafted most of the figures.

REFERENCES

1. K. A. Norton, "Transmission Loss in Radio Propagation," Proc. I. R. E., 41, 146-152, (1953).

2. K. A. Norton, "Transmission Loss of Space Waves Propagated over Irregular Terrain," I. R. E., Trans. AP-3, 152-166, (1952).

3. K. A. Norton, P. L. Rice, and L. E. Vogler, "The Use of Angular Distance in Estimating Transmission Loss and Fading Range for Propagation Through a Turbulent Atmosphere over Irregular Terrain," Proc. I. R. E., 43, 1488-1526, (1955).

4. Kenneth A. Norton, "Propagation Over Rough Terrain," Naval Electronics Laboratory Symposium, July 25, 1959, Report No. 173, U. S. N. E. L., San Diego, California.

5. A. P. Barsis, "Comparison of Calculated and Measured Fields within the Radio Horizon for the 92 to 1046 Mc Range," Private Communication, Jan. 1955.

6. R. E. McGavin and L. J. Maloney, "A Study at 1046 Mc of the Reflection Coefficient of Irregular Terrain at Grazing Angles," J. Research NBS, 63-D (Radio Propagation), Sept. (1959).

7. A. L. Durkee, "Results of Microwave Propagation Tests on a 40-Mile Overland Path," Proc. I. R. E., 36 (2), 197-205, (1948).

8. J. Z. Millar and L. A. Byam, "A Microwave Propagation Test," Proc. I. R. E., 38 (6), 619-626, (1950).

9. Kenneth A. Norton, "Space and Surface Waves in Radio Propagation," Physical Review, 52 (2), 132-133, (1937).

10. Kenneth A. Norton, "The Propagation of Radio Waves Over the Surface of the Earth and in the Upper Atmosphere," Proc. I. R. E., 25 (9), 1203-1236, (1937).

11. Kenneth A. Norton, "The Calculation of Ground-Wave Field Intensity Over a Finitely Conducting Spherical Earth," Proc. I. R. E., 29 (12), 623-639, (1941)

12. Kenneth A. Norton, "Ground Wave Propagation," Federal Communications Commission Report No. 47475 prepared for the Fourth Annual Broadcast Engineering Conference held Feb. 10-21, 1941 at Ohio State University.

13. Kenneth A. Norton, "The Polarization of Downcoming Ionospheric Radio Waves," Report prepared in connection with a National Bureau of Standards Project on Direction Finding Sponsored by the National Defense Research Committee, 1942.

14. W. H. Wise, "The Physical Reality of Zenneck's Surface Wave," Bell System Technical Journal, 16, 35-44, (1937).

15. James R. Wait, "Excitation of Surface Waves on Conducting, Stratified, Dielectric Clad and Corrugated Surfaces," Journal Research, NBS, 59, 365, (1957).

16. R. S. Kirby, J. W. Herbstreit, and K. A. Norton, "Service Range for Air-to-Ground and Air-to-Air Communications at Frequencies Above 50 Mc," Proc. I. R. E., 40, 525-536, (1952).

17. Kenneth A. Norton and Philip L. Rice, "Gapless Coverage in Air-to-Ground Communications at Frequencies Above 50 Mc," Proc. I. R. E., 40 (4), 470-474, (1952).

18. Kenneth A. Norton and J. W. Herbstreit, "Wright Field Letters," Private Communication, Jan. 1955.

19. Kenneth A. Norton, Morris Schulkin, and Robert S. Kirby, "Ground-Wave Propagation Over Irregular Terrain at Frequencies Above 50 Mc," Reference C to the Report of the Federal Communications Commission Ad Hoc Committee for the Evaluation of the Radio Propagation Factors Concerning the Television and Frequency Modulation Broadcasting Services in the Frequency Range between 50 and 250 Mc, May 1949.

20. R. S. Kirby, J. C. Harman, F. M. Capps, and R. N. Jones, "Effective Radio Ground-Conductivity Measurements in the United States," National Bureau of Standards Circular 546, Feb. 1954.

21. H. E. Bussey, "Microwave Attenuation Statistics Estimated from Rainfall and Water Vapor Statistics," Proc. I. R. E., 38, 781-785, (1950) (CRPL Preprint 50-7).

22. Bradford R. Bean, "Some Meteorological Effects on Scattered Radio Waves," Trans. of I. R. E., PGCS, 4, 32-38, (1956).

23. B. R. Bean and R. L. Abbott, "Oxygen and Water Vapor Absorption of Radio Waves in the Atmosphere," Geofis. Pura e Appl., 37 (2), 127, (1957).

24. "Instructions for the Use of Basic Radio Propagation Predictions," NBS Circular 465, 1947, Superintendent of Documents, Government Printing Office, Washington 25, D. C.

25. "Basic Radio Propagation Predictions - Three Months in Advance," CRPL Series D, Superintendent of Documents, Government Printing Office, Washington 25, D. C.

26. J. R. Wait, "The Mode Theory of VLF Ionospheric Propagation for Finite Ground Conductivity," Proc. I. R. E., 45 (6), 760-767, (1957).

27. J. R. Wait, "The Attenuation vs Frequency Characteristics of VLF Radio Waves," Proc. I. R. E., 45 (6), 768-771, (1957).

28. Jack N. Brown, "Round-the-World Signals at Very Low Frequency," J. Geophys. Research, 54, 367-372, (1949) (1949).

29. G. Millington, "Ground Wave Propagation Over an Inhomogeneous Smooth Earth; Part 1," Proc. Inst. Elec. Engrs., 96, 53, (1949).

30. James R. Wait and James Householder, "Mixed-path Ground-Wave Propagation; Part 1 - Short Distances," J. Research NBS, 57, 1-15, (1956); Part 2 - "Larger Distances," J. Research NBS, 59, 19-26, (1957).

31. T. N. Gautier, "The Ionosphere," Scientific American, 193 (3), 126-137, (1955).

32. J. R. Johler, W. J. Kellar, and L. C. Walters, "Phase of the Low Radio Frequency Ground Wave," National Bureau of Standards Circular 573, June 26, 1956.

33. J. R. Wait and H. H. Howe, "Amplitude and Phase Curves for Ground Wave Propagation in the Band 200 Cycles Per Second to 500 Kilocycles," National Bureau of Standards Circular 574, (1956).

34. J. R. Wait and A. Murphy, "Multiple Reflections Between the Earth and the Ionosphere in VLF Propagation," Geofis. Pura e Appl. (Milano) 35, (III), 61-72, (1956)

35. B. G. Pressy, G. E. Ashwell, and C. S. Fowler, "The Measurement of the Phase Velocity of Ground Wave Propagation at Low Frequencies Over a Land Path," Proc. Inst. Elec. Engrs., 100 (Pt. III), 73-84, (1953).

36. G. Hefley, C. England, W. Kellar and R. Dyer, "Skywave Delays at 100 kc and Noise Signal Interference in the 100 kc Navigation Band," Private Communication, June, 1953.

37. A. B. Schneider, "Phase Variations With Range of the Ground Wave Signal from C. W. Transmitters in the 70-130 kc Band," Jour. British Inst. Radio Engrs., 12 (3), 181-194, (1955).

38. R. H. Doherty, "Pulsed Sky Wave Phenomena Observed at 100 kc," Private Communication, Feb. 1957.

39. J. R. Wait, "Pattern of a Flush-Mounted Microwave Antenna," J. Research NBS, 59, 255-259, (1957).

40. J. R. Wait, and Alyce M. Conda, "Pattern of an Antenna on a Curved Lossy Surface," I. R. E. Trans., AP-6, 348-360, (1958).

41. S. O. Rice, "Diffraction of Plane Radio Waves by a Parabolic Cylinder," Bell System Tech. Jour., 33, 417-504, (1954).

42. V. A. Fock, "Fresnel Diffraction from Convex Bodies," Uspekhi Fizicheskikh Nauk (Progress of Physical Sciences), 43, 587-599, (1951) also, Paper No. IX, Astia Document No. AD 117276: "A series of translations of 13 papers by Fock," U. S. Department of Commerce, Office of Technical Services, Washington 25, D. C., June, 1957.

43. H. Bremmer, "Terrestrial Radio Waves," Elsevier Publishing Co., 1949, Chapter XI.

(44) Omitted in Revision.

45. J. S. Belrose, "Some Investigations of the Lowest Ionosphere," a dissertation submitted for the degree of Doctor of Philosophy in the University of Cambridge in England, December, 1956.

46. A. D. Watt, E. L. Maxwell and E. H. Whelan, "Low Frequency Propagation Paths in Arctic Areas," J. Research NBS, 63-D (Radio Propagation), 99 , (1959).

47. D. F. Martyn, "The Propagation of Medium Radio Waves in the Ionosphere," Proc. Phys. Soc., 47, 323-339, (1935).

48. Paul O. Laitinen and George W. Haydon, "Analysis and Prediction of Sky-Wave Field Intensities in the High Frequency Band," Technical Report No. 9, Signal Corps Radio Propagation Agency, Ft. Monmouth, New Jersey.

49. A. N. Kazantsev, "Theoretical Calculations of Ionospheric Absorption in the Different Areas of Change of Ionization as a Function of Height," Proceedings of the Academy of Sciences of the U. S. S. R., 1956, No. 9.

50. A. N. Kazantsev, "Absorption of Short Radio Waves in the Ionosphere and the Intensity of the Electric Field at the Point of Reception," Proceedings of the Academy of Sciences of the U. S. S. R., 1947, No. 9.

51. D. K. Bailey, R. Bateman, and R. C. Kirby, "Radio Transmission at VHF by Scattering and Other Processes in the Lower Ionosphere," Proc. IRE, 43, 1181-1230, (1955).

52. R. C. Kirby, "VHF Propagation by Ionospheric Scattering - A Survey of Experimental Results," IRE Trans. Commun. Syst. CS-4 (1), 17-27, (1956).

53. R. C. Kirby, "Extreme Useful Range of VHF Transmission by Scatter from the Lower Ionosphere," IRE Convention Record, 1958.

54. A. D. Wheelon, "Radio Frequency and Scattering Angle Dependence of Ionospheric Scatter Propagation at VHF," J. Geophys. Research, 62, 93-112, (1957).

55. A. D. Wheelon, "Diurnal Variations of Signal Level and Scattering Heights for VHF Propagation," J. Geophys. Research, 62, 255-266, (1957).

56. A. D. Wheelon, "Refractive Corrections to Scatter Propagation," J. Geophys. Research, 62, 343-349, (1957).

57. K. A. Norton, "Point-to-Point Radio Relaying via the Scatter Mode of Tropospheric Propagation," IRE Trans. Commun. Syst. CS-4 (1), 39-49, (1956).

58. K. A. Norton, "Recent Experimental Evidence Favoring the pK_1 (p) Correlation Function for Describing the Turbulence of Refractivity in the Troposphere and Stratosphere," Proc. Joint Commission on Radio Meteorology held under the auspices of the International Scientific Radio Union at New York University, August, 1957 (in press).

59. B. R. Bean, "Prolonged Space-Wave Fadeouts at 1046 Mc Observed in Cheyenne Mt. Propagation Program," Proc. IRE, 42 (5), 848-853, (1954).

60. M. Katzin, R. W. Bauchman, and W. Binnian, "3 and 9 Centimeter Propagation in Low Ocean Ducts," Proc. IRE, 35 (9), 891-905, (1947).

61. B. R. Bean, "The Atmospheric Bending of Radio Waves," Proc. International Conference on Electromagnetic Wave Propagation, Liege, Belgium, October, 1958, (in press).

62. H. G. Booker and W. Walkinshaw, "The Mode Theory of Tropospheric Refraction and Its Relation to Wave-Guides and Diffraction," Meteorological Factors in Radio-Wave Propagation - a report of a conference held on 8 April 1946 at the Royal Institution, London, by the Physical Society and the Royal Meteorological Society; published by the Physical Society of London, pp. 80-127.

63. J. E. Freehafer, W. T. Fishback, W. H. Furry and D. E. Kerr, "Theory of Propagation in a Horizontally Stratified Atmosphere," Chapter 2, "Propagation of Short Radio Waves," Vol. 13, Radiation Laboratory Series, McGraw-Hill Book Co., 1951.

64. C. L. Pekeris, "Wave Theoretical Interpretation of Propagation of 10-centimeter and 3-centimeter Waves in Low-Level Ocean Ducts," Proc. IRE, 35 (5), 453-462, (1947).

65. J. C. Schelling, C. R. Burrows, and E. B. Ferrell, "Ultra-Short-Wave Propagation," Proc. IRE, 21 (3), 427-463, (1933).

66. B. R. Bean and F. M. Meaney, "Some Applications of the Monthly Median Refractivity Gradient in Tropospheric Propagation," Proc. IRE, 43, 1419-1431, (1955).

67. B. R. Bean and G. Thayer, "Models of the Atmospheric Radio Refractive Index," Proc. IRE, 47, 740-755, (1959).

68. Study Programme No. 90, "Tropospheric Wave Propagation," Documents of the VIIIth Plenary Assembly, Warsaw, 1956, vol. 1, pp. 538-539, Published by the International Telecommunication Union, Geneva, 1957.

69. B. R. Bean and J. D. Horn, "The Radio Refractive Index Climate Near the Ground," J. Research NBS, 63-D, (Radio Propagation), Sept. (1959).

70. P. L. Rice, A. G. Longley, and K. A. Norton, "Prediction of the Cumulative Distribution with Time of Ground Wave and Tropospheric Wave Transmission Loss," Private Communication, June 1958.

71. K. A. Norton, L. E. Vogler, W. V. Mansfield, and P. J. Short, "The Probability Distribution of the Amplitude of a Constant Vector Plus a Rayleigh-Distributed Vector," Proc. IRE. 43 (10), 1354-1361, (1955)

72. CCIR Report No. 65: "Report on Revision of Atmospheric Radio Noise Data," Warsaw, 1956; available as a separate document from the International Telecommunications Union, Geneva, or in Vol. I of the Documents of the VIIIth Plenary Assembly of the CCIR (Warsaw, 1956).

73. R. W. Plush, A. D. Watt, and E. F. Florman, "Carrier-to-Noise Requirements for Teletype Communication via a Fading UHF Carrier," Private Communication, July, 1958.

Appendix I

The Attenuation of Radio Waves Propagated Between a Perfectly Reflecting Spherical Ionospheric Layer and a Spherical Earth

The attenuation with which we are here concerning ourselves is that due to the spreading of the energy over larger and larger areas as it progresses further and further from the transmitting antenna.

For the sake of clarity in presentation, several simpler problems will be solved first in order to illustrate the principles involved. Consider first the attenuation of waves emanating from an isotropic radiator in free space as in Fig. I-1. The total energy passing through the differential elements of area, dA_1 and, dA, normal to the radius vector and at the unit of distance R_1 and at R, respectively, will be equal.

$$dA_1 = R_1\, d\psi\, r_1\, d\chi = R_1^2 \cos\psi\, d\psi\, d\chi \tag{I-1}$$

$$dA = R^2 \cos\psi\, d\psi\, d\chi \tag{I-2}$$

Now, if we let p_1 and p_2 represent the energy density per unit area at the distances R_1 and R, we obtain:

$$p_1\, dA_1 = p_2\, dA \tag{I-3}$$

$$(p_2/p_1) = (dA_1/dA) = R_1^2/R^2 \tag{I-4}$$

Thus we see that the field intensity (i. e., the energy density) is inversely proportional in free space to the square of the distance

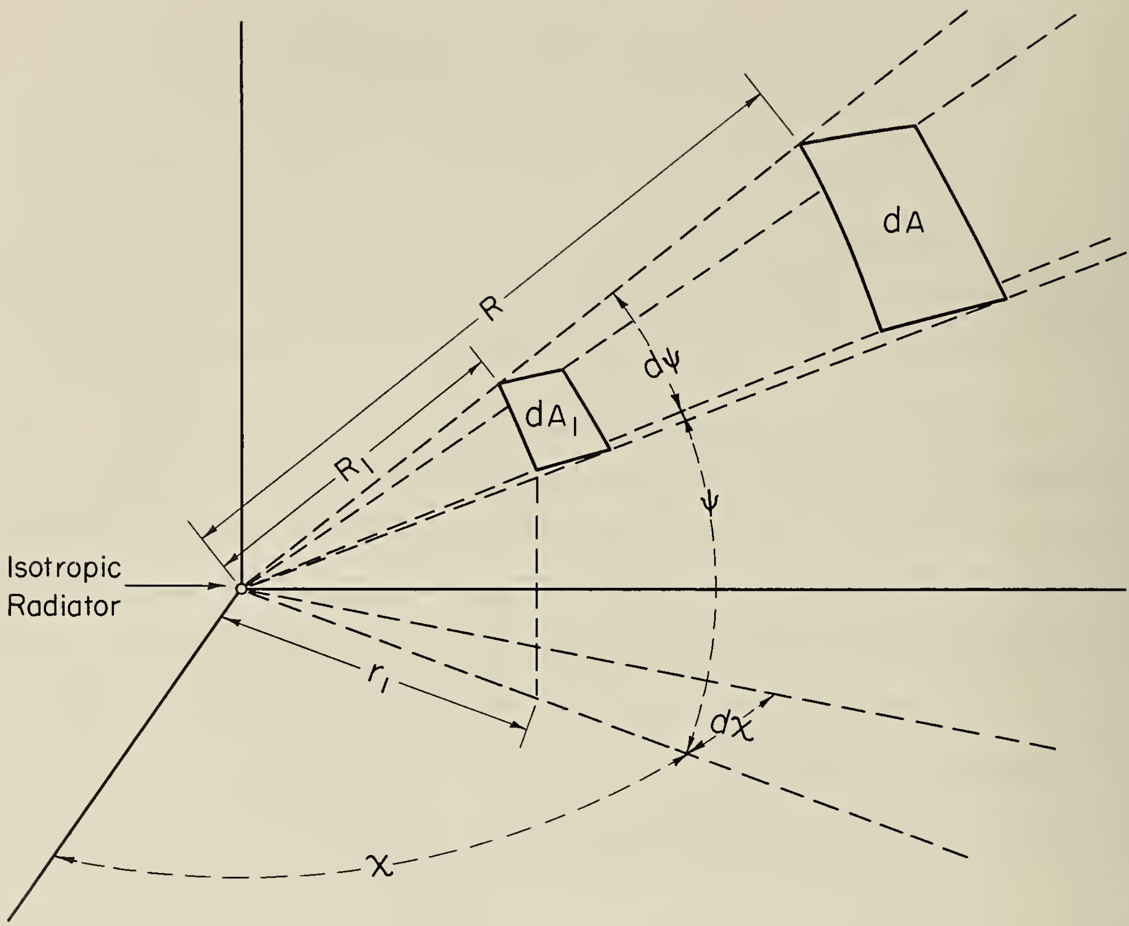

Figure I-1

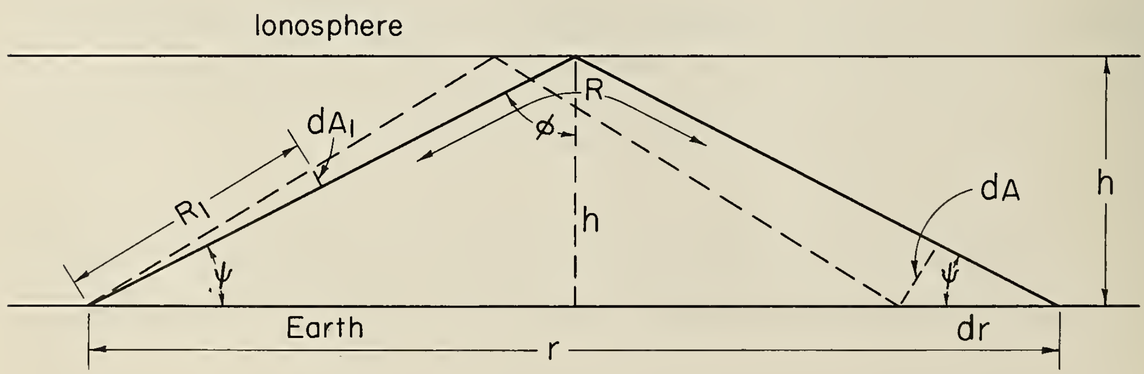

Figure I-2

from the source. In terms of transmission loss, this result may be expressed:

$$L_{bf}(R) = L_{bf}(R_1) + 20 \log_{10}(R/R_1) \qquad \text{(I-5)}$$

Consider next—see Fig. I-2—the attenuation of waves reflected from a plane perfectly conducting ionosphere at a height, h, above a plane earth and with no atmospheric refraction; in this case we have:

$$dA = - r\, d\chi \sin\psi\, dr = R^2 \cos\psi\, d\psi\, d\chi \qquad \text{(I-6)}$$

In this case again we find that the attenuation of waves reflected from a plane ionosphere is the same as in (I-5).

Finally consider—see Fig. I-3—the attenuation of waves reflected from a perfectly conducting spherical ionosphere and a perfectly conducting spherical earth with the effects of atmospheric refraction included:

$$dA = - y\, d\chi \sin\psi\, dr \qquad \text{(I-7)}$$

$$dr = 2\, a\, d\theta \qquad \text{(I-8)}$$

$$y = a \sin 2\theta \qquad \text{(I-9)}$$

$$dA = - 2a^2 \sin 2\theta \sin\psi\, d\theta\, d\chi \qquad \text{(I-10)}$$

By Snell's law:

$$\frac{\cos(\psi + \theta - \tau)}{\cos\psi} = C = \frac{\{1 + N_o \cdot 10^{-6} \exp(-c_s h_s)\}(a + h_s)}{\{1 + N_o \cdot 10^{-6} \exp(-c_s h)\}(a + h)} \qquad \text{(I-11)}$$

$$C = \cos(\theta - \tau) - \tan\psi \sin(\theta - \tau) \qquad \text{(I-12)}$$

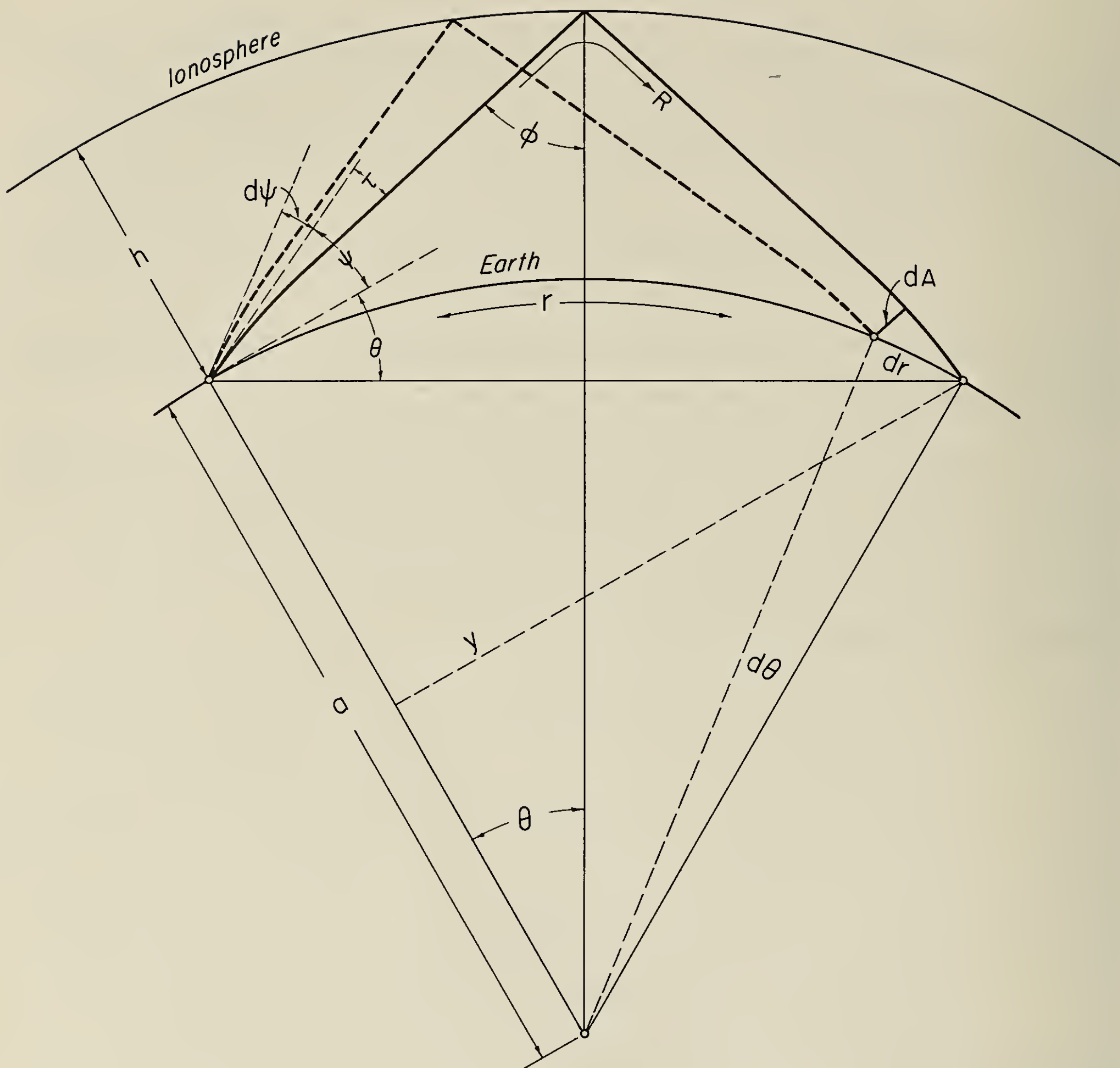

Figure I-3

Since C is a constant, independent of θ, τ and ψ, we find:

$$dC = \frac{\partial C}{\partial \theta} d\theta + \frac{\partial C}{\partial \tau} d\tau + \frac{\partial C}{\partial \psi} d\psi = 0 \qquad \text{(I-13)}$$

Thus $$(d\theta/d\psi) = - \left\{ \frac{\partial C}{\partial \psi} \Big/ \frac{\partial C}{\partial \theta} \right\} - \left\{ \frac{\partial C}{\partial \tau} \Big/ \frac{\partial C}{\partial \theta} \right\} \frac{d\tau}{d\psi} \qquad \text{(I-14)}$$

$$(d\theta/d\psi) = - \frac{\sin(\theta - \tau)}{\cos\psi \cos\phi} + \frac{d\tau}{d\psi} \qquad \text{(I-15)}$$

In the particular case when $\psi = 0$:

$$(d\theta/d\psi)_{\psi = o} = -1 + (d\tau/d\psi)_{\psi = o} = -k \qquad \text{(I-16) *}$$

$$L(R) = L_{bf}(R_1) + 10 \log_{10}\left(\frac{dA}{dA_1}\right) = L_{bf}(R) - C_1(R) \qquad \text{(I-17)}$$

Thus, if we substitute (I-10) and (I-1) in the above and solve for $C_1(R)$, we obtain:

$$C_1(R) = 10 \log_{10}\left(\frac{R^2 \, dA_1}{R_1^2 \, dA}\right) = 10 \log_{10}\left\{ \frac{R^2 \cot\psi}{-2a^2 \sin 2\theta (d\theta/d\psi)} \right\} \qquad \text{(I-18)}$$

The function $C_1(R)$ is a convergence factor, expressed in decibels, which measures how much stronger the field intensity at the receiving point is for one reflection at a spherical ionosphere than it would be if it were plane.

The generalization of this expression to m reflections at the ionosphere may be obtained by noting that the only changes required in the above analysis are:

* Note that k here refers to the ratio between the effective and actual radii of the earth.

$$dr = 2ma\,d\theta \tag{I-19}$$

$$y = a \sin 2m\theta \tag{I-20}$$

Thus the convergence factor for m ionospheric reflections may be written:

$$C_m(R) = 10 \log_{10}\left\{\frac{R}{-2ma\sin\psi\,(d\theta/d\psi)}\right\}_v \cdot \left\{\frac{R\cos\psi}{a\sin 2m\theta}\right\}_h \tag{I-21}$$

The above expression has been divided into two factors with subscripts v and h so that the convergence of the rays in the vertical and horizontal planes, respectively, can be considered separately.

If we introduce the approximate expression $R \simeq 2ma\sin\theta/\sin\phi_o$ into (I-21) above, we obtain:

$$C_m(R) \cong 10 \log_{10}\left\{\frac{\sin\theta}{-\sin\phi_o\sin\psi\,(d\theta/d\psi)}\right\}_v \cdot \left\{\frac{2m\sin\theta\cos\psi}{\sin\phi_o\sin 2m\theta}\right\}_h \tag{I-21a}$$

The above expression indicates that the convergence in the vertical plane at points far removed from a caustic is independent of the number of ionospheric reflections for a given angle, ψ.

Note that the convergence in the vertical plane becomes infinite when ψ approaches zero; this infinite convergence is demonstrated on Fig. 25. Similarly, the convergence in the horizontal plane becomes infinite at the antipode of the transmitter where $2m\theta = \pi$. Actually, of course, the received energy is finite at these points, and we may use Airy's integral to evaluate the convergence in the vertical plane when $\psi \leq 0$. It can be shown [1/] by the solution of the two dimensional wave equation that:

$$C_v(R) = 10 \log_{10}\left\{\frac{-\Omega}{\Omega''(\psi)}\right\}_v \tag{I-22}$$

where $\Omega = 2\pi R/\lambda$ is the phase of the waves at the receiving point. If we multiply the numerator and denominator of the first term in (I-21) by $2\pi/\lambda$ and compare the results with (I-22), we find:

$$\Omega''(\psi) = 4\pi m\,(a/\lambda)\,\sin\psi\,(d\theta/d\psi)$$

Now we see that the above second derivative of the phase is equal to zero when the convergence factor becomes infinite; this is the definition of a caustic and the convergence at this caustic may be evaluated by means of the third derivative at this point:

$$\Omega'''(\psi) = -\,4\pi m\,k(a/\lambda) \qquad (\psi \leq 0)$$

Thus, at the caustic in the vertical plane, $C_v(R)$ may be expressed:[1]

$$C_v(R) = 10\,\log_{10}\left\{\frac{\Omega\,2\pi\,\{A_i(0)\}^2}{\left[\frac{1}{2}\,\Omega'''\right]^{2/3}}\right\} \qquad \text{(I-23)}$$

In the above $A_i(0)$ is the Airy integral[2] with argument zero: $2\pi\,\{A_i(0)\}^2 = 0.79196357$.

From the above results we obtain the following expression for $C_m(R)$ at the caustic in the vertical plane:

$$C_m(R) = 10\,\log_{10}\left\{\frac{2\pi(R/\lambda)\,0.792}{[2\pi m\,k(a/\lambda)]^{2/3}}\right\}_v \cdot \left\{\frac{R}{a\,\sin 2m(\theta_m - k\psi)}\right\}_h (\psi \leq 0)$$

(I-24)

The convergence at the antipode of the transmitter is of a somewhat different nature. Note, in particular, that there is no point of stationary phase with respect to variations in the azimuth angle, χ, since the waves appear to be arriving from all directions at this particular point. The following treatment of this problem is due to J. R. Wait.[10]

Using a cylindrical coordinate system centered at the antipode (i.e., ρ, χ, z), we may obtain the following axially symmetric solution of the wave equation, for a time factor $\exp(i\omega t)$:

$$E_z = A \exp[-ik(R_a + z \sin \psi)] J_o(k \rho \cos \psi) \tag{I-25}$$

$$H_\chi = B \exp[-ik (R_a + z \sin \psi) J_1(k \rho \cos \psi) \tag{I-25a}$$

where $k = 2\pi/\lambda$, R_a is the distance along the ray path to the antipode, A and B are constants, and J_o and J_1 denote Bessel functions. For the ground wave and for those ionospheric modes for which m is sufficiently small so that ψ is negative at the antipode, ψ should be set equal to zero in (I-25) and (I-25a). Note that, in addition to the oscillations with time, the magnitudes of E_z and H_χ oscillate with the distance ρ from the antipode, E_z having its maximum value at the antipode while H_χ is equal to zero at the antipode. Note also that the variation with ρ is the same, independent of the azimuth angle, χ; this would be expected since we have assumed that our source radiates uniformly in all directions. When $k\rho \cos \psi >> 1$, we may replace the Bessel functions by the first terms in their asymptotic expansions and obtain:

$$E_z = A \exp(-ikz \sin \psi) \left\{ \frac{\exp\{i[k(\rho \cos \psi - R_a) - \pi/4]\} + \exp\{-i[k(\rho \cos + R_a) - \pi/4]\}}{\sqrt{2\pi k \rho \cos \psi}} \right\} \tag{I-26}$$

$$H_\phi = -i B \exp(-ikz \sin \psi \left\{ \frac{\exp\{i[k(\rho \cos \psi - R_a) - \pi/4]\} - \exp\{-i[k(\rho \cos \psi + R_a) - \pi/4]\}}{\sqrt{2\pi k \rho \cos \psi}} \right\} \tag{I-26a}$$

The two exponential terms in the above may be identified with waves arriving from opposite directions at a receiving point at a distance ρ from the antipode along great circle paths of lengths $R_a - \rho \cos \psi$ and

$R_a + \rho \cos \psi$, respectively. It is the interference between these two waves which causes the oscillations in the magnitude of the field near the antipode.

To complete our solution we need only evaluate the constants A and B. Rather than doing this directly, we note by (I-21) that the geometrical theory indicates that the focusing in the horizontal plane not too near the antipode is given by:

$$c_h = \frac{R \cos \psi}{a \sin 2m\theta} \qquad (2m\theta < \pi) \tag{I-27}$$

and if we multiply (I-27) by the square of the ratio of $|E_z|$ as given by (I-25) and by the first term in (I-26), we obtain the following expression for c_h which must be used instead of (I-27) at points very near the antipode:

$$c_h = \frac{R \cos \psi}{a \sin 2m\theta} \cdot [J_o(k\rho \cos \psi)]^2 \, 2\pi k \rho \cos \psi \tag{I-28}$$

When we note that $\rho = a \sin(\pi - 2m\theta)$, the above reduces to:

$$c_h = 2\pi k R \cos^2 \psi \, [J_o(k \rho \cos \psi)]^2 \tag{I-29}$$

For the ground wave $R = \pi a$ and $\psi = 0$; thus, at the antipode $c_h = 2\pi^2 ka$ and $C_h = 10 \log_{10} c_h = 34.210 + 10 \log_{10} f_{kc}$, and this clearly represents an extremely large focusing effect for the ground wave at and near this point. The focusing in the horizontal plane for the sky wave modes is only slightly different,* but we must add to this the focusing in the vertical plane to obtain the total focusing for these modes. (I-29) is for a vertical electric dipole receiving antenna; if a horizontal magnetic dipole were used for reception, then the J_o should be replaced by J_1.

* Note that $\cos \psi > 0.995$ for $m \leq 16$, and $\cos \psi = 1$ for $m \leq 8$ when $h = 90$ km.

Using a cylindrical coordinate system centered at the antipode (i.e., ρ, χ, z), we may obtain the following axially symmetric solution of the wave equation, for a time factor $\exp(i\omega t)$:

$$E_z = A \exp[-ik(R_a + z \sin \psi)] J_o(k \rho \cos \psi) \tag{I-25}$$

$$H_\chi = B \exp[-ik(R_a + z \sin \psi) J_1(k \rho \cos \psi) \tag{I-25a}$$

where $k = 2\pi/\lambda$, R_a is the distance along the ray path to the antipode, A and B are constants, and J_o and J_1 denote Bessel functions. For the ground wave and for those ionospheric modes for which m is sufficiently small so that ψ is negative at the antipode, ψ should be set equal to zero in (I-25) and (I-25a). Note that, in addition to the oscillations with time, the magnitudes of E_z and H_χ oscillate with the distance ρ from the antipode, E_z having its maximum value at the antipode while H_χ is equal to zero at the antipode. Note also that the variation with ρ is the same, independent of the azimuth angle, χ; this would be expected since we have assumed that our source radiates uniformly in all directions. When $k\rho \cos \psi >> 1$, we may replace the Bessel functions by the first terms in their asymptotic expansions and obtain:

$$E_z = A \exp(-ikz \sin \psi)\left\{\frac{\exp\{i[k(\rho \cos \psi - R_a) - \pi/4]\} + \exp\{-i[k(\rho \cos + R_a) - \pi/4]\}}{\sqrt{2\pi k \rho \cos \psi}}\right\} \tag{I-26}$$

$$H_\phi = -i B \exp(-ikz \sin \psi \left\{\frac{\exp\{i[k(\rho \cos \psi - R_a) - \pi/4]\} - \exp\{-i[k(\rho \cos \psi + R_a) - \pi/4]\}}{\sqrt{2 \pi k \rho \cos \psi}}\right\} \tag{I-26a}$$

The two exponential terms in the above may be identified with waves arriving from opposite directions at a receiving point at a distance ρ from the antipode along great circle paths of lengths $R_a - \rho \cos \psi$ and

$R_a + \rho \cos \psi$, respectively. It is the interference between these two waves which causes the oscillations in the magnitude of the field near the antipode.

To complete our solution we need only evaluate the constants A and B. Rather than doing this directly, we note by (I-21) that the geometrical theory indicates that the focusing in the horizontal plane not too near the antipode is given by:

$$c_h = \frac{R \cos \psi}{a \sin 2m\theta} \qquad (2m\theta < \pi) \tag{I-27}$$

and if we multiply (I-27) by the square of the ratio of $|E_z|$ as given by (I-25) and by the first term in (I-26), we obtain the following expression for c_h which must be used instead of (I-27) at points very near the antipode:

$$c_h = \frac{R \cos \psi}{a \sin 2m\theta} \cdot [J_o(k \rho \cos \psi)]^2 \, 2\pi k \rho \cos \psi \tag{I-28}$$

When we note that $\rho = a \sin(\pi - 2m\theta)$, the above reduces to:

$$c_h = 2\pi k R \cos^2 \psi \, [J_o(k \rho \cos \psi)]^2 \tag{I-29}$$

For the ground wave $R = \pi a$ and $\psi = 0$; thus, at the antipode $c_h = 2\pi^2 k a$ and $C_h = 10 \log_{10} c_h = 34.210 + 10 \log_{10} f_{kc}$, and this clearly represents an extremely large focusing effect for the ground wave at and near this point. The focusing in the horizontal plane for the sky wave modes is only slightly different,* but we must add to this the focusing in the vertical plane to obtain the total focusing for these modes. (I-29) is for a vertical electric dipole receiving antenna; if a horizontal magnetic dipole were used for reception, then the J_o should be replaced by J_1.

---

* Note that $\cos \psi > 0.995$ for $m \leq 16$, and $\cos \psi = 1$ for $m \leq 8$ when $h = 90$ km.

All of the above discussion applies to the case when the effective reflecting surface of the ionosphere is smooth and concentric with the surface of the earth. In practice, as the sun rises and sets, or as the geomagnetic latitude of the reflection point is varied, the surface of the ionosphere will undoubtedly change in such a way that its radius of curvature and slope relative to a tangent plane on the earth will vary over appreciable ranges, and this will cause $C_m(R)$ to vary up and down relative to the values expected on the basis of the above analysis. However, except near the antipode, it seems plausible to assume that the median values of $C_m(R)$ may not be much influenced by such changes. The magnitude of the antipodal anomaly will be substantially reduced by these macroscopic perturbations of the spherical concentric shell model assumed for our calculations. Note also that there will be concentric rings around the antipode at which the expected field will be equal to zero. The radii of these concentric rings are the same, regardless of the number, m, of ionospheric reflections, and are determined by the zeros of the Bessel functions; for the electric field, the first two such rings have radii equal to 0.38λ and 0.88λ. Note, however, that the geographical location of the centers of the antipodal anomalies may be expected to be somewhat different for the different modes for the actual non-concentric ionosphere, and thus these zeros are not likely to be observable unless some means is used to exploit their different times of arrival. The shifts in the geographical locations of the anomalies caused by these macroscopic changes in the ionosphere would be expected to result in a net increase in the fading range in the neighborhood of the antipode.

In addition to these systematic macroscopic changes in the ionosphere, the reflecting surface of the ionosphere will be locally rough, and we will see in the following analysis how this local roughness may be expected to reduce the median values of convergence as computed above for a smooth concentric ionosphere.

We have seen above that the convergence depends, at a given receiving point, upon the smooth variation of the phase of the received waves with changes in elevation angle and azimuth. If we let σ_Ω denote the standard deviation of the phase of the waves received via m hops, then we may use Rayleigh's criterion of ionospheric roughness (see Section 2 for a discussion of Rayleigh's criterion as applied to ground roughness) to calculate σ_Ω in terms of the variance, σ_h^2, of the local effective reflection heights, h, of the ionosphere at the points of stationary phase.

$$\sigma_\Omega = \frac{720° \, \sigma_h \cos\phi \sqrt{m}}{\lambda} \tag{I-30}$$

Note that the variance, σ_Ω^2, of phase consists of components arising from (a) a drift of a fixed pattern of ionospheric irregularities relative to a reference great-circle-smooth-concentric-ionosphere path, (b) changes in the shape of these irregularities with time, and (c) changes in the locations of the reflection points in the horizontal plane.

Brennan and Phillips[3/] find that variations with time of the intensity and phase of a one-hop transmission at 543 kc over a 380 mile path at night indicate rather conclusively that they may be described adequately most of the time by assuming that the received waves consist of a steady component with constant phase and approximately constant amplitude plus a random Rayleigh distributed component of relative intensity k^2 and random relative phase; the amplitude distribution expected in this case is given on Fig. 5 with $K \equiv 10 \log_{10} k^2$. The fixed component may be identified with a specular reflection expected from the reference smooth surface while the random component arises from the surface roughness. It now becomes clear how ionospheric roughness may be expected to affect the convergence; the specular component will be increased $C_m(R)$ db whereas the random component, since its phase is random, will not be increased at all. If we write $C_m(R) \equiv 10 \log_{10} c_m$, then we find the following expression for the convergence factor $C_m(R, p)$ exceeded 100 p % of the time in terms of the values of $k^2(1 - p)$ exceeded 100(1 - p)% of the time:

$$C_m(R, p) = 10 \log_{10} \left\{ \frac{c_m + k^2(1 - p)}{1 + k^2(1 - p)} \right\} \tag{I-31}$$

Note that $k^2(1 - p)$ approaches zero as p approaches zero, and thus $C_m(R, p)$ approaches $C_m(R)$, the value expected for a smooth ionosphere, as p approaches zero. On the other hand, $k^2(1 - p)$ approaches ∞ for a perfectly rough ionosphere, and in this case there will be no convergence and $C_m(R, p)$ approaches zero.

The values of k^2 to be used in (I-31) may, in principle, be determined from observations of the variations in either the amplitude or the phase of the waves corresponding to a single mode of propagation. However, it is ordinarily better in practice to use the variations in phase as an index to k^2 since the amplitudes of the received waves also vary with ionospheric absorption, and it is sometimes difficult to separate out these absorption variations from the amplitude variations arising from surface roughness alone. In Table I-1 are tabulated some experimental measurements of σ_Ω. In some cases the required variance was observed directly, but in other cases it had to be estimated from phase difference measurements made on paths with one common terminal, but with their other terminals

Table I-1
Estimates of the Variance of Phase on Ionospheric Paths

No.	Freq.	Distance	SOURCE	TIME	MONTH	$\sigma_{obs.}$	S		σ_{Ω}	MODE		σ_h
	kc	Statute Miles	REFERENCE NUMBER			Degrees	λ	$\sqrt{2(1-\rho^2}$		m	$\cos\phi$	km_1
1	16	3230	PIERCE (4)	DAY	FEB.	8.06			8.06	3	0.146	0.829
2	16	3230	PIERCE (4)	NIGHT	FEB.	16.1			16.1	3	0.170	1.424
3	17.2	640	REDGMENT (5)	DAY	SEPT.	1.9	10	1.00	1.9	1	0.174	0.265
4	17.2	640	REDGMENT (5)	NIGHT	SEPT.	9.3	10	1.00	9.3	1	0.206	1.093
5	17.2	640	REDGMENT (5)	DAY	JAN.	5.2	10	1.00	5.2	1	0.174	0.726
6	17.2	640	REDGMENT (5)	NIGHT	JAN.	13.3	10	1.00	13.3	1	0.206	1.563
7	18.4	3488	REDGMENT (5)	DAY	JUNE JULY	7.1	10	1.00	7.1	3	0.144	0.643
8	18.4	3488	REDGMENT (5)	NIGHT	JUNE JULY	10.0	10	1.00	10.0	3	0.169	0.775
9	18.4	3488	REDGMENT (5)	DAY	DEC.	6.5	10	1.00	6.5	3	0.144	0.588
10	18.4	3488	REDGMENT (5)	NIGHT	DEC.	6.5	10	1.00	6.5	3	0.169	0.503
11	60	3230	PIERCE (4)	DAY	DEC.	2.8			2.8	3	0.146	0.077
12	100	2350	DOHERTY (6)	NIGHT	APRIL	10.8	> 40	1.41	7.64	1	0.165	0.193
13	115	780	FLORMAN (7)	NIGHT	MARCH	13.3	11	1.00	13.3	1	0.189	0.255
14	115	780	FLORMAN (7)	DAY	MARCH	2.7	11	1.00	2.7	1	0.158	0.062
15	418	1250	FLORMAN (7)	NIGHT	MARCH	51	41	1.41	36.1	1	0.167	0.216
16	543	380	BRENNAN (3)	NIGHT	JAN. TO APRIL	34	3.39	0.83	41.0	1	0.371	0.085
17	556	454	REDGMENT (5)	NIGHT	APRIL MAY	19	1.85	0.63	30.2	1	0.334	0.068

separated by S wavelengths. In this latter case the observed phase difference was related to σ_{Ω}^{2} as follows:

$$\sigma_{obs.}^{2} = 2(1 - \rho^{2}) \sigma_{\Omega}^{2} \tag{I-32}$$

In the above ρ is the correlation between the phase variations along the two independent paths. The correlation will vary from $\rho = 1$ for $S = 0$ to $\rho \cong 0$ for $S > 40\lambda$. Although direct measurements of ρ do not appear to be available in the literature, it seems reasonable to assume that ρ will be of the same order of magnitude as the correlation between the amplitude variations on paths separated a distance S at one end. Measurements of the latter correlation were reported in reference 3, and these data constituted the basis for the estimates in Table I-1.

Using (I-30) estimates of σ_h can also be made, and these are also given in Table I-1 and shown on Fig. I-4. Although the data are quite scattered, the curved lines labelled day and night, respectively, represent the estimates used in this report for calculating the median values of σ_{Ω} using (I-30). It should be noted that σ_{Ω} is itself a random variable which changes over wide ranges from hour to hour and from day to day. For example, an analysis of the data in reference 3 shows that the observed phase differences, $\sigma_{obs.}$, ranged from 5.3° to more than 180°, 10% of the values exceeded 118°, 50% exceeded 34° and 90% exceeded 14°. We will see below that the maximum value of $\sigma_{obs.}$ to be expected in practice is $103.9 \times \sqrt{2} = 147°$, which corresponds to $k^{2} = \infty$, and only 5% of their observed values exceeded this value.

The relation between σ_{Ω} and k^{2} has been obtained on the assumption that the data fit the Rice[8/] distribution of a constant vector plus a Rayleigh distributed vector. By integrating over the joint

MEDIAN EFFECTIVE IONOSPHERIC ROUGHNESS PARAMETER, σ_h
OBTAINED FROM OBSERVATIONS OF σ_Ω
σ_Ω (DEGREES) $\equiv 2.4\, f_{kc} \cos\phi\, \sigma_h$ (km)

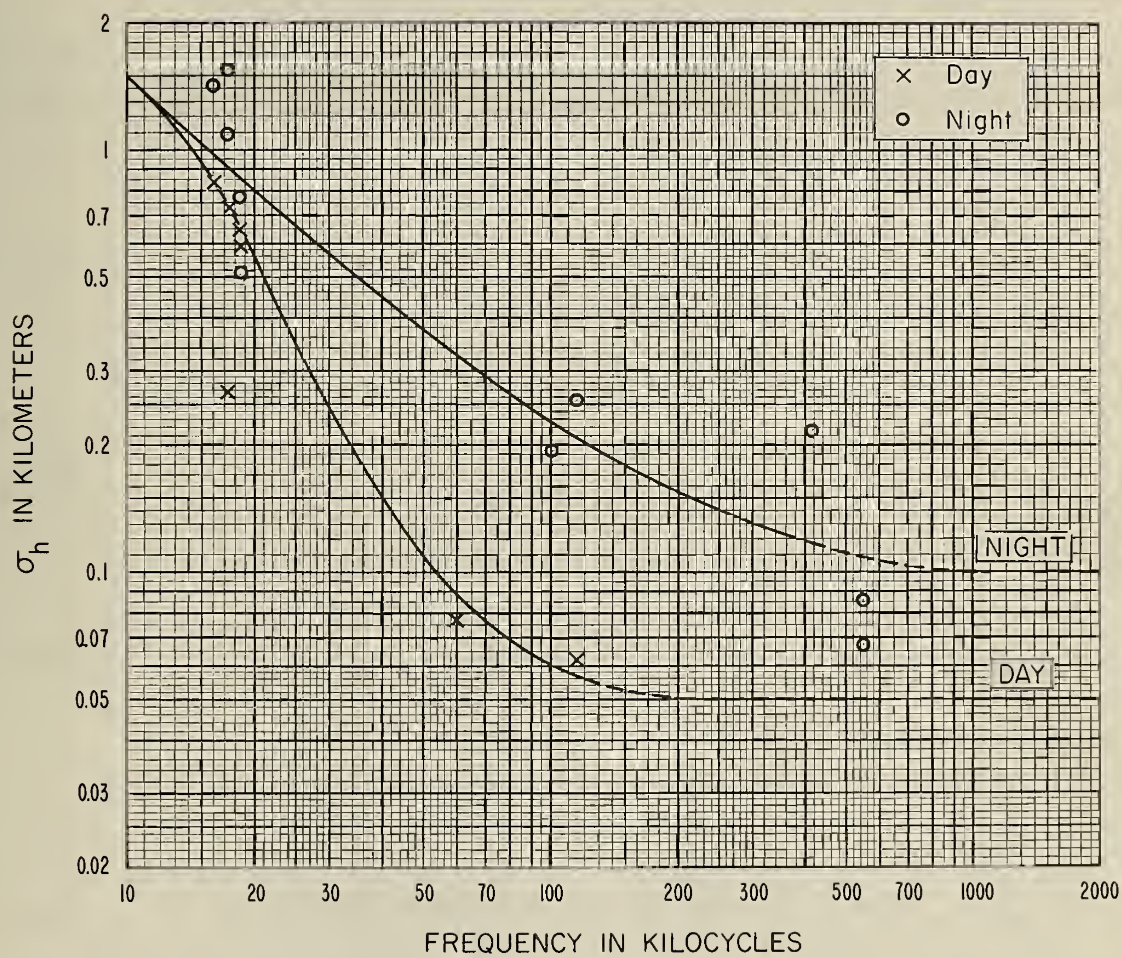

Figure I-4

probability distribution given by Rice for all of the variables except Ω, we obtain the following expression for the probability density function for Ω with k^2 as a parameter:

$$2\pi p(\Omega) = \{1 + \sqrt{\pi}\, z \exp(z^2)[1 + \operatorname{erf}(z)]\} \exp(-1/k^2) \tag{I-33}$$

where $z \equiv \frac{\cos \Omega}{k}$. Fig. I-5 shows $p(\Omega)$ is symmetrically distributed about zero for all values of k^2. When k^2 is very small, $\sin \Omega$ is distributed approximately normally about zero with variance $\sigma^2_{\sin \Omega} = k^2/2$. When k^2 approaches infinity, Ω is uniformly distributed between - 180° and +180° and σ_Ω approaches 103.923 degrees. Fig. I-6 gives the cumulative distribution defined by:

$$P[\Omega(t) > \Omega(P)] = 1 - \int_{-\pi}^{\Omega(P)} p(\Omega)\, d\Omega \tag{I-34}$$

The mean absolute value $|\bar{\Omega}|$ and variance σ^2_Ω are also of interest:

$$|\bar{\Omega}| = 2 \int_0^{\pi} \Omega\, p(\Omega)\, d\Omega \tag{I-35}$$

$$\sigma^2_\Omega = 2 \int_0^{\pi} \Omega^2\, p(\Omega)\, d\Omega \tag{I-36}$$

For many applications the cumulative distribution of the absolute value of $|\Omega(t)|$ is of greater interest:—

$$P'[\,|\Omega(t)| > \Omega(P')] = 2P[\Omega(t) > \Omega(P)] \tag{I-37}$$

The distribution of P' is given in a recent paper [9] and several of its percentage points, together with $|\bar{\Omega}|$ and σ_Ω are shown on Fig. I-7 as a function of k^2. By using the median values of σ_Ω determined from Fig. I-4, we may use the results shown on Fig. I-7 to determine the median values of $k^2(0.5)$ required for the evaluation of $C_m(R, 0.5)$.

THE PROBABILITY DENSITY FUNCTION $p(\Omega)$

$$p(\Omega)=\frac{1}{2\pi}\left\{1+\sqrt{\pi}\ \frac{\cos\Omega}{k}\exp\left(\frac{\cos^2\Omega}{k^2}\right)\left[1+\operatorname{erf}\left(\frac{\cos\Omega}{k}\right)\right]\right\}\exp\left(-\frac{1}{k^2}\right)$$

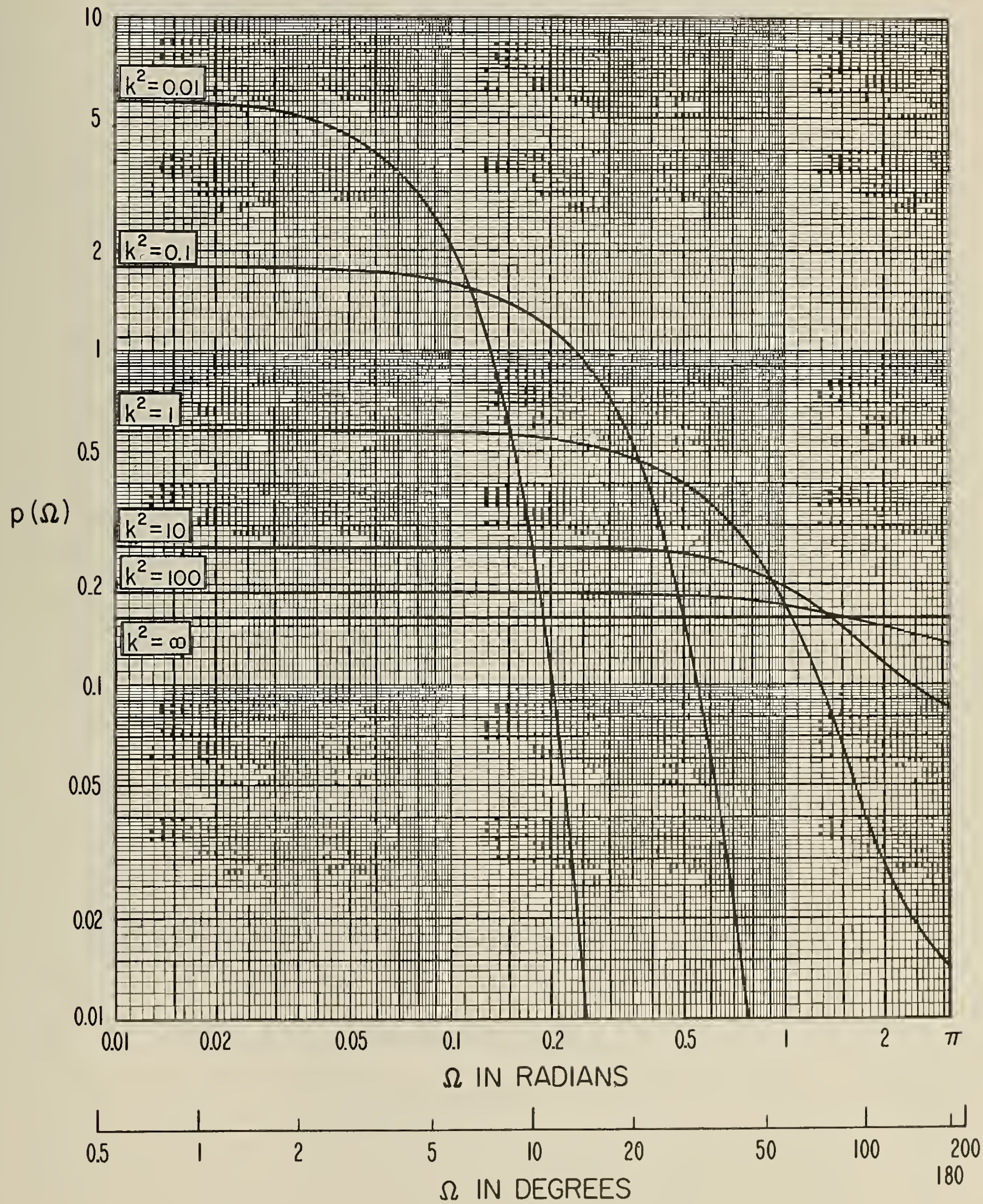

Figure I-5

THE CUMULATIVE DISTRIBUTION OF $\Omega(t)$

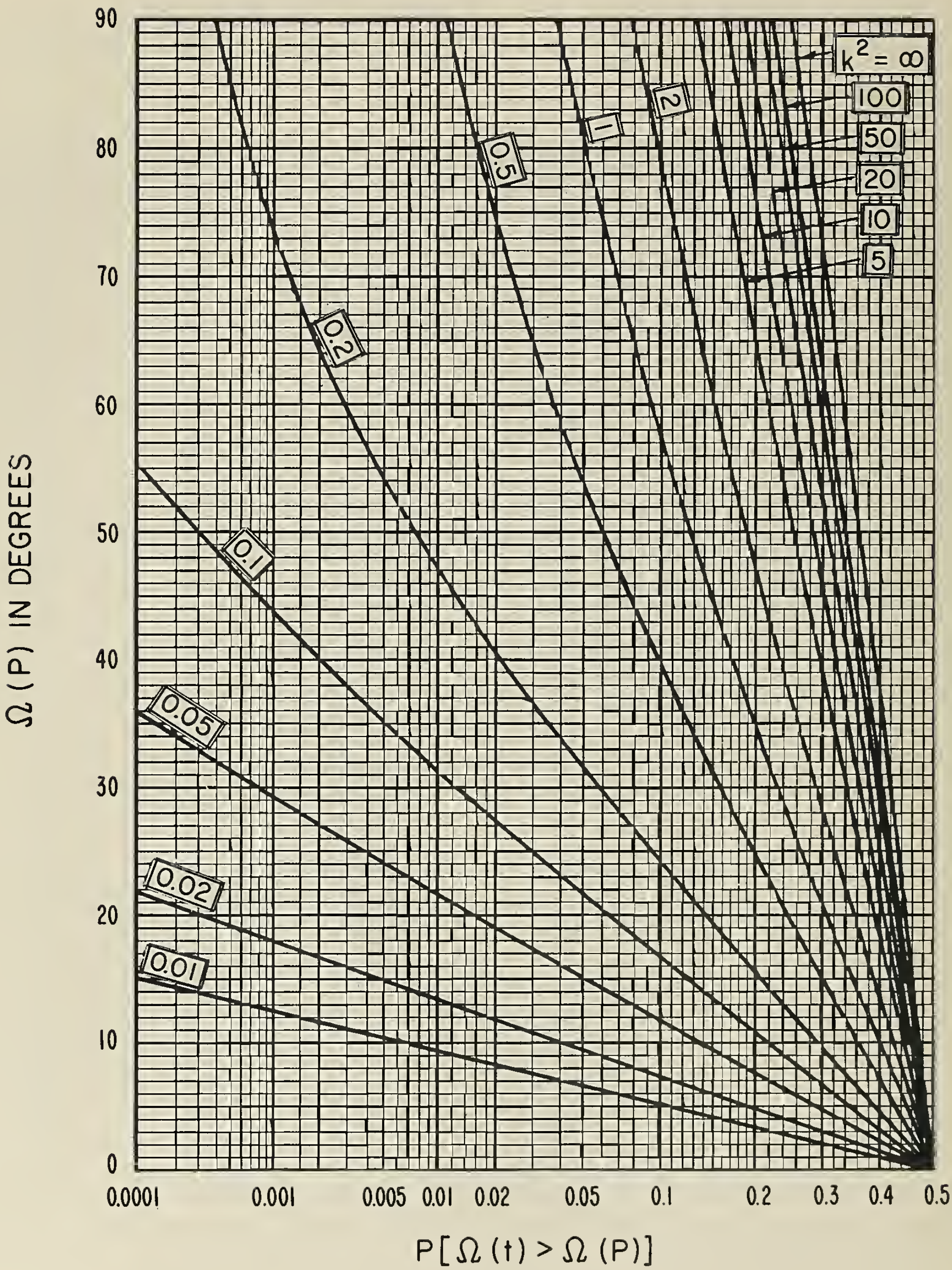

Figure I-6

STATISTICS OF THE DISTRIBUTION OF THE PHASE OF A CONSTANT VECTOR PLUS A RAYLEIGH DISTRIBUTED VECTOR

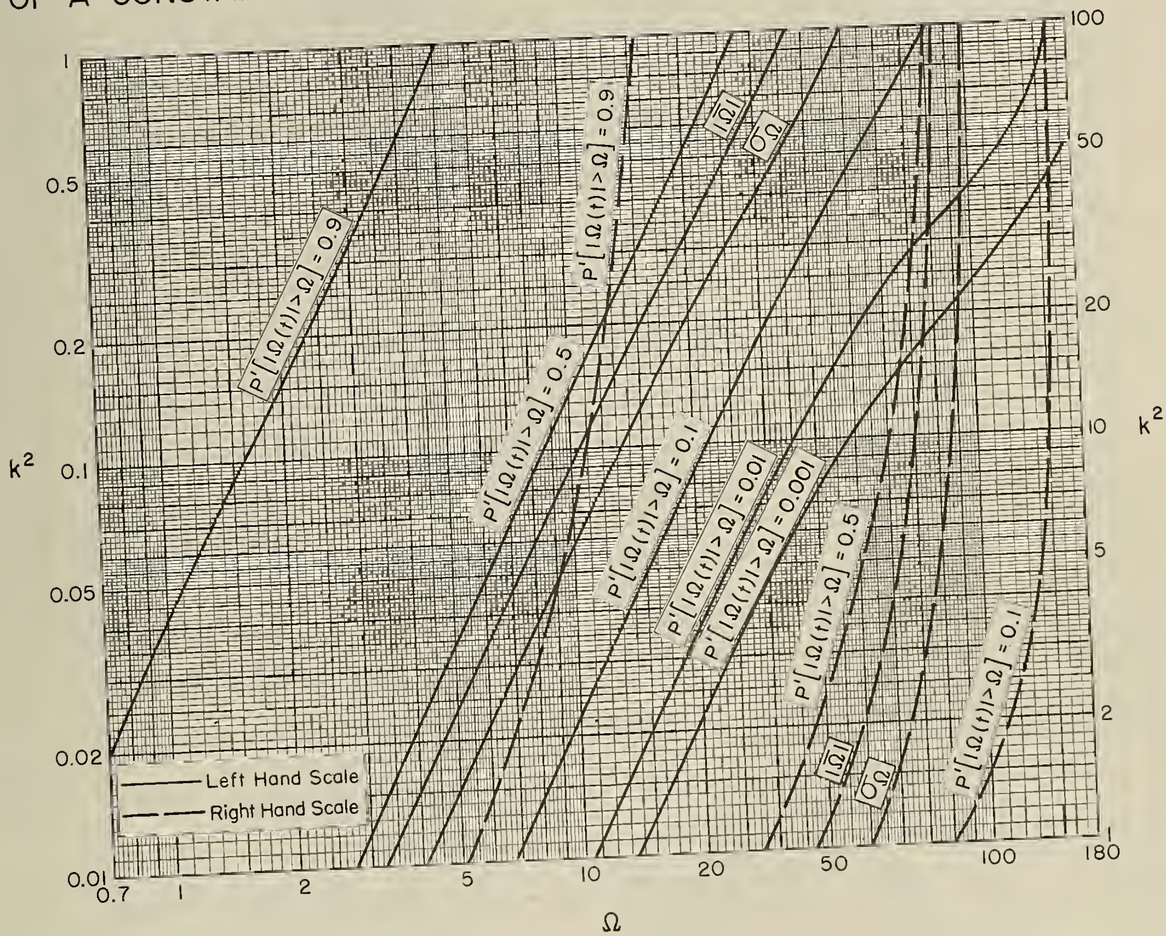

Figure I-7

Table I-2 below gives the values of $|\bar{\Omega}|$ and of σ_Ω for several values of k^2.

Table I-2

k^2	$\lvert\bar{\Omega}\rvert$ radians	σ_Ω radians	$\lvert\bar{\Omega}\rvert$ degrees	σ_Ω degrees
0.01	0.056514	0.070890	3.2380	4.0617
0.02	0.080059	0.10051	4.5871	5.7590
0.05	0.12726	0.16023	7.2915	9.1803
0.1	0.18172	0.23013	10.412	13.185
0.2	0.26330	0.34032	15.086	19.499
0.5	0.44605	0.60664	25.557	34.758
1	0.64346	0.87134	36.868	49.924
2	0.85196	1.1175	48.813	64.031
5	1.0876	1.3661	62.313	78.270
10	1.2217	1.4972	69.999	85.785
20	1.3212	1.5907	75.701	91.142
50	1.4119	1.6735	80.896	95.884
100	1.4582	1.7149	83.547	98.259
200	1.4911	1.7441	85.431	99.929
500	1.5203	1.7698	87.107	101.40
1000	1.5351	1.7827	87.953	102.14
∞	$\pi/2$	$\pi/\sqrt{3}$	90.000	103.92

An analysis was made in reference 3 of both the amplitude variations on single paths as well as the phase differences between paths separated by 3.39 wavelengths at one end. Using their observed median standard deviation of $\sigma_{obs.} = 34°$, the median value $\sigma_{\Omega} = 41°$ given in Table I-1 was estimated; this value corresponds by Fig. I-7 to $k^2(0.5) = 0.68$. The analysis of their amplitude variations gives directly the estimate $k^2(0.5) = 2/\overline{a}^2 = 0.854$, and this latter estimate is somewhat larger, as might have been expected, since the amplitude variations are biased by changes in absorption.

References to Appendix I

1. L. H. Doherty, "Geometrical optics and the field at a caustic with applications to radio wave propagation between aircraft," Cornell University Report EE 138.

2. British Association Mathematical Tables, Part Volume B; British University Press, Cambridge, 1946.

3. D. G. Brennan and M. Lindeman Phillips, "Phase and amplitude variability in medium-frequency ionospheric transmission," Technical Report No. 93, Massachusetts Institute of Technology Lincoln Laboratory, September, 1957; note that the a in this report, which is used as a parameter describing the Rice distribution of a constant plus a Rayleigh distributed vector, is equal to $\sqrt{2}/k$ where k^2 denotes the relative intensity of the random component as used in this appendix.

4. John A. Pierce, "Intercontinental frequency comparison by very-low-frequency radio transmission," Proc. IRE, vol. 45, no. 6, pp. 794-803, June, 1957.

5. P. G. Redgment and D. W. Watson, "Phase-correlation of medium and very-low-frequency waves using a baseline of several wavelengths," Admiralty Signal and Radar Est., Lythe Hill House, Haslemere, Surrey, England, Monograph No. 836, October, 1948.

6. R. H. Doherty, "Pulse Sky Wave Phenomena Observed at 100 kc," Private Communication, Feb. 6, 1957

7. Private communication from E. F. Florman of the Boulder Laboratories of the National Bureau of Standards.

8. S. O. Rice, "Properties of a sine wave plus random noise," Bell System Technical Journal, vol. 27, pp. 109-157, Jan., 1948; the joint probability distribution is given by equation (4.6).

9. K. A. Norton, E. L. Shultz, and H. Yarbrough, "The probability distribution of the phase of the resultant vector sum of a constant vector plus a Rayleigh-distributed vector," Jour. Appl. Phys., vol. 23, pp. 137-141; January, 1952. Note that the k in this reference is a power ratio rather than a voltage ratio and that the formulas and graphs give the distribution of $|\phi|$.

10. Private communication from J. R. Wait of the National Bureau of Standards, Boulder Laboratories.

Appendix II

The Physics of Ionospheric Scatter Propagation

Wheelon [54] [55] [56] gives the following formula for the scattered power, p_s, relative to the power, p_f, expected for propagation over the same distance in free space:

$$(p_s/p_f) = 4\pi\, b \sec \phi\, \sigma(k^2) \tag{II-1}$$

$$\sigma(k^2) = \text{constant}\; r_e^2 < [d\, N_e/dh]^2\, \ell_o^5 > f(k^2) \tag{II-2}$$

$$f(k^2) = [1 + k^2 \ell_o^2]^{-5/2}\, [1 + (k^2 \ell_s^2)^{2/3}]^{-2}\, [1 + (k^2 \ell_s^2)^2]^{-4/3} \tag{II-3}$$

The dimensionless constant in (II-2) is of the order of unity, and will be set equal to one in the subsequent analysis; k^2 is defined by (32). $[d\, N_e/dh]$ is the gradient of the electron density expressed in electrons/cubic meter/meter; b is the effective thickness of the scattering layer expressed in meters; the classical electron radius, $r_e = 2.81785 \times 10^{-15}$ meters and ℓ_o is the scale of turbulence expressed in meters.

Note that when $f = f_{MUF}$ we have $k^2 = 0$ and $f(0) = 1$. The constant $S(0.5) = -8.4$ db determined from the radio data may be readily identified with:

$$S(0.5) = 10 \log_{10} 4\pi\, b\, \sigma(0) = -8.4 \tag{II-4}$$

Consequently it follows that:

$$4\pi\, b\, r_e^2 < [d\, N_e/dh]^2\, \ell_o^5 > = 0.1445 \tag{II-5}$$

If we let b = 10,000 meters, we obtain:

$$< [d\, N_e/dh]^2\, \ell_o^5 > = 14.48 \times 10^{22} \tag{II-6}$$

Note that the average indicated by < > is taken over the scattering volume. In the troposphere it has been found that ℓ_o is a random variable with respect to time at a fixed point and with respect to location at a fixed time; more specifically, $L = 10 \log_{10} \ell_o$ has been found to be normally distributed about its median value ℓ_{om} with $\sigma_L = 5$ db. It seems not unreasonable to assume a similar variability for ℓ_o in the ionosphere. Similarly we may assume that $[d\, N_e/dh]^2$ is log-normally distributed about its median value $[d\, N_e/dh]_m^2$ with a similar standard deviation, i.e., about 5 db. On these assumptions it can be shown[55] by simple statistical analysis that:

$$< [d\, N_e/dh]^2\, \ell_o^5 > = [d\, N_e/dh]_m^2\, \ell_{om}^5 \exp[0.02651\, \sigma^2] \tag{II-7}$$

In the above, σ denotes the standard deviation, expressed in decibels, of $10 \log_{10}\{[d\, N_e/dh]^2\, \ell_o^5\}$; if we neglect any correlation between the variations of $[d\, N_e/dh]$ and of ℓ_o, then $\sigma^2 \cong (5)^2 + (25)^2 = 650$ and $\exp[0.02651\, \sigma^2] = 3.045 \times 10^7$. If we combine (II-7) and (II-6) and set $\ell_{om} = 100$ meters, we obtain $[d\, N_e/dh]_m = 690$ electrons/c.c/kilometer. If this value is compared with the value 3,800 electrons/c.c./kilometer expected with $\sigma^2 = 0$, we see the importance of allowing for this statistical correction; the actual value probably lies somewhere between these two estimates, and can be estimated more precisely only when more adequate information becomes available relative to the variances of these variables.

The above analysis refers to the scatter expected for frequencies just above the E layer MUF. The forward scatter on the higher frequencies where S was actually evaluated becomes independent of ℓ_o since $[1 + k^2 \ell_o^2]^{-5/2} = k^{-5} \ell_o^{-5}$ when $k^2 \ell_o^2 >> 1$. In this case the correction factor should be determined for $\sigma^2 = 25$, i.e., $\exp[0.0265\ \sigma^2] = 1.940$ and the expected median gradient on these assumptions is then 2700 electrons/c.c./km.

It appears from the above analysis that S may increase with decreasing frequency because of the increasing importance of the variance of ℓ_o at these lower frequencies. This statistical factor should not be ignored in analyses of ionospheric scatter data. However, it was suppressed in the present analysis because of the lack of definitive data on σ^2.

Note that scale lengths of the order of $\ell_{om} = 100$ meters and electron density gradients of the order of 1,000 electrons/c.c./km. are not unreasonable values to assume for the lower ionosphere, and we conclude that Wheelon's theory provides a useful description of ionospheric turbulence which is not inconsistent with our knowledge of the ionosphere.

Appendix III

An Additional Height-Gain Factor in Transmission Loss

In free space the field strength e, expressed in volts per meter at a distance d, expressed in meters, from an isotropic transmitting antenna radiating p_r watts may be determined from the relation:

$$\frac{e^2}{z} = \frac{p_r}{4\pi d^2} \qquad \text{(III-1)}$$

(Radiation from an isotropic antenna in free space)

where $z = 4\pi c \cdot 10^{-7}$ = impedance of free space expressed in ohms, and $c = 2.997925 \cdot 10^{8}$ meters per second = velocity of light in free space.

Now consider the intensity of the radiation field of a short vertical electric dipole antenna of length ℓ and at a height h_a above a perfectly conducting plane. By re-distributing the field in the space above the plane, the radiation resistance is modified by the presence of the surface as follows:

$$R_e = \frac{2\pi z \ell^2}{3\lambda^2}\left[1 + \Delta_a\right] \qquad \text{(III-2)*}$$

$$\Delta_a = \frac{3}{(2k\,h_a)^2}\left[\frac{\sin(2k\,h_a)}{2k\,h_a} - \cos(2k\,h_a)\right] \qquad \text{(III-3)*}$$

* These relations are derived by S. A. Schelkunoff in Chapters VI and IX of the book "Electromagnetic Waves," D. Van Nostrand Company, 1943.

In the above $k = 2\pi/\lambda = 2\pi f/c$, i.e., λ is the wavelength in free space. Note that Δ_a approaches zero at large heights above the surface, and R_e approaches its free space value. On the other hand $\Delta_a = 1$ for $h_a = 0$, and the radiation resistance is then just twice its free space value. Using (III-2) we find that the field intensity of the short dipole over the perfectly conducting plane surface may be expressed:

$$\frac{e^2}{z} = \frac{p_r (3/2)[2 \cos\psi \cos(k h_a \sin\psi)]^2}{4\pi d^2 [1 + \Delta_a]} \tag{III-4}$$

(Radiation from a short vertical electric dipole over a perfectly conducting surface)

Note that the factor (3/2) is just the free space gain of the short dipole antenna. Since $\Delta_a = 1$ for $h_a = 0$, the field intensity is 3 db greater when $\psi = 0$ for a dipole on the surface of a perfectly conducting plane than for a short dipole in free space. In more familiar units (III-4) with $h_a = \psi = 0$ may be expressed:

$$e(\mu v/\text{meter}) = 299{,}896.2 \sqrt{p(kw)}/d_{km} \qquad (h_a = \psi = 0) \tag{III-5}$$

Furthermore, the effective absorbing area of a short vertical electric dipole antenna at a height h_b above a perfectly conducting plane may be expressed:

$$a_e = \frac{\lambda^2 (3/2) \cos^2\psi}{4\pi[1 + \Delta_b]} \tag{III-6}$$

where Δ_b is defined by (III-3) with h_a replaced by h_b.

Combining (III-4) and (III-6) we may express the transmission loss in decibels between short vertical electric dipoles at heights h_a and h_b above a perfectly conducting plane as follows:

$$L = L_{bf} - G_t - G_r + A \qquad \text{(III-7)}$$

$$A = -20 \log_{10}[2 \cos^2 \psi \cos (k h_a \sin \psi)] + L_a + L_b \qquad \text{(III-8)}$$

$$L_{a,b} = 10 \log_{10} [1 + \Delta_{a,b}] \qquad \text{(III-9)}$$

Note that L_{bf} is the basic transmission loss expected in free space, $G_t = G_r = 1.761$ db, and that the transmission loss, A, relative to free space contains two height gain factors which are not ordinarily considered in field strength calculations. No allowance was made in the calculations in this report for the additional losses L_a and L_b which arise from the redistribution of the field intensity in space which, in turn, is associated with the proximity of the antennas to the ground. Thus the transmission losses shown on Figs. 7, 8, 16, 17, 18, 19, 20, 21, 27, 31, 32, 33, 34, 35, 36, 37, 38, 39, 40, etc. are too small by an amount ranging from about 6 db at very low frequencies and low antenna heights to zero at the higher frequencies. Fig. III-1 shows this additional loss as a function of antenna height (h/λ), expressed in wavelengths, for the case of a perfectly reflecting surface, and this should also represent a good approximation in those cases where the antennas are erected over large ground screens.

It is of interest, although not surprising, to note that the transmission loss between vertical electric dipoles on the surface of a perfectly conducting plane ($h_a = h_b = \psi = 0$) is the same as if the dipoles were in free space, even though the field intensity at the surface is 3 db greater.

It should be noted that Schelkunoff identified the factors in (III-2) somewhat differently; thus he considered the ground to be an integral part of the antennas, and set $G_t = 10 \log_{10} \{(3/2) \cdot 2/[1 + \Delta_a]\}$,

$G_r = 10 \log_{10}\{(3/2)\cdot 2/[1+\Delta_b]\}$ and $A = -20 \log_{10}[\cos^2\psi \cos(k h_a \sin\psi)]$. It seems to this writer that the terms $10 \log_{10}[1+\Delta_{a,b}]$ should be excluded from G_t and G_r. Thus, according to this approach, G_t and G_r are the free space gains of the antennas, independently of their location, and the path antenna gain G_p, when measured by replacing the actual antennas by isotropic antennas, will still be approximately equal to $G_t + G_r$.

Suppose now that we use small loop antennas of area S, with their axes normal to the plane of propagation, parallel to the perfectly conducting surface and at heights h_a and h_b, respectively. In this case:

$$R_m = \frac{8\pi^3 z S^2}{3\lambda^4} [1 + \Delta'_b] \tag{III-10}$$

$$\Delta'_b = (3/2)\left[\left(1 - \frac{1}{(2k h_b)^2}\right) \frac{\sin(2k h_b)}{2k h_b} + \frac{\cos(2k h_b)}{(2k h_b)^2}\right] \tag{III-11}$$

$$a_e = \frac{\lambda^2 (3/2)}{4\pi [1 + \Delta'_b]} \tag{III-12}$$

$$A = -20 \log_{10} [2 \cos(k h_a \sin\psi)] + L'_a + L'_b \tag{III-13}$$

Note that Δ'_b approaches zero at large heights and $\Delta'_b = 1$ for $h_b = 0$.

Consider next the transmission loss between two small loop antennas at heights h_a and h_b, respectively, above a perfectly conducting surface with their axes normal to this surface. In this case:

$$R_m = \frac{8\pi^3 z S^2}{3\lambda^4} [1 - \Delta] \tag{III-14}$$

$$A = -20 \log_{10} [2 \cos^2 \psi \sin (k h_a \sin \psi)] + L''_a + L''_b \qquad \text{(III-15)}$$

$$L''_{a,b} = 10 \log_{10} [1 - \Delta_{a,b}] \qquad \text{(III-16)}$$

The factor L'' is also shown as a function of (h/λ) on Fig. III-1.

Finally consider the transmission loss between two short horizontal electric dipoles of length ℓ, normal to the plane of propagation and at heights h_a and h_b, respectively, above a perfectly conducting plane surface. In this case:

$$R_e = \frac{2\pi z \ell^2}{3\lambda^2} [1 - \Delta'] \qquad \text{(III-17)}$$

$$A = -20 \log_{10} [2 \sin (k h_a \sin \psi)] + L'''_a + L'''_b \qquad \text{(III-18)}$$

$$L'''_{a,b} = 10 \log_{10} [1 - \Delta'_{a,b}] \qquad \text{(III-19)}$$

Note that L''' and L'' both approach $(-\infty)$ as h approaches zero, but the radiation resistance R simultaneously approaches zero, and it would be difficult in practice to keep the radiated power constant as the antennas are brought nearer and nearer to the surface. When h_a and h_b are both much less than a wavelength, A, as defined by (III-15) for horizontal loops becomes independent of these heights and equal to $A = 20 \log_{10}(kd/5)$; similarly A, as defined by (III-18) for horizontal electric dipoles approaches $20 \log_{10}(2\,kd/5)$ for h_a and h_b much less than a wavelength.

Since the factors L'''_a and L'''_b were omitted in calculating the transmission losses shown on Figs. 9 and 10, these values are much too large at the lower frequencies since the 30-foot antennas are in this case only a small fraction of a wavelength above the surface.

All of the above results refer to the case of a perfectly conducting plane surface and to distances $d >> \lambda$. For a finitely conducting ground, the factor $2 \cos (k h_a \sin \psi)$ in (III-8) and (III-13) or the factor $2 \sin (k h_a \sin \psi)$ in (III-15) and (III-18) must be replaced by the appropriate attenuation factor, 2 W, relative to the free space field. For example, for electric dipoles over a flat earth of finite conductivity and with $h_a = h_b = 0$:

$$W = \left| 1 + i \sqrt{\pi p} \exp(-p) \operatorname{erfc}(-i \sqrt{p}) \right| \tag{III-20}$$

Here p denotes Sommerfeld's numerical distance as defined in reference 13 where a comprehensive discussion is given of the radiation fields of electric and magnetic dipoles over a finitely conducting plane earth. Furthermore, Δ and Δ' will be modified when the antennas are located over a finite ground, 1/ 2/ 3/ 4/ but this difference will often largely be cancelled in practice if a large ground screen is used under the antennas. Although (III-14) indicates that R_m approaches zero as the vertical magnetic dipoles approach the perfectly conducting surface, Wait 1/ has shown that R_m becomes very large when such loops are brought near a finitely conducting ground.

It is sometimes convenient to be able to relate the basic transmission loss, ℓ_b, to the field strength e:

$$p_a/\ell_b = p_a = (e^2/z) \cdot (\lambda^2/4\pi) \tag{III-21}$$

(Isotropic antennas in free space)

Expressed in decibels, we obtain from (III-21):

$$L_b = 77.216 + 20 \log_{10} f_{kc} + P_r - E_b \tag{III-22}$$

(Isotropic antennas in free space)

In the above, P_r is the radiated power expressed in db above one kilowatt, and E_b is the field strength in db above one microvolt per meter. If antennas with free space gains G_t and G_r are used, we find that $E_t = E_b + G_t$, and the transmission loss between these antennas in free space may be expressed:

$$L = L_b - G_t - G_r = 77.216 + 20 \log_{10} f_{kc} + P_r - E_t - G_r \qquad \text{(III-23)}$$

(Antennas with gains G_t and G_r in free space)

For a half wave dipole transmitting antenna $G_t = 2.15$ db, and we obtain from the above the relation given at the bottom of page two of the report.

References

1. James R. Wait, "Radiation resistance of a small circular loop in the presence of a conducting ground," Jour. of App. Phys., vol. 24, no. 5, 646-649, May, 1953.

2. James R. Wait and Walter J. Surtees, "Impedance of a top-loaded antenna of arbitrary length over a circular grounded screen," Jour. of Applied Phys., vol. 25, no. 5, 553-555, May, 1954.

3. J. R. Wait and W. A. Pope, "Input resistance of L. F. unipole aerials," Wireless Engineer, vol. 32, 131-138, May, 1955.

4. J. R. Wait, "Effect of the ground screen on the field radiated from a monopole," IRE Trans. on Antennas and Propagation, vol. AP-4, no. 2, April, 1956.

TRANSMISSION LOSS ARISING FROM A CHANGE IN THE RADIATION RESISTANCE OF SHORT DIPOLE ANTENNAS NEAR A PERFECTLY CONDUCTING SURFACE

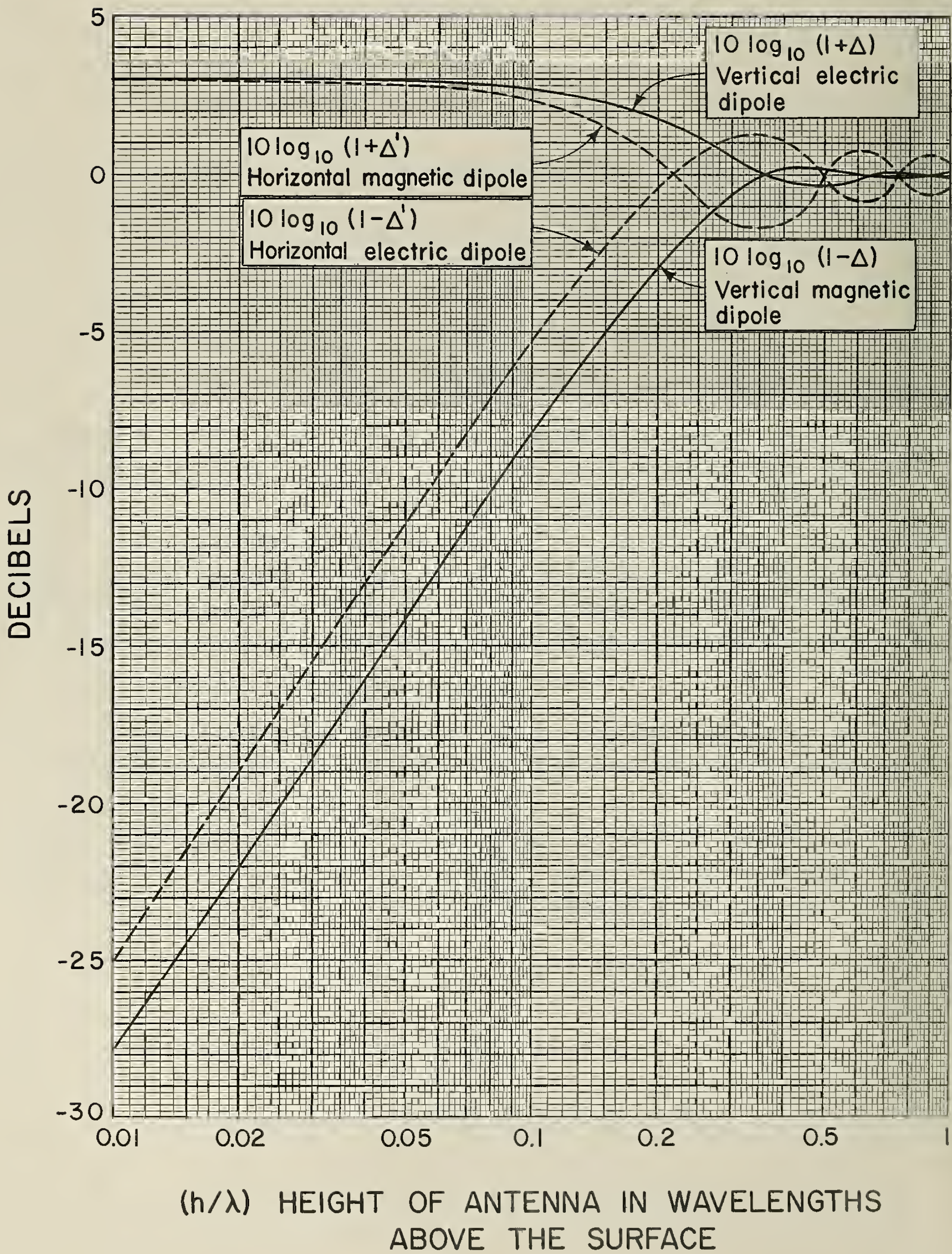

Figure III-1

USCOMM-NB

NBS

AUG 1980